Ph.D. Dissertation in Agricultural Biotechnology

Engineering of *Saccharomyces cerevisiae* as a Novel Expression Platform of Endolysin for Biocontrol of *Staphylococcus aureus*

*Saccharomyces cerevisiae*를 이용한
엔도라이신의 신규 발현 플랫폼 구축과
*Staphylococcus aureus*의 생물방제에 관한 연구

February, 2020

The Graduate School
Seoul National University
Department of Agricultural Biotechnology

Jihwan Chun

Engineering of *Saccharomyces cerevisiae* as a Novel Expression Platform of Endolysin for Biocontrol of *Staphylococcus aureus*

Advisor: Sangryeol Ryu

Submitting a Ph.D. Dissertation
in Agricultural Biotechnology

February, 2020

The Graduate School
Seoul National University
Department of Agricultural Biotechnology
Jihwan Chun

Confirming the Ph.D. Dissertation written by
Jihwan Chun
February, 2020

Chair	_____	(Seal)
Vice Chair	_____	(Seal)
Examiner	_____	(Seal)
Examiner	_____	(Seal)
Examiner	_____	(Seal)

Abstract

Chun, Jihwan

Department of Agricultural Biotechnology

The Graduate School

Seoul National University

Despite the countless efforts to fend off the threat of bacterial pathogens, the arms race between prokaryotes and mankind has never been eased. Nonetheless, thanks to the extensive studies about many of the pathogens, we are gaining more and more insight into the characteristics of pathogenic bacteria. Among them, *Staphylococcus aureus* has been recognized as one of the most important pathogen, in terms of both community and clinical acquisition. In addition to the numerous illnesses caused by *S. aureus*, its resistance to various antibiotic agents, including the most powerful ones, is a significant threat to public health. Moreover, its ability to provoke pathogenesis in both humans and livestock animals has intensified the challenging issues to a greater extent.

Recently, the breakthrough in bioinformatics allowed us with abundant genetic and genomic information about many pathogenic bacteria. However, such data is still quite limited to a few laboratory strains or significant isolates, which may not be relevant enough to represent the

characteristics of bacterial isolates from other part of the globe. Hence, I speculated that it is necessary to study the genome of domestically isolated pathogenic *S. aureus* (*S. aureus* FORC_059) and elucidate its features involved in virulence and antibiotic resistance. I have elucidated the entire sequences of a clinical *S. aureus* isolate from Korea, and functionally annotated its genomic features. Not only the genomic structures but the detailed information about the genes contributing to the virulence or antibiotic resistance were revealed in terms of genotypic and phenotypic approaches. Furthermore, similarities and differences in genomic properties were compared with an isolate originated from food poisoning outbreak in Korea. From the genomics study, I learned that both clinical and food isolated *S. aureus* strains carry multiple virulence factors and resistance genes, and some critical features are highly prone to horizontal gene transfer. Considering the prevalence of such genetic diversifications, it became apparent that we need an alternative strategy to control this pathogen regardless of its antibiotic resistance.

In this respect, study of bacteriophage has been diverged to develop alternative methodologies for the biocontrol of pathogenic bacteria. Since it is perceived that virtually every bacterial strain has one or more corresponding phages, the application of phage could have been a promising solution. However, due to several reasons, such as host-dependent replication, host specificity, lysogenic lifecycle, host defense systems, application of phage could not resolve the antibiotic crisis. Therefore, phage lysins,

especially phage endolysins, have received more and more attention. So far, studies about phage endolysins were mostly focused on the discovery or development of novel endolysins, together with their characterization. Since such researches relied on bacterial expression platforms, application of endolysin was rather limited. In order to develop industrially applicable platform, I have engineered yeast *Saccharomyces cerevisiae* strains to build novel endolysin expression platform based on surface display and secretion system, and investigated the antibacterial effect of yeast-expressed endolysin LysSA11 toward *S. aureus*. This is by far the first study to express phage endolysin in yeast by both surface display and secretion.

Surface display of LysSA11 on *S. cerevisiae* EBY100 strain was mediated by fusion with a-agglutinin subunit Aga2p at C-terminus in pYD5 plasmid. Galactose-induced *S. cerevisiae* EBY100/pYD5-LysSA11 cultures were harvested at early- (OD_{600} = 6) and late-exponential (OD_{600} = 13) phases, in regard to growth and galactose consumption pattern. Expression of LysSA11-Aga2p fusion protein at each growth phase was confirmed by western blot assay, and it was revealed that the fusion protein was glycosylated. The harvested cultures were also examined by flow cytometry, and based on the surface display properties of LysSA11 at each growth phase, I could learn that the amount of surface-displayed LysSA11 increases over time during exponential growth. When yeast cells were simply transferred from culture media to reaction buffer (100 mM sodium phosphate, 200 mM sodium chloride, pH 7.4), yeast-displayed LysSA11 exhibited antibacterial

activities against a type strain *S. aureus* ATCC 13301, and a clinical isolate *S. aureus* FORC_059. By applying approximately 3×10^8 CFU/mL of induced yeast cells to *S. aureus* ATCC 13301, yeast-displayed LysSA11 from early-, mid-, or late-exponential phase could eliminate approximately 1×10^5 CFU/mL within 7 h, 6 h, and 2 h or reaction. In addition, once the staphylococcal populations were inhibited, they did not grow back until 10 h, implying that the *S. aureus* could not develop any resistance. Likewise, approximately 2×10^5 CFU/mL of *S. aureus* FORC_059 was totally reduced within 4 h when treated with the equivalent population of late-exponentially induced yeast cells. Moreover, stability of yeast-displayed LysSA11 was notably improved, as the antibacterial activity against *S. aureus* ATCC 13301 was merely affected in the absence of any stabilizing agent during 14 days of storage at 4℃. On the contrary, purified LysSA11 from *Escherichia coli* system was dramatically deteriorated in the absence of glycerol, retaining only 19.2% and 11.5% of initial activity after 7 and 14 days.

Secretion of LysSA11 was tested from two different recombinant yeast strains, YVH10/pYDS-K-LysSA11 and EBY100/p404TEF1-LysSA11. Specifically, the former used inducible GAL1 promoter, while the latter used constitutive TEF1 promoter, which can express the target protein without any supplementation of inducing agent. At first, both strains were grown at 30℃, and the expression of LysSA11 and its antibacterial activity were investigated. In terms of YVH10/pYDS-K-LysSA11, induced cultures were harvested at early- (OD_{600} = 5) or late-exponential phase (OD_{600} = 16) based on growth

and galactose consumption, and EBY100/p404TEF1-LysSA11 cultures were harvested at late-exponential phase (OD_{600} = 10). The intracellular expression and secretion of LysSA11 was confirmed in both types of recombinant yeast strains. Specifically, it was confirmed that LysSA11 secreted from YVH10/pYDS-K-LysSA11 was glycosylated. Secreted LysSA11 in each culture supernatant was concentrated to a volume 150 times smaller than the initial status, and treated to approximately 2×10^4 CFU/mL of *S. aureus* ATCC 13301 to examine antibacterial activity. Culture concentrate of YVH10/pYDS-K-LysSA11 exhibited 4-log CFU reduction within 4 h, while its counterpart of EBY100/p404TEF1-LysSA11 did not show any activity. Then, YVH10/pYDS-K-LysSA11 strain was cultured in different conditions (low cell density/high cell density, 20℃/30℃) and the secretion and antibacterial activity were analyzed. As a result, low cell density culture at 30℃ harvested at early-exponential phase and high cell density culture at 20℃ harvested at late-exponential phase turned out to confer sufficient activity to inhibit the given population of *S. aureus* ATCC 13301.

In the current study, I employed bioinformatics tools to genomically study *S. aureus*, developed novel endolysin expression platforms by engineering surface display and secretion systems in yeast *S. cerevisiae*, and validated the applicability for the biocontrol of *S. aureus*. The acquired results urge the necessity for novel antibacterial agents, and will pave the road to exploit yeast for advanced application strategies of endolysins.

Keywords: *Staphylococcus aureus*, bacteriophage endolysin, *Saccharomyces cerevisiae*, yeast surface display, yeast protein secretion, biocontrol agent

Student Number : 2014-21911

Contents

Abstract ..... - 1 -

Contents ..... - 7 -

List of Figures ..... - 13 -

List of Tables ..... - 16 -

Chapter I. ..... - 17 -

Introduction ..... - 17 -

I.1. *Staphylococcus aureus* ..... - 18 -

I.2. Bacteriophage ..... - 20 -

I.3. Bacteriophage endolysin ..... - 25 -

I.4. *Saccharomyces cerevisiae* ..... - 30 -

I.5. Purpose of this research ..... - 35 -

Chapter II. Genomics study of *Staphylococcus aureus* ..... - 37 -

II.1. Introduction ..... - 38 -

II.2. Materials and Methods ..... - 41 -

II.2.1. Strains, culture media, and growth conditions ..... - 41 -

II.2.2. Bacterial species identification ..... - 41 -

II.2.3. Genomic DNA preparation ..... - 41 -

II.2.4. Whole-genome sequencing ..... - 42 -

II.2.5. *De novo* assembly ..... - 43 -

II.2.6. Genome annotation ..... - 43 -

II.2.7. COG analysis ..... - 44 -

II.2.8. Virulence factor analysis ..... - 45 -
II.2.9. Comparative genome analysis ..... - 45 -
II.2.10. Hemolysis test ..... - 45 -
II.2.11. Antimicrobial susceptibility test ..... - 46 -
II.3. Results and Discussion ..... - 48 -
II.3.1. Genomic properties of *S. aureus* FORC_059 ..... - 48 -
II.3.2. Genotypic and phenotypic properties of *S. aureus* FORC_059 ..... - 54 -
II.3.3. Comparative genome analysis of *S. aureus* FORC_059 .- 65 -
Chapter III. Development of a novel endolysin expression platform by utilizing yeast surface display system ..... - 69 -
III.1. Introduction ..... - 70 -
III.2. Materials and Methods ..... - 75 -
III.2.1. Strains, culture media, and growth conditions ..... - 75 -
III.2.2. Cloning, expression, and purification of LysSA11 with variant His-tag orientations ..... - 75 -
III.2.3. Lytic activity test of purified LysSA11 ..... - 77 -
III.2.4. Recombinant yeast construction for surface display of LysSA11 ..... - 77 -
III.2.5. Expression of yeast-displayed LysSA11 ..... - 78 -
III.2.6. Analyzing physiological properties of recombinant yeast during LysSA11 expression ..... - 79 -
III.2.7. Immunoblot assay of LysSA11-Aga2p fusion protein ... - 80 -

III.2.8. Glycosylation analysis of LysSA11-Aga2p fusion protein ..... - 81 -
III.2.9. Flow cytometry (FACS) analysis recombinant yeast ..... - 83 -
III.2.10. Antibacterial activity analysis of yeast-displayed LysSA11 ..... - 83 -
III.2.11. Stability analysis of yeast-displayed and purified LysSA11 in storage condition ..... - 84 -
III.2.12 Antibacterial activity analysis of surface-displayed LysSA11 in cryo-lysed yeast ..... - 85 -
III.2.13. Statistical analysis ..... - 86 -
III.3. Results and Discussion ..... - 90 -
III.3.1. Determination of optimal orientation for LysSA11 fusion protein ..... - 90 -
III.3.2. Construction of recombinant *S. cerevisiae* strains ..... - 93 -
III.3.3. Physiological traits of the recombinant yeast during LysSA11 induction ..... - 95 -
III.3.4. Expression of LysSA11-Aga2p fusion protein in the recombinant yeast ..... - 99 -
III.3.5. Glycosylation of LysSA11-Aga2p fusion protein ..... - 101 -
III.3.6. Characterization of surface-displayed LysSA11 in the recombinant yeast ..... - 106 -
III.3.7. Antibacterial activity of yeast-displayed LysSA11 against *S. aureus* ATCC 13301 ..... - 109 -

III.3.8. Antibacterial activity of yeast-displayed LysSA11 against *S. aureus* FORC_059 ..... - 116 -
III.3.9. Protein stability of yeast-displayed LysSA11 ..... - 118 -
Chapter IV. Development of a novel endolysin expression platform by utilizing yeast secretion system..... - 124 -
IV.1. Introduction ..... - 125 -
IV.2. Materials and Methods..... - 129 -
IV.2.1. Strains, culture media, and growth conditions ..... - 129 -
IV.2.2. Recombinant yeast construction for inducible secretion of LysSA11..... - 130 -
IV.2.3. Recombinant yeast construction for constitutive secretion of LysSA11..... - 131 -
IV.2.4. Galactose-induced expression of yeast-secreted LysSA11 from low-density population..... - 132 -
IV.2.5. Galactose-induced expression of yeast-secreted LysSA11 from high-density population..... - 133 -
IV.2.6. Constitutive expression of yeast-secreted LysSA11 from low-density population..... - 133 -
IV.2.7. Analyzing physiological properties of recombinant yeast during LysSA11 expression ..... - 134 -
IV.2.8. Harvesting and concentrating secreted LysSA11 in yeast culture ..... - 135 -
IV.2.9. Immunoblot assay of intracellular or secreted LysSA11 from

yeast .....- 136 -
IV.2.10. Glycosylation analysis of yeast-secreted LysSA11 ....- 138 -
IV.2.11. Zymography of yeast-secreted LysSA11 .....- 139 -
IV.2.12. Antibacterial activity analysis of yeast-secreted LysSA11 .....- 140 -
IV.2.13. Antibacterial activity assessment of LysSA11-secreting yeast .....- 141 -
IV.2.14. Statistical analysis .....- 142 -
IV.3. Results and Discussion.....- 146 -
IV.3.1. Determination of optimal expression system for LysSA11 secretion .....- 146 -
IV.3.2. Construction of recombinant *S. cerevisiae* strains.....- 148 -
IV.3.3. Physiological traits of the recombinant yeast with inducible expression system .....- 152 -
IV.3.4. Physiological traits of the recombinant yeast with constitutive expression system .....- 156 -
IV.3.5. Confirming the expression of LysSA11 in inducible system .....- 158 -
IV.3.6. Confirming the expression of LysSA11 in constitutive system .....- 166 -
IV.3.7. Antibacterial activity of yeast-secreted LysSA11 against *S. aureus* ATCC 13301.....- 168 -
IV.3.8. Antibacterial activity of LysSA11-secreting yeast against *S.*

aureus ATCC 13301..... - 175 -

References ..... - 177 -

국문 초록 ..... - 213 -

List of Figures

Figure II-1. Genome map of *S. aureus* FORC_059. .....- 52 -

Figure II-2. Hemolysis assay of *S. aureus* FORC_059. .....- 57 -

Figure II-3. Antibiotic susceptibility assay of *S. aureus* FORC_059. .....- 63 -

Figure II-4. Comparative genome analysis of *S. aureus* FORC_059 and FORC_001.....- 68 -

Figure III-1. Overview of YSD-based novel endolysin expression platform. .....- 89 -

Figure III-2. Evaluation of LysSA11 fusion protein with divergent orientations for optimal bactericidal activity.....- 92 -

Figure III-3. Schematic diagram of pYD5-LysSA11 shuttle vector and LysSA11-Aga2p fusion protein. .....- 94 -

Figure III-4. Physiological behaviors of recombinant *S. cerevisiae* EBY100 strains in glucose and galactose media.....- 97 -

Figure III-5. Expression of LysSA11-Aga2p fusion protein....- 100 -

Figure III-6. Glycosylation of LysSA11-Aga2p fusion protein. .....- 103 -

Figure III-7. Characteristics of yeast cells with surface-displayed LysSA11. .....- 108 -

Figure III-8. Antibacterial activity of yeast-displayed LysSA11 from different growth stages against *S. aureus* ATCC 13301. ..... - 112 -

Figure III-9. Population variation of *S. aureus* ATCC 13301 upon treatment of divergent recombinant yeast strains. ..... - 113 -

Figure III-10. Antibacterial activity of yeast-displayed LysSA11 against *S. aureus* ATCC 13301 in acidic environment. ..... - 114 -

Figure III-11. Antibacterial activity of yeast-displayed LysSA11 against staphylococcal clinical isolate FORC_059. . - 117 -

Figure III-12. Antibacterial activity of yeast-displayed and purified LysSA11 after refrigerated storage..... - 119 -

Figure III-13. Antibacterial activity of yeast-displayed LysSA11 in cryo-lysed yeast. ..... - 121 -

Figure IV-1. Overview of yeast secretion-based endolysin expression platform ..... - 145 -

Figure IV-2. Schematic diagram of pYDS-K-LysSA11 shuttle vector and LysSA11 secretion cassette. ..... - 149 -

Figure IV-3. Schematic diagram of p404TEF1-LysSA11 shuttle vector and LysSA11 secretion cassette. ..... - 151 -

Figure IV-4. Physiological behaviors of recombinant *S. cerevisiae* YVH10 strains in glucose and galactose media at 30℃. ..... - 154 -

Figure IV-5. Growth of recombinant *S. cerevisiae* EBY100 strains in glucose media at 30℃. ..... - 157 -

Figure IV-6. Expression of LysSA11 in *S. cerevisiae* YVH10/pYDS-K-LysSA11 at 30℃. ..... - 159 -

Figure IV-7. Glycosylation of LysSA11 secreted from *S. cerevisiae* YVH10/pYDS-K-LysSA11. ..... - 162 -

Figure IV-8. Zymography of LysSA11 secreted from *S. cerevisiae* YVH10/pYDS-K-LysSA11. ..... - 165 -

Figure IV-9. Expression of LysSA11 in *S. cerevisiae* EBY100/p404TEF1-LysSA11 at 30℃. ..... - 167 -

Figure IV-10. Antibacterial activity of yeast-secreted LysSA11 from different hosts. ..... - 170 -

Figure IV-11. Antibacterial activity of LysSA11 secreted from inducible host with various induction conditions..... - 174 -

Figure IV-12. Antibacterial activity of LysSA11-secreting inducible yeast visualized on solid culture matrix. ..... - 176 -

List of Tables

Table II-1. Primers used in Chapter II. ..... - 47 -

Table II-2. Genome assembly results of *S. aureus* FORC_059.. - 50 -

Table II-3. Genome annotation summary of *S. aureus* FORC_059.

..... - 53 -

Table II-4. Virulence factors of *S. aureus* FORC_059. ..... - 58 -

Table II-5. Antibiotic susceptibility of *S. aureus* FORC_059. ... - 64 -

Table III-1. Plasmids and primers used in this chapter. ..... - 88 -

Table IV-1. Plasmids and primers used in this chapter..... - 144 -

Chapter I.

Introduction

I.1. *Staphylococcus aureus*

Staphylococcus aureus is a non-sporulating, non-motile, Gram-positive, coagulase positive coccoid bacterium of the Firmicutes phylum (*Medical Microbiology. 4th Edition*, 1996). *S. aureus* is a member of human commensal microbiota, especially from nasal mucosa and skin. It is an opportunistic pathogen, provoking various diseases, such as skin abscesses, endocarditis, pneumonia, bacteremia, and toxic shock syndrome (Lowy, 1998). Moreover, this pathogen has been recognized as one of the most widespread cause of community-associated and nosocomial clinical infections (P R & M, 2013). Most importantly, the emergence and accumulation of antibiotic-resistant strains, including methicillin-resistant *S. aureus* (MRSA), have become a serious problem worldwide (Lee et al., 2018).

Pathogenesis of *S. aureus* occurs through an orchestrated activity of various virulence factors. Staphylococcal surface proteins promote attachment to biotic or abiotic surfaces, allowing the pathogen to make contact with its host (Foster, Geoghegan, Ganesh, & Höök, 2013). Some of the virulence factors contribute to host immune evasion. *S. aureus* possess an array of diverse toxins, among which enterotoxins are mostly involved in food-poisoning or toxic shock syndrome, while hemolysins can trigger hemolysis (Otto, 2014). Furthermore, resistance to numerous antibiotics makes *S. aureus* a significant threat (Chambers & DeLeo, 2009). Specifically,

some multidrug-resistant strains have acquired resistance against glycopeptides including vancomycin.

In addition to clinical infections, *S. aureus* is a common cause of food-borne outbreaks, whose symptoms include sudden start of nausea, vomiting, stomach cramps, and diarrhea. In Korea, *S. aureus* has been reported as the fifth leading cause of bacterial food-borne outbreaks, following pathogenic *E. coli*, *Salmonella*, *Clostridium*, and *Campylobacter* (Center for Disease et al., 2019). Not only humans, but livestock animals could also suffer from *S. aureus* infections, such as dermatitis, pneumonia, septicemia, osteomyelitis, and meningitis in swine, bovine mastitis in cattle, and septic arthritis, bumblefoot disease, and gangrenous dermatitis in poultry (Quinn, 1994). Furthermore, it has been reported that *S. aureus* can be transmitted from humans to livestock animals or vice versa (Hasman et al., 2010; Lowder et al., 2009; Voss, Loeffen, Bakker, Klaassen, & Wulf, 2005). It could be assumed that once *S. aureus* outbreaks occur, it may spread out very quickly through various routes, and therefore development of novel methodologies to prevent the dissemination and neutralize the pathogen is inevitable.

I.2. Bacteriophage

As one of the most abundant living entities on the globe, bacteriophages (phages) have been studied for several decades. The nature of phage to infect and affect the host bacteria has been a great interest. There have been numerous phages reported so far, among which tailed double-stranded DNA phages, the order *Caudovirales*, are regarded to account for 96% of known phages (Ackermann, 2006). The order *Caudovirales* is further classified into four families; *Siphoviridae* (54%), *Myoviridae* (26%), *Podoviridae* (17%), and *Ackermannviridae* (1%) (Adriaenssens et al., 2018). Morphological traits lie on the basis of the classification: icosahedral head and long, non-contractile, flexible, thin tail (*Siphoviridae*) ("Family - Siphoviridae," 2012); relatively larger icosahedral head and long, contractile, rigid, thick tail (*Myoviridae*) ("Family - Myoviridae," 2012); short, non-contractile tail (*Podoviridae*) ("Family - Podoviridae," 2012); icosahedral head, contractile tail, thin base plate, prong- and star-like adsorption organelle (*Ackermannviridae*) (Adriaenssens et al., 2012). On the other hand, such classifications cannot be applied in genomic point of view, since phage genomes share limited sequence similarity. In fact, phages with common host may retain similar nucleotide sequences to some extent, but those infecting different hosts or even within a same group, phages would rarely share any genomic architectures. More interestingly, phage genes with no significant

sequence similarity may encode proteins having similar biological functions (Bérard et al., 2016; Hatfull, 2008). Instead, phages can be grouped into “types”, whose members share similarities in the life cycles, gene order, transcription pattern, and the ability to infect closely related bacterial hosts (Casjens, 2005; Grose & Casjens, 2014). Even though the actual nucleotide sequence may differ, functional genes can exhibit syntenic relationship, that phages of the same type can harbor gene modules arranged in the same manner with one another.

No matter how they differ, all of these phages undergo one of several life cycles: the lytic (virulent) cycle, in which they propagate and destroy the host cell; the lysogenic (temperate) cycle, in which the phage genome coexists with bacterial chromosome via integrated form; the pseudolysogenic cycle, in which the phage genome exists in episomal form; the chronic infection, in which phage progeny is continuously released from the host without lysis (Weinbauer, 2004).

The life of phage is not a strictly destined scenario, but involves multiple decision making processes to determine the most favorable mode of growth (Erez et al., 2017; Oppenheim, Kobiler, Stavans, Court, & Adhya, 2005; Silpe & Bassler, 2019). When the lytic cycle is activated, the genetic functions of host are compromised and preoccupied with the reproduction of phages, and eventually, newly assembled virion particles are released by host cell lysis. Since multiple proteins are orchestrated during lysis, the gene

cassettes are elaborately regulated (R. Young, 2014). In Gram-negative hosts, it was reported that phages employ holin, endolysin, and spanin proteins for lysis (Berry, Rajaure, Pang, & Young, 2012). In terms of Gram-positive bacteria, since they lack outer membrane, phages require holin and endolysin proteins to lyse the host (Vincent A. Fischetti, 2011), and such structural characteristics allow efficient disruption of the cell wall by exogenous treatment of endolysin (Schmelcher, Donovan, & Loessner, 2012). On the other hand, under specific circumstances, phages may choose to initiate lysogenic pathway, during which their genetic materials are integrated into the host genome and stably maintained as prophage state until induction of lytic cycle (Oppenheim et al., 2005). Moreover, during lysogeny, the infected host (lysogen) becomes immune to additional infection by homologous phages. Significantly, prophages may contribute to the genetic diversity of the host through horizontal gene transfer mediated by lysogenic conversion, giving rise to various changes in their physiology, adaptation, and virulence, including bacterial virulence factors and antibiotic resistance (Brown-Jaque, Calero-Cáceres, & Muniesa, 2015; Fortier & Sekulovic, 2013; Jamet et al., 2017). Meanwhile, upon infection of starving host cells, phage genome can enter pseudolysogeny and remain in the form of an episome, which can further be passed to successive generation in an asymmetrical manner (Cenens, Makumi, Mebrhatu, Lavigne, & Aertsen, 2013). In terms of chronic infection, which was reported from several filamentous phages, the progeny

virus exits the host without lethal damages (Marciano, Russel, & Simon, 1999).

Based on the versatile biological characteristics, numerous researches have been conducted to develop and utilize phages as natural antimicrobial agents (Alisky, Iczkowski, Rapoport, & Troitsky, 1998). Especially, lytic (virulent) phages have been widely studied for human therapy (Lin, Koskella, & Lin, 2017), veterinary medicine (Squires, 2018), agriculture (Svircev, Roach, & Castle, 2018), food safety (Moye, Woolston, & Sulakvelidze, 2018), and environmental protection (Withey, Cartmell, Avery, & Stephenson, 2005). In fact, phages could be used as sanitizing agents in food production facilities, and some of them were actually approved of GRAS (generally regarded as safe) status by FDA (Sharma, 2013; Sulakvelidze, 2013).

The benefits of using phages over conventional antibiotics can be as follows: i) high host specificity of phage prevents undesirable damage to off-target commensal bacteria, ii) the nature of phage to only infect targeted bacteria poses low inherent cytotoxicity to human, iii) the abundance of phage species makes it much more cost-efficient to discover phages than developing a new antibiotic molecule (Loc-Carrillo & Abedon, 2011). Nevertheless, the use of phages is still very limited due to some intrinsic issues (Fernández, Gutiérrez, Rodríguez, & García, 2018). As previously mentioned, phages which undergo obligatory lytic lifecycle can be utilized for antimicrobial purposes. Since lysogenic phages have contributed to the genetic

diversification of bacteria by sometimes transducing toxin or antibiotic resistance genes, the genetic and physiological traits have to be investigated. Moreover, the ability of bacteria to develop resistance against phages makes it challenging. In fact, bacteria have evolved to have a variety of defense mechanisms against phage infection, such as preventing the adsorption of phage or the injection of DNA, digesting foreign DNA, or activating abortive infection system (Labrie, Samson, & Moineau, 2010). Most importantly, due to its parasitic nature, phages cannot directly inhibit their target hosts (Stone, Campbell, Grant, & McAuliffe, 2019). In other words, phages alone cannot exhibit any inhibitory activity, since they require certain period of time to infect and multiply to kill the host. Taken together, it is obvious that more studies are required to develop effective and efficient strategies to utilize phages for the biocontrol of pathogenic bacteria.

I.3. Bacteriophage endolysin

Endolysins are phage-encoded lytic enzymes employed for host lysis at the end of phage multiplication cycle, contributing to the eventual liberation of newly synthesized virions (Schmelcher et al., 2012). It is a type of peptidoglycan hydrolases, capable of recognition and degradation of specific targets of bacterial peptidoglycan structure. Upon phage infection, endolysin-mediated host cell lysis occurs from the intracellular space, otherwise called as 'lysis from within', in which other proteins are involved to assist the action of endolysin (Catalão, Gil, Moniz-Pereira, São-José, & Pimentel, 2013). Among them, phage holin plays a critical role to accomplish cell lysis by perforating the cytoplasmic membrane, thereby releasing endolysins accumulated in the cytoplasm and allowing them to attack the cell wall (R. Young, 2014). Moreover, it has been studied that many other proteins are involved to finely control the procedures and timing of bacterial cell lysis (Catalão et al., 2013). Interestingly, phages capable of secreting endolysins without the use of holins have been reported in both Gram-positive and Gram-negative systems (São-José, Parreira, Vieira, & Santos, 2000; Xu, Struck, Deaton, Wang, & Young, 2004).

Endolysins have different structural characteristics in regard to the cell wall structure of host bacteria. The endolysins encoded by phages infecting Gram-negative bacteria are generally small (molecular weight of 15 to 20

kDa), since they are composed of a single domain for the cleavage of a specifically conserved peptidoglycan structure, the cross-linkage between meso-diaminopimelic acid and D-alanine of the peptides of two adjacent glycan chains (Briers & Lavigne, 2015). Due to the distinct structure of Gram-negative bacterial peptidoglycan, these endolysins can virtually act on the peptidoglycan of any other strains within a same species (Walmagh et al., 2013). However, the existence of outer membrane protects the peptidoglycan from extracellular endolysins.

On the other hand, endolysins from phages of Gram-positive bacteria or mycobacteria have a typical modular architecture comprising at least two distinguishing functional regions (Vincent A Fischetti, 2008). In general, being connected by a flexible linker, the N-terminal region carries one or two catalytic domain (enzymatically active domain, EAD) and the C-terminus segment carries cell wall binding domains (CBD). As the EAD confers the catalytic mechanism of the enzyme, endoysins can be categorized into 5 functional types based on the EAD: *N*-acetylmuramidases (lysozymes), endo-β-*N*-acetylglucosaminidases, lytic transglycosylases (cleave the *N*-acetylmuramic acid – *N*-acetyl glucosamine moiety of the peptidoglycan), *N*-acetyl-muramoyl-*L*-alanine amidases (hydrolyze the amide bond between *N*-acetylmuramic acid and *L*-alanine residues in the oligopeptide cross-linking chains), and endopeptidases (attack the interconnecting peptide bonds within the same peptidoglycan units) (Loessner, 2005). Except for the lytic

transglycosylases, all 4 types of endolysins are hydrolases, and among them, *N*-acetyl-muramoyl-*L*-alanine amidase (often abbreviated as 'amidase') is the most frequently and earliest identified peptidoglycan hydrolase (Schmelcher et al., 2012). Meanwhile, it has been revealed that the CBD guide the endolysin to the substrate and maintain the protein to be securely bound to the cell wall debris after cell lysis, thereby preventing collateral damage of potential new host cells nearby (Vincent A Fischetti, 2008). The most crucial function of CBD is to endow specificity to an endolysin for certain types of cell wall by recognizing and binding the ligand molecules. Consequently, it can be assumed that the host range of endolysin is mostly determined by CBD.

Especially for most of the endolysins derived from staphylococcal phages, a modular architecture of N-terminal endopeptidase, centrally located amidase, and C-terminal SH3b-type CBD, is relatively well conserved (Schmelcher, Shen, et al., 2015). In most cases, the N-terminal endopeptidase is a cysteine-, histidine-dependent amidohydrolase/peptidase (CHAP), which cleaves the bond between D-alanine of the stem peptide and the pentaglycine bridge of the staphylococcal peptidoglycan (Becker et al., 2009). The EAD in the central region often displays amidase activity (amidase 2 or amidase 3), breaking between the sugar strands and the stem peptide (Navarre, Ton-That, Faull, & Schneewind, 1999). It is reported that the C-terminal SH3b domain needs an intact pentaglycine bridge for full binding activity, as shown for the SH3b-like cell wall-targeting domain (CWT) of lysostaphin, the bacteriocin

of *Staphylococcus simulans* bv. staphylolyticus (Gründling & Schneewind, 2006). However, the CBD of some staphylococcal endolysins turned out to be unrelated to the common SH3b domain (Chang, Kim, & Ryu, 2017). In most cases of the dual-EAD staphylococcal endolysins, lytic activity relies mostly on the N-terminal CHAP endopeptidase domain (Becker et al., 2015; Sanz-Gaitero, Keary, Garcia-Doval, Coffey, & van Raaij, 2014).

In the notion of application as an antimicrobial agent, endolysin is a highly competent candidate to substitute conventional antibiotics, regarding its biological properties (Schmelcher et al., 2012). First of all, the extensive use of broad-range antibiotics has accelerated the dissemination of resistance genes within bacterial community, due to their non-specific activity to target pathogens and commensal bacteria. However, endolysins is capable of acting on bacteria within a certain genus or species, due to its target-specific nature (Nelson et al., 2012). Moreover, the relatively low structural diversity and extracellularly exposed nature of peptidoglycans in Gram-positive bacteria have made it unfavorable for bacterial cells to develop resistance against endolysins (Vincent A. Fischetti, 2005). Although there were some reports about resistance to peptidoglycan hydrolases other than endolysins, such as a few *S. aureus* strains being resistant to lysostaphin (Gründling, Missiakas, & Schneewind, 2006), no resistance mechanisms have been observed for phage endolysins so far. In addition, endolysins can act synergistically when used in combination with each other or with other antimicrobial agents (Becker,

Foster-Frey, & Donovan, 2008; Schmelcher, Powell, Camp, Pohl, & Donovan, 2015). Most importantly, despite the fact that antibodies against endolysins can be raised, no adverse side effect or anaphylaxis nor any severe interference with endolysin activity *in vivo* was reported (Vincent A. Fischetti, 2010; Rashel et al., 2007).

To date, the advances in endolysin research have led to the development of a commercial endoysin-based therapeutic agent for the biocontrol of *S. aureus*, SAL200 (Jun et al., 2013). Preclinical tests (good laboratory practice (GLP)-compliant safety evaluation) of SAL200 in rat and dog models have yielded favorable results (Jun et al., 2014), and a further study has been conducted in monkeys to analyze its pharmacokinetics (Jun et al., 2016), in which no significant adverse effect was observed. Recently, research of SAL200 was conducted as a part of the first in-human phase 1 study of endolysin-based therapeutic agent for intravenous administration (Jun et al., 2017). Despite the favorable results, there still resides a few issues to be resolved. Repeated exposure to SAL200 in rats and dogs for over 10 days triggered immune response, which is doubted to be due to residual lipopolysaccharide endotoxin originating from the bacterial expression host (Jun et al., 2014). Also, comparable to other proteins, SAL200 has low half-life in human blood plasma ranging from 0.04 to 0.38 h (Jun et al., 2017), implying that a lot more improvements are required for efficient uses.

I.4. *Saccharomyces cerevisiae*

In general, production of recombinant proteins has been most frequently studied in prokaryotes, specifically *Escherichia coli* expression system (Rosano & Ceccarelli, 2014) due to several benefits: i) fast growth kinetics, ii) ease of obtaining high cell density culture, and iii) ease of transformation with recombinant DNA. Despite the advantages, some of its biological properties could be hurdles for further applications of endolysins. The presence of lipopolysaccharide (LPS) in *E. coli* host is detrimental for recombinant proteins produced for therapeutic purposes (Petsch & Anspach, 2000). Due to the high toxicity of LPS, recombinant therapeutic proteins have to be purified to thoroughly remove the endotoxin for further applications. In addition, protein production itself can be problematic in *E. coli* system. Accumulation of recombinant protein in the cytoplasm may lead to increased instability and formation of inclusion bodies (IBs) (Carrió & Villaverde, 2002). Even if the final product is in a soluble form, the polypeptide contents may lack proper activity due to improper folding (Martínez-Alonso, González-Montalbán, García-Fruitós, & Villaverde, 2008). Finally, successfully produced soluble and active proteins have to undergo complicated and labor-intensive processes to be prepared in a purified and concentrated form.

Being the most well-established eukaryotic expression host with

broad utility, yeast can offer solutions to aforementioned issues. Among several eukaryotic host systems, yeast could excel others by combining the advantages of unicellular organisms with the capability of eukaryotes to carry out protein processing (protein folding, assembly, and post-translational modifications) (Porro, Sauer, Branduardi, & Mattanovich, 2005). Its ability to quality control the production of polypeptides in cellular organelles can help preventing the formation of misfolded polypeptides (C. L. Young & Robinson, 2014). Recently, production of fully humanized sialylated glycoproteins have become available, thanks to the breakthroughs in glycoengineering of the yeast *Pichia pastoris* (Hamilton & Gerngross, 2007). Moreover, *Saccharomyces cerevisiae* is classified as generally regarded as safe (GRAS) organism by U.S. Food and Drug Administration (FDA), thereby ensuring endotoxin-free production of desired proteins. Previous studies have demonstrated that soluble form of eukaryotic proteins, such as single-chain T cell receptor (scTCR) or bovine pancreatic trypsin inhibitor (BPTI), were successfully obtained using the yeast system (Kowalski, Parekh, & Wittrup, 1998; Shusta, Kieke, Parke, Kranz, & Wittrup, 1999). Recently, it was reported that yeast *S. cerevisiae* could intracellularly express and utilize a prokaryotic protein called encapsulin (Humphries et al., 2018). In addition, it was confirmed that yeast is capable of intracellularly producing or secreting endolysin LysA2 in a functionally active form (Khatibi, Roach, Donovan, Hughes, & Bischoff, 2014; J.-S. Kim, M. A. Daum, Y.-S. Jin, & M. J. Miller,

2018).

Among several yeast expression systems, yeast surface display (YSD) system has been widely utilized as a platform for recombinant protein production and engineering in various ways (Mattanovich et al., 2012). Originally, YSD was designed to facilitate antibody engineering, especially for the screening and sorting of antibodies with enhanced binding affinity or augmented specificity (Boder & Wittrup, 1997; Gai & Wittrup, 2007). Recently, YSD system has been widely utilized for the engineering and construction of whole-cell biocatalyst for several purposes, including advancements in protein stability, biomass turnover, or bio-adsorption (Gai & Wittrup, 2007; Kuroda & Ueda, 2013; Shusta et al., 1999). Specifically, it has been reported that immobilization of a metabolic enzyme by YSD could greatly improve protein stability and reusability (Parthasarathy, Bajaj, & Boder, 2005).

In the YSD system, recombinant proteins are expressed and extracellularly displayed by anchor proteins. Among several anchors, a-agglutinin mating protein subunits, Aga1p and Aga2p, can be employed in *Saccharomyces cerevisiae* host (Cherf & Cochran, 2015). Regarding the activity domain, protein of interest can be fused to the N- or C- terminus of Aga2p, which forms two disulfide bonds with β 1,6-glucan-anchored Aga1p subunit embedded in the cell wall, and surface-displayed upon expression. Subsequently, displayed proteins can be detected by incorporated epitope tags,

and examined for the activity. Throughout the procedures, properly folded products are secreted and displayed, hence protein aggregation due to excessive accumulation in the cytoplasm is less likely to occur. Most importantly, the immobilization of active protein on the cell surface makes it unnecessary to further purify and concentrate proteins for further applications.

Yeast secretion system has also been developed and optimized for the production of heterologous proteins (Porro et al., 2005). Many yeast systems have been exploited for protein production for pharmaceutical, food, and other industries (Vieira Gomes, Souza Carmo, Silva Carvalho, Mendonça Bahia, & Parachin, 2018). In respect to pharmaceutical proteins, *S. cerevisiae* has been engineered for the production of insulin, insulin analogs, human serum albumin, hepatitis vaccines (Martínez, Liu, Petranovic, & Nielsen, 2012). The advantage of yeast over bacterial system in pharmaceutical protein production rooted from the ability to do post-translational processing and secrete proteins in functionally active forms. The rapid growth and high-density fermentation of yeast in chemically defined media also facilitated industrial applications.

In *S. cerevisiae* and other yeast strains, protein of interest can be secreted by adding appropriate secretion signal sequence. One of the most commonly used signal peptide is the *S. cerevisiae* α-mating factor (α-MF). It has been reported that the use of entire processing sequence of prepro α-MF could achieve high secretion level of target protein in both nonmethylotrophic

and methylotrophic yeasts (*S. cerevisiae*, *K. lactis*, and *P. pastoris*) (Porro et al., 2005). Upon expression, nascent protein is further processed in endoplasmic reticulum (ER) and Golgi, such as signal peptide cleavage, or glycosylation (Banfield, 2011; Walker & Lively, 2013). If unfolded proteins accumulate in the ER, unfolded protein response (UPR) is induced, and the proteins may be rescued or degraded. Through such modification and quality control mechanisms, heterologous proteins can be successfully secreted in an active form for further applications.

I.5. Purpose of this research

As an important community-associated and nosocomial bacterial pathogen, *S. aureus* has been extensively studied. However, studies about *S. aureus* isolated from Korea has not been focused on the genomic level. Genomic studies on clinical or environmental isolates of *S. aureus* can give more insight to the pathogenic features, such as virulence and antibiotic resistance.

Based on the understandings about the pathogen, novel biocontrol strategies could be developed. Through several decades of fight against antibiotic-resistant bacteria, many approaches to substitute conventional antibiotic agents have been made. Bacteriophage endolysin has been recognized as one of the candidate antibacterial agents against Gram-positive pathogens. However, the development of commercially available endolysin has been very challenging due to low productivity and stability. Moreover, conventional recombinant endolysin expression system mostly relies on *E. coli* host, in which intrinsic issues, such as endotoxin contamination, are present. As a well-established protein expression host, *Saccharomyces cerevisiae* can make itself an appropriate expression platform for endolysin.

Hence, the objectives of this study are (i) analyze the whole genome sequence of *S. aureus* isolate and reveal the pathogenic characteristics in genotypic and phenotypic level, (ii) develop a functional endolysin

expression platform based on yeast surface display system, (iii) develop a functional endolysin expression platform based on yeast secretion system, and (iv) evaluate the efficacy and efficiency of each expression platform for the biocontrol of *S. aureus*.

Chapter II.

Genomics study of *Staphylococcus aureus*

II.1. Introduction

Staphylococcus aureus is a Gram-positive, coagulase positive coccoid bacterium of the Firmicutes phylum with non-sporulating, non-motile properties (*Medical Microbiology. 4th Edition*, 1996). *S. aureus* is a component of human commensal microbiota, but also an opportunistic pathogen causing various diseases (Lowy, 1998). It has been known as one of the most widespread causes of community-associated and nosocomial clinical infections (P R & M, 2013). Above all, the prevalence and accumulation of antibiotic-resistant strains, such as methicillin-resistant *S. aureus* (MRSA), is a serious problem worldwide (Lee et al., 2018). In Korea, *S. aureus* has been reported as the fifth leading cause of bacterial food-borne outbreaks, following pathogenic *E. coli*, *Salmonella*, *Clostridium*, and *Campylobacter* (Center for Disease et al., 2019). Not only humans, but livestock animals could also suffer from *S. aureus* infections, such as dermatitis, pneumonia, septicemia, osteomyelitis, and meningitis in swine, bovine mastitis in cattle, and septic arthritis, bumblefoot disease, and gangrenous dermatitis in poultry (Quinn, 1994). Furthermore, it has been reported that *S. aureus* can be transmitted from humans to livestock animals or vice versa (Hasman et al., 2010; Lowder et al., 2009; Voss et al., 2005).

In regard to this, the pivotal role of molecular typing techniques in microbiology have greatly contributed to the clinical and public health by

unveiling the evolutionary and phylogeographic dispersion of medically important microbes (van Belkum, 2003). Nucleic acid-based typing approaches such as pulsed field gel electrophoresis (PFGE) (Schwartz & Cantor, 1984), multi-locus sequence typing (MLST) (Maiden et al., 1998), or the use of DNA arrays (Dunne Jr, Pouseele, Monecke, Ehricht, & van Belkum, 2018) have been proven useful to assess epidemiological relatedness among strains of most of the health-care associated species (Sabat et al., 2013). Nevertheless, most infections in the clinical setting are caused by strains belonging to a relatively restricted number of lineages especially for highly prevalent MRSA. Such strains cannot always be differentiated in sufficient detail by means of the classical DNA-based methods (Sabat et al., 2013). More recently, improvements in both the time-to-results and the affordability of whole-genome sequencing (WGS) promised to overcome this limitation by providing access to complete microbial genomes (Harris et al., 2010; Salipante et al., 2015). Both the WGS discriminatory power and its versatility helped to highlight transmission pathways (Gordon et al., 2014; Köser et al., 2012). To date, WGS is the sole approach that yields insight into both the macro- and the micro-evolutionary dynamics of bacterial pathogens over different periods of time and in different geographical locations. WGS is “portable” and has sufficient discriminatory power to reconstruct both intercontinental and local transmission of MRSA lineages. This will facilitate better tracking of emergent lineages within the community (Fridkin et al.,

2005).

II.2. Materials and Methods

II.2.1. Strains, culture media, and growth conditions

Staphylococcus aureus FORC_059 (Accession number: CP020354) strain was acquired from Seoul Samsung hospital. It was isolated from the blood of a patient, and was originally named as F2603. *S. aureus* FORC_059 was cultivated in tryptic soy broth/agar (TSB/TSA) (BD Difco) with aeration at 37℃, 220 rpm/static.

II.2.2. Bacterial species identification

Prior to whole-genome sequencing, 16S rRNA sequence of *S. aureus* FORC_059 strain was amplified and analyzed. The nucleotide sequence of forward and reverse primers are listed in Table II-1. The amplicon was amplified with PrimeSTAR® HS DNA polymerase (TaKaRa Bio), and purified with Wizard® SV Gel and PCR Clean-up system (Promega). The purified PCR product was analyzed by Sanger sequencing, and the resulting nucleotide sequence was tested by sequence alignment at BLASTn database (Z. Zhang, Schwartz, Wagner, & Miller, 2000).

II.2.3. Genomic DNA preparation

S. aureus FORC_059 strain was streaked on TSA plate, and a single

colony was inoculated to 3 mL of TSB media and cultivated for overnight. The enriched culture was sub-cultured in 50 mL of TSB for 4 h, and the mid-exponentially grown cells were collected by centrifugation at 10,000 × *g* for 5 min. After discarding supernatant, the genomic DNA (gDNA) was isolated by using G-spin™ for bacteria genomic DNA extraction kit (iNtRON bio).

II.2.4. Whole-genome sequencing

The whole genome sequence of *S. aureus* FORC_059 was analyzed by PacBio RS II sequencing platform (ver. 1.1) (Pacific Biosciences), using SMRT (Single Molecule Real-Time) sequencing technique. A total of 5 μg of gDNA was used for library preparation. The SMRTbell® library was constructed with SMRTbell® template prep kit 1.0 (Pacific Biosciences) following manufacturer's instructions. Small fragments lower than 20 kb of SMRTbell template were removed using BluePippin size selection system (Sage Science) for large-insert library. The constructed library was validated by Aglient 2100 Bioanalyzer (Agilent Technologies). After annealing sequencing primer to the SMRTbell template, DNA polymerase was bound to the complex using DNA/Polymerase binding kit P6 v2 (Pacific Biosciences). The polymerase-SMRTbell-adaptor complex was then loaded into SMRT cells, and the library was sequenced using one SMRT cell with C4 chemistry (DNA sequencing reagent 4.0), and 240 min movies were captured for each SMRT cell using PacBio RS II sequencing platform (Pacific Biosciences).

II.2.5. *De novo* assembly

De novo assembly was conducted by using HGAP (hierarchical genome assembly process) (ver. 2.3) workflow, including consensus polishing with Quiver (Chin et al., 2013). Taking into account that the estimated size of the genome was 2,797,605 bp, and the average coverage was 347×, error correction was performed based on the longest seed bases (150,017,244 bp) with rest of the shorter reads. Subsequent to HGAP, the size of N50 contig and the total contig were acquired. The structure of each contig was verified by using MUMmer (ver. 3.5) (Kurtz et al., 2004). Any self-similar ends identified were trimmed by manual genome closure.

II.2.6. Genome annotation

Assembled contigs were imported to CLC Main Workbench (ver. 7.7.1) (QIAGEN), and minor modifications were performed if needed. The resulting sequence information was exported in fasta format, and the ORF (open reading frame) prediction was conducted by GeneMarkS program (Besemer, Lomsadze, & Borodovsky, 2001) and RAST (Rapid Annotation using Subsystem Technology) (Aziz et al., 2008) database. In terms of RAST, the annotation scheme followed “classic RAST”, based on GLIMMER-3 (Gene Locator and Interpolated Markov ModelER) system (Delcher, Bratke, Powers, & Salzberg, 2007). The output files of GeneMarkS and RAST were

processed by using Artemis software (ver. 16.0.0) (T. Carver, Harris, Berriman, Parkhill, & McQuillan, 2012), and the prediction data were comparatively analyzed. While RAST database provides functional prediction of each predicted ORF, GeneMarkS program only provides the location information. Hence functional prediction of ORFs retrieved from GeneMarkS was conducted by protein Multi BLAST (Camacho et al., 2009) using CLC Genomics Workbench (ver. 9.0) (QIAGEN). The resulting functional predictions were selected based on E-value. When functional prediction was completed, the ORFs were rearranged, starting from chromosomal replication initiator *dnaA*, and the GC skew was plotted for confirmation. Additionally, tRNA sequences were predicted by Aragorn software (Laslett & Canback, 2004), and rRNA sequences were predicted by RNAmmer software (Lagesen et al., 2007). All the prediction data were merged and processed by Sequin software (ver. 15.10) (NCBI), and the resulting data was validated by Microbial Genome Submission Check software (NCBI). Errors (complete overlap, RNA overlap, frameshift) were amended prior to submission. Finally, BioProject and BioSample information were newly created, and the complete annotation data was submitted to NCBI database.

II.2.7. COG analysis

Based on the annotation data, protein products of the predicted ORFs

were categorized by COG database (Clusters of Orthologous Groups of proteins) (Tatusov, Galperin, Natale, & Koonin, 2000). COG analysis data retrieved from the database were then processed by Artemis software (ver. 16.0.0) (T. Carver et al., 2012). Based on COG classifications and the G+C content of each ORF, circular genome map of each contig was created by GeneScene software (ver. 0.99.8.0) (DNASTAR).

II.2.8. Virulence factor analysis

Virulence factors of *S. aureus* were identified referring to VFDB (virulence factor database) (Chen et al., 2005). Complete genome annotation data in GenBank format were uploaded to VFDB, and virulence factors were systematically screened by the automated analysis pipeline, VFanalyzer.

II.2.9. Comparative genome analysis

Complete genome data of *S. aureus* strains were compared by ACT (Artemis comparison tool) analysis (T. J. Carver et al., 2005). The raw data of ACT analysis were trimmed by setting a cutoff at alignment length of 5,000.

II.2.10. Hemolysis test

S. aureus FORC_059 strain was cultivated on sheep blood agar (MBcell) at 37℃, static for overnight to examine the hemolytic activity.

II.2.11. Antimicrobial susceptibility test

The response of *S. aureus* FORC_059 to an array of antibiotic agents was tested by Kirby-Bauer method (Hudzicki, 2009). Single colony of *S. aureus* FORC_059 streaked on TSA plate was inoculated to 3 mL of TSB for overnight, and then sub-cultured for 2 h. The culture was pelleted and re-suspended to 0.85% saline water to turbidity of 0.5, based on Densicheck calibration standard turbidometer (BIOMERIEUX). On Mueller-Hinton agar (Oxoid Ltd.), 1 mL of the re-suspended culture was evenly plated. Excess inoculum was removed, and the agar plate was dried for 15 min. Antibiotic susceptibility discs containing specific antibiotics (Oxoid Ltd.) were dispensed on agar plate. Subsequently, the agar plates were incubated at 37℃, static for overnight, and the result was assessed according to CLSI antimicrobial susceptibility criteria (Humphries et al., 2018).

Table II-1. Primers used in Chapter II.

Primers (5'→3')		
Name	**Sequence**	**Reference**
27F	AGAGTTTGATCMTGGCTCAG	(Srinivasan et al., 2015)
1492R	CGGTTACCTTGTTACGACTT	

II.3. Results and Discussion

II.3.1. Genomic properties of *S. aureus* FORC_059

Staphylococcus aureus FORC_059 is a clinical isolated from blood of a patient in Korea. Initially, it was named as *S. aureus* F2603 by Seoul Samsung hospital, and later renamed as FORC_059 by FORC (Food-borne pathogen Omics Research Center) project. Upon acquisition, bacterial species was identified by 16S rRNA sequencing, and clinical isolate was verified as *S. aureus*.

Subsequently, genomic DNA of *S. aureus* FORC_059 was prepared, and the whole genome sequence was elucidated and assembled by PacBio RS II platform and HGAP protocol, respectively. The result of *de novo* assembly is as follows: mean subread length, 10,642; number of subreads, 109,914; polished contig total length, 2,797,605; number of contigs, 2 (Table II-2). In regard to the fact that coverage indicate the repetition of sequencing, it could be assumed that coverage of 418.1× guarantees the fidelity of sequence data.

Assembly data was further analyzed for the prediction of ORFs (open reading frames) and their functional annotation by RAST (Aziz et al., 2008), GeneMarkS (Besemer et al., 2001), protein BLAST (Camacho et al., 2009), Aragorn (Laslett & Canback, 2004), and RNAmmer (Lagesen et al., 2007). The genome of *S. aureus* FORC_059 was predicted to include two circular

contigs, which were identified as a chromosome and a plasmid. On the chromosome, 2,531 ORFs were predicted as CDS (coding sequence), and 75.8% of the CDS were functionally annotated. In addition, 61 tRNA coding sequences and 19 rRNA coding sequences were predicted (Figure II-1A). Meanwhile, 43 ORFs were predicted on the plasmid, and 69.8% of them were functionally annotated (Figure II-1B). Annotation data of both contigs were deposited to NCBI database. According to NCBI genome database, in which 10,752 genome assemblies of *S. aureus* are deposited, the median total length of *S. aureus* is 2.84 Mb, with 2,764 median protein counts and 32.7% median GC content. Therefore, it can be concluded that *S. aureus* FORC_059 shows average genomic features of staphylococci. The result of analysis is visualized in Figure II-1, and summarized in Table II-3.

Table II-2. Genome assembly results of *S. aureus* FORC_059.

Assembly results				
Sample name	**Mean subread length**	**Number of subreads**	**Polished contig total length**	**Coverage**
S. aureus FORC_059	10,642	109,914	2,797,605	418.1 ×
Contig information				
Data	**Form**	**Contig length**		**GC contents (%)**
Contig 1	Circular	2,707,649		32.84
Contig 2	Circular	35,269		30.45

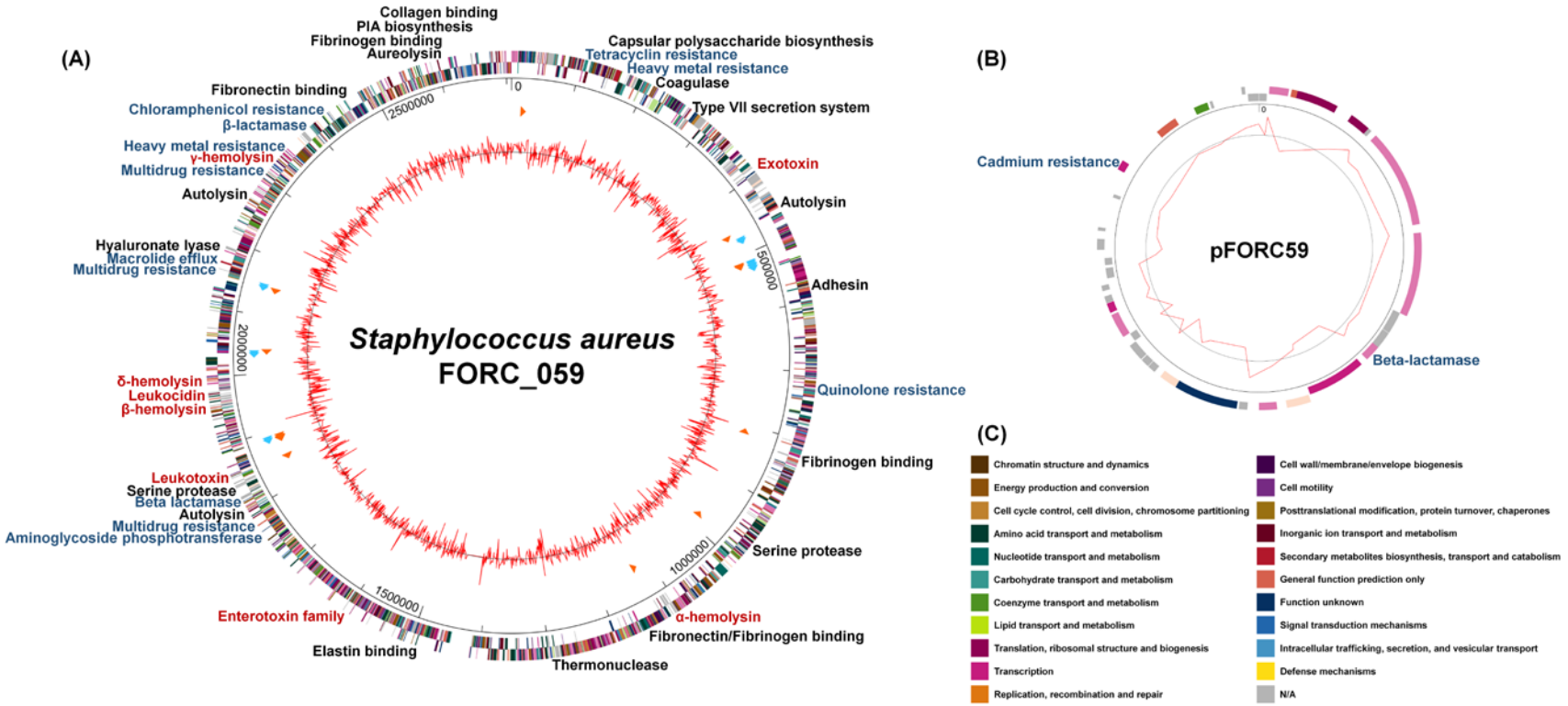
(A)
Staphylococcus aureus
FORC_059
0
500000
1000000
1500000
2000000
2500000
Collagen binding
PIA biosynthesis
Fibrinogen binding
Aureolysin
Capsular polysaccharide biosynthesis
Tetracyclin resistance
Heavy metal resistance
Coagulase
Type VII secretion system
Exotoxin
Autolysin
Adhesin
Quinolone resistance
Fibrinogen binding
Serine protease
α-hemolysin
Fibronectin/Fibrinogen binding
Thermonuclease
Elastin binding
Enterotoxin family
Leukotoxin
Serine protease
Beta lactamase
Autolysin
Multidrug resistance
Aminoglycoside phosphotransferase
δ-hemolysin
Leukocidin
β-hemolysin
Hyaluronate lyase
Macrolide efflux
Multidrug resistance
Autolysin
Heavy metal resistance
γ-hemolysin
Multidrug resistance
Fibronectin binding
Chloramphenicol resistance
β-lactamase
(B)
pFORC59
Cadmium resistance
Beta-lactamase
(C)
Chromatin structure and dynamics
Energy production and conversion
Cell cycle control, cell division, chromosome partitioning
Amino acid transport and metabolism
Nucleotide transport and metabolism
Carbohydrate transport and metabolism
Coenzyme transport and metabolism
Lipid transport and metabolism
Translation, ribosomal structure and biogenesis
Transcription
Replication, recombination and repair
Cell wall/membrane/envelope biogenesis
Cell motility
Posttranslational modification, protein turnover, chaperones
Inorganic ion transport and metabolism
Secondary metabolites biosynthesis, transport and catabolism
General function prediction only
Function unknown
Signal transduction mechanisms
Intracellular trafficking, secretion, and vesicular transport
Defense mechanisms
N/A

Figure II-1. Genome map of *S. aureus* FORC_059.

Genomic features of the chromosome (A) and plasmid (B) of *S. aureus* FORC_059 were illustrated. The outermost rings indicate predicted ORFs on plus or minus strands. The ring with red peaks indicates GC content. Between those rings, light blue arrows represent rRNAs and orange arrows represent tRNAs. Each ORF was categorized into functional groups, which were represented by different colors. Based on the annotation data, ORFs predicted to encode proteins contributing to virulence or antibiotic resistance were marked on the maps: red, toxins; blue, antibiotic resistance; black, other virulence factors. (C) COG (Clusters of Orthologous Groups of proteins) groups of the annotated ORFs were classified and represented by different colors.

Table II-3. Genome annotation summary of *S. aureus* FORC_059.

Name	Contig type	Size (bp)	Predicted CDS	Annotated gene	Hypothetical protein	tRNA	rRNA	Accession number
S. aureus FORC_059	Chromosome	2,707,649	2,531	1,919	612	61	19	CP020354
	Plasmid	35,269	43	30	13	-	-	CP020355

II.3.2. Genotypic and phenotypic properties of *S. aureus* FORC_059

Genetic features of *Staphylococcus aureus* FORC_059 were analyzed based on the annotation data and virulence factor report (Table II-4). First of all, *S. aureus* FORC_059 could be determined as a MSSA (methicillin susceptible *Staphylococcus aureus*), since *mecA* gene was not identified (Sakoulas et al., 2001). In fact, the genetic elements involved in biofilm formation of MSSA strains, such as *ica* operon (FORC_059_2478 ~ FORC_059_2482) required for biosynthesis of PIA (polysaccharide intercellular adhesin) (Cramton et al., 1999; Rohde, Knobloch, Horstkotte, & Mack, 2001), were identified, supporting the idea that *S. aureus* FORC_059 could be an MSSA strain (McCarthy et al., 2015). In a previous study, it was reported that *ica* operon was highly conserved in clinical isolates of *S. aureus* from bacteremia patients (Fowler Jr et al., 2001). Since FORC_059 was isolated from bacteremia patient, it could be assumed that *ica* operon can be utilized as a biomarker to identify *S. aureus* with clinical significance.

In addition to biofilm forming activity, some ORFs were predicted as virulence factors for immune evasion and persistent infection. Among several strategies to escape from host immune system, clinical *S. aureus* strains express capsular polysaccharide CP5 and CP8 to avoid phagocytic killing (Nanra et al., 2013). Plus, *S. aureus* uses protein A (SpA) to inhibit

opsonophagocytosis by interfering with complement binding region (Fcγ) of functional antibodies to recognize and bind to the pathogen (Peterson, Verhoef, Sabath, & Quie, 1977). Serine proteases are also known to contribute to the growth and survival of *S. aureus in vivo* (Rice, Peralta, Bast, de Azavedo, & McGavin, 2001). In *S. aureus* FORC_059, CDS for capsular polysaccharide biosynthesis (FORC_059_0112,0113,0115,0116, and 0117), protein A (FORC_059_0069), and serine proteases (FORC_059_0924, 1699 ~ 1704) were identified.

Most importantly, *S. aureus* is very well known for its variety of exotoxins, which can be roughly classified into hemolysins and pyrogenic toxin superantigens (PTSAgs) (Dinges, Orwin, & Schlievert, 2000). The exotoxins categorized into PTSAgs include toxic shock syndrome toxin-1 (TSST-1) and staphylococcal enterotoxins (SEs) (Ortega, Abriouel, Lucas, & Gálvez, 2010). Specifically, SEs preformed on food by *S. aureus* contamination have been recognized as the cause of staphylococcal food poisoning. Moreover, SEs and TSST-1 can also cause a systemic illness, toxic shock syndrome (TSS), which can become fatal to some extent. Interestingly, the genes for such toxins were not identified on the genome of *S. aureus* FORC_059. This finding imply that the FORC_059 strain may not have originated from food sources. However, such implication does not necessarily undermine the pathogenic impact of this clinical isolate, since all four hemolysins were identified (alpha, FORC_059_1037; beta, FORC_059_1827;

gamma, FORC_059_2239 ~ 2241; delta, FORC_059_1862). In fact, hemolytic activity of *S. aureus* FORC_059 was confirmed by hemolysis assay conducted on blood agar (Figure II-2).

Alongside with toxins and virulence factors, genes predicted to be involved in the development of antibiotic resistance were identified. The ORFs for such genes were categorized according to the antibiotic agent against which they build up resistance, such as β-lactamase, fluoroquinolone, aminoglycoside, macrolide, and specifically methicillin. As listed in Table II-4, several genes related to antibiotic resistance were predicted, and their actual phenotypic representation was examined by conducting antibiotic susceptibility assay (Figure II-3, Table II-5). Referring to CLSI antimicrobial susceptibility criteria (Humphries et al., 2018), it could be learned that *S. aureus* FORC_059 is resistant to ampicillin, erythromycin, nalidixic acid, and ciprofloxacin. This could also be confirmed from the annotation data: metallo-β-lactamase family protein, FORC_059_1634; β-lactamase, FORC_059_1706, 2261, p014, p015; macrolide-efflux protein, FORC_059_2005; quinolone resistance protein, FORC_059_0662. As previously mentioned, *S. aureus* FORC_059 did not have resistance against methicillin, since it was susceptible to a methicillin-derivative, oxacillin, in agreement to the absence of any ORF to be predicted as *mecA* gene.

Figure II-2. Hemolysis assay of *S. aureus* FORC_059.

Hemolytic activity of *S. aureus* FORC_059 was assessed by streaking on sheep blood agar plate. Hemolysis of red blood cells is visualized as the halo appearing around the streaked colonies.

Table II-4. Virulence factors of *S. aureus* FORC_059.

Locus tag	Annotation	Location (nt)
Adherence		
FORC_059_0069	Protein A, von Willebrand factor binding protein Spa	complement (76623..78053)
FORC_059_0423	Autolysin precursor	455288..456292
FORC_059_0520	Adhesin SdrC	580606..583656
FORC_059_0521	Bone sialoprotein-binding protein Bbp-like Adhesin SdrE	584023..587985
FORC_059_0522	Bone sialoprotein-binding protein Bbp-like Adhesin SdrE	588379..591858
FORC_059_0756	Clumping factor ClfA, fibrinogen-binding protein	828954..831812
FORC_059_1033	Extracellular fibrinogen-binding protein Efb	1108432..1108929
FORC_059_1087	Fibronectin/fibrinogen-binding protein	complement (1162200..1163897)
FORC_059_1374	Elastin binding protein EbpS	complement (1493854..1495314)
FORC_059_1660	Autolysin	complement (1800236..1801090)
FORC_059_1825	Extracellular adherence protein of broad specificity Eap/Map	complement (1965726..1966016)
FORC_059_1826	Extracellular adherence protein of broad specificity Eap/Map	complement (1966027..1967775)
FORC_059_2124	Bifunctional autolysin Atl / N-acetylmuramoyl-L-Alanine amidase / Endo-beta-N-acetylglucosaminidase	complement (2266006..2266782)
FORC_059_2313	Fibronectin binding protein FnbB	complement (2462318..2465143)
FORC_059_2314	Fibronectin binding protein FnbA	complement (2465821..2469003)
FORC_059_2443	Clumping factor ClfB, fibrinogen-binding protein	complement (2604615..2607374)
FORC_059_2478	Biofilm operon *icaABCD* HTH-type negative transcriptional regulator IcaR	complement (2655804.2656364.)

FORC_059_2479	Polysaccharide intercellular adhesin (PIA) biosynthesis N-glycosyltransferase IcaA	2656567..2657766
FORC_059_2480	Polysaccharide intercellular adhesin (PIA) biosynthesis protein IcaD	2657730..2658035
FORC_059_2481	Polysaccharide intercellular adhesin (PIA) biosynthesis deacetylase IcaB	2658032..2658904
FORC_059_2482	Polysaccharide intercellular adhesin (PIA) biosynthesis protein IcaC	2658891..2659943
FORC_059_2506	Collagen binding protein Cna	complement (2681290..2684841)
Host immune evasion		
FORC_059_0112	Capsular polysaccharide biosynthesis protein CapD	125914..126942
FORC_059_0113	Capsular polysaccharide synthesis enzyme Cap5F	126955..128064
FORC_059_0115	Capsular polysaccharide synthesis enzyme Cap8H	129195..130274
FORC_059_0116	Capsular polysaccharide synthesis enzyme Cap8I	130267..131661
FORC_059_0117	Capsular polysaccharide synthesis enzyme Cap8J	131658..132215
Exoenzyme		
FORC_059_0183	Coagulase	214699..216660
FORC_059_0924	Glutamyl endopeptidase precursor, serine proteinase SspA	complement (994424..995488)
FORC_059_1217	Thermonuclease	1297856..1298389
FORC_059_1699	Serine protease	complement (1831795..1832514)
FORC_059_1700	Serine protease	complement (1832665..1833381)
FORC_059_1701	Serine protease	complement (1833539..1834258)
FORC_059_1702	Serine protease	complement (1834379..1835098)
FORC_059_1703	Serine protease	complement (1835156..1835878)
FORC_059_1704	Serine protease	complement (1836003..1836710)

FORC_059_2028	Hyaluronate lyase precursor	2186129..2188576
FORC_059_2346	Esterase/lipase	complement (2501704..2502672)
Secretion system		
Type VII secretion system		
FORC_059_0238	ESAT-6/Esx family secreted protein EsxA/YukE	277684..277977
FORC_059_0239	Putative secretion accessory protein EsaA/YueB	278061..281090
FORC_059_0240	Putative secretion system component EssA	281090..281548
FORC_059_0241	Putative secretion accessory protein EsaB/YukD	281520..281762
FORC_059_0242	Putative secretion system component EssB/YukC	281775..283109
FORC_059_0243	FtsK/SpoIIIE family protein, putative EssC component of Type VII secretion system	283131..287579
FORC_059_2397	Putative EsaC protein-like protein	complement (2556048..2556344)
Toxin		
FORC_059_364	Exotoxin 6	399697..400377
FORC_059_365	Exotoxin 7	400663..401358
FORC_059_366	Exotoxin 8	401649..402719
FORC_059_368	Exotoxin 8	403084..404031
FORC_059_369	Exotoxin 10	404395..405099
FORC_059_371	Exotoxin 1	406665..407360
FORC_059_372	Exotoxin 8	407699..408397
FORC_059_373	Exotoxin 13	408776..409474

FORC_059_374	Exotoxin 4	409833..410516
FORC_059_377	Exotoxin 15	413992..414684
FORC_059_1037	Alpha-hemolysin precursor	complement (1111715..1112674)
FORC_059_1495	Enterotoxin family protein	complement (1605931..1606635)
FORC_059_1711	Leukotoxin LukD	complement (1840837..1841820)
FORC_059_1712	Leukotoxin LukE	complement (1841822..1842757)
FORC_059_1827	Beta-hemolysin	1968161..1969156
FORC_059_1828	Leukocidin LukF-PV	complement (1969394..1970410)
FORC_059_1829	Leukocidin LukS-PV	complement (1970432..1971487)
FORC_059_1862	Delta-hemolysin	complement (1998771..1998905)
FORC_059_2239	Gamma-hemolysin component A	2383163..2384128
FORC_059_2240	Gamma-hemolysin component B	2384695..2385642
FORC_059_2241	Gamma-hemolysin component C	2385644..2386621
Antibiotics resistant genes		
FORC_059_0096	Tetracycline resistance protein-like protein	106152..107504
FORC_059_0290	Multi antimicrobial extrusion protein (Na(+)/drug antiporter), MDR efflux pump MATE family	331000..332355
FORC_059_1646	Multidrug resistance protein B	complement (1786605..1787786)
FORC_059_1994	Multidrug resistance protein B	complement (2151639..2152982)
FORC_059_2173	Multidrug resistance protein	complement (2313867..2314514)
FORC_059_2272	Chloramphenicol resistance protein	complement (2422883..2424067)

FORC_059_2281	Antibiotic resistance protein	complement (2431719..2432912)
β-lactam resistant genes		
FORC_059_1634	Metallo-β-lactamase family protein	complement (1765776..1766660)
FORC_059_1706	Putative β-lactamase	1837674..1838252
FORC_059_2261	β-lactamase	2409025..2410521
FORC_059_p014	β-lactamase	complement (13955..15754)
FORC_059_p015	β-lactamase class A	15819..16664
Fluoroquinolone resistance		
FORC_059_0662	Quinolone resistance protein norA	724336..725502
Aminoglycoside resistance		
FORC_059_1636	Aminoglycoside phosphotransferase family protein	complement (1767748..1768539)
Macrolide resistance		
FORC_059_2005	Macrolide-efflux protein	complement (2163987..2165024)
Methicillin resistance		
FORC_059_1268	tRNA-dependent lipid II-Gly--Gly/lipid II-GlyGly--Gly ligase/methicillin resistance key factor FemA	1355519..1356781
FORC_059_1269	tRNA-dependent lipid II-GlyGlyGly--Gly/lipid II-GlyGlyGlyGly--Gly ligase/methicillin resistance factor FemB	1356800..1358059

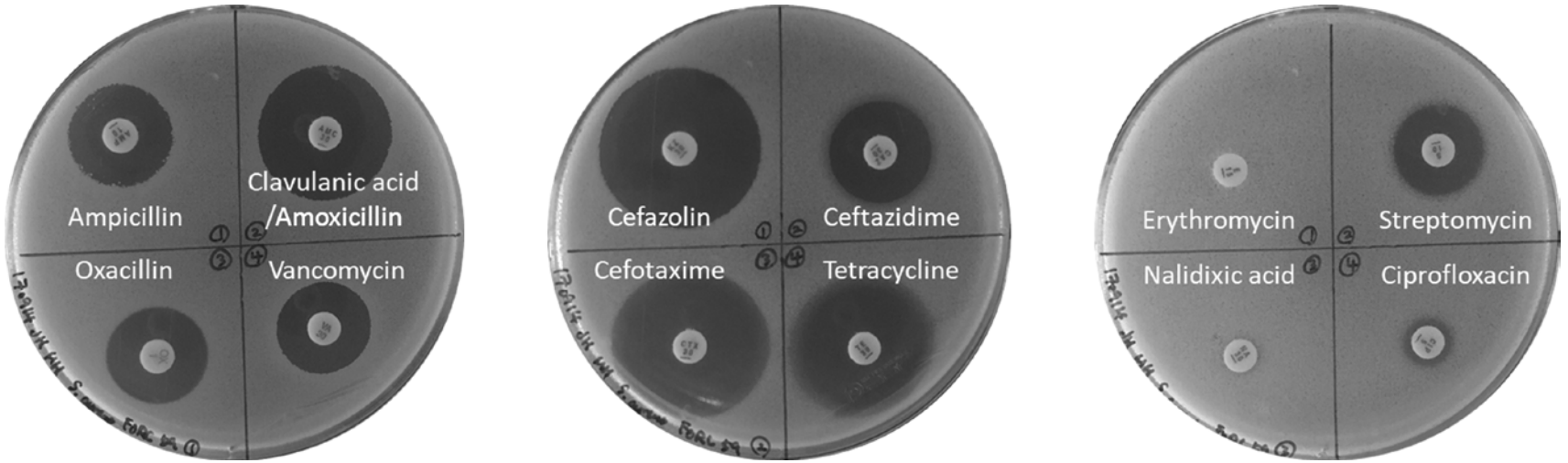

Figure II-3. Antibiotic susceptibility assay of *S. aureus* FORC_059.

Antibiotic susceptibility of *S. aureus* FORC_059 was tested by conducting disc diffusion assay with 12 different antibiotic agents. The diameter of each inhibition zone was measured and the resistance phenotype was determined referring to CLSI antimicrobial susceptibility criteria (Humphries et al., 2018).

Table II-5. Antibiotic susceptibility of *S. aureus* FORC_059.

Antibiotic agent	Disc content	Class	Zone diameter (mm)	Resistance standard (mm)
Ampicillin	10 μg	β-lactam	16	≤ 28
Amoxicillin/clavulanic acid	30 μg	β-lactam	22	≤ 19
Cefotaxime	30 μg	3rd cephalosporin	28	≤ 14
Ceftazidime	30 μg	3rd cephalosporin	18	≤ 14
Cefazolin	30 μg	1st cephalosporin	28	≤ 14
Erythromycin	15 μg	Macrolide	0	≤ 13
Tetracycline	30 μg	Tetracycline	28	≤ 14
Streptomycin	10 μg	Aminoglycoside	15	≤ 12
Nalidixic acid	30 μg	Synthetic quinolone	0	≤ 13
Ciprofloxacin	5 μg	2nd fluoroquinolone	8	≤ 15
Oxacillin	1 μg	Penicillinase-resistant β-lactam	18	≤ 10
Vancomycin	30 μg	Glycopeptide	17	≤ 14

II.3.3. Comparative genome analysis of *S. aureus* FORC_059

The genomic features of *S. aureus* FORC_059 was analyzed in comparison with *S. aureus* FORC_001, a food isolate originating from bean paste related to an outbreak, in Korea (Lim et al., 2015). The chromosome of each strain had 96% of coverage with 99.02% of percent identity. The genomic difference between the food and clinical isolates was elucidated by comparing their complete genome sequence using Artemis comparison tool (ACT) (T. J. Carver et al., 2005) (Figure II-4). Each genome greatly differed at the region between the gene encoding β-hemolysin and the group of genes comprising staphylococcal pathogenicity island (SaPI) and *agr* (accessory gene regulator) operon. Despite a few phage-associated genetic elements predicted on the chromosome, *S. aureus* FORC_059 did not harbor any group of genes to make up a prophage. On the other hand, on the chromosome of *S. aureus* FORC_001, nearly fifty ORFs spanning almost 4.3 kb were predicted to be phage genes, implying the presence of a prophage. Regarding the fact that SaPI is known as a kind of mobile genetic elements, and capable of carrying and disseminating superantigen genes, it could be assumed that virulence genes including toxic shock syndrome toxin-1 (TSST-1) in *S. aureus* FORC_001 may be readily transmitted by prophage induction (Novick, Christie, & Penadés, 2010). For example, the virulence genes within SaPI could be mobilized due to SOS response induced by antibiotic treatments

followed by abort of phage lysogeny, resulting in horizontal gene transfer to other available populations (Maiques et al., 2006). Moreover, due to the absence of prophage on the chromosome of FORC_059 strain, the introduction of genes involved in the virulence or antibiotic resistance could be highly available (Cervera-Alamar et al., 2018).

Considering the high prevalence and the molecular aspects of pathogenic *S. aureus* strains in food-poisoning outbreaks in Korea (Cha et al., 2006), it could be concluded that these pathogens from both environmental and clinical settings are an obvious threat to public health. In addition, the high possibilities of antibiotic-induced horizontal gene transfer among pathogenic bacteria would hamper the efforts to fight against them. Hence, it is evident that development of alternative strategies, other than conventional antibiotics, is very much needed for the biocontrol of pathogenic *S. aureus*.

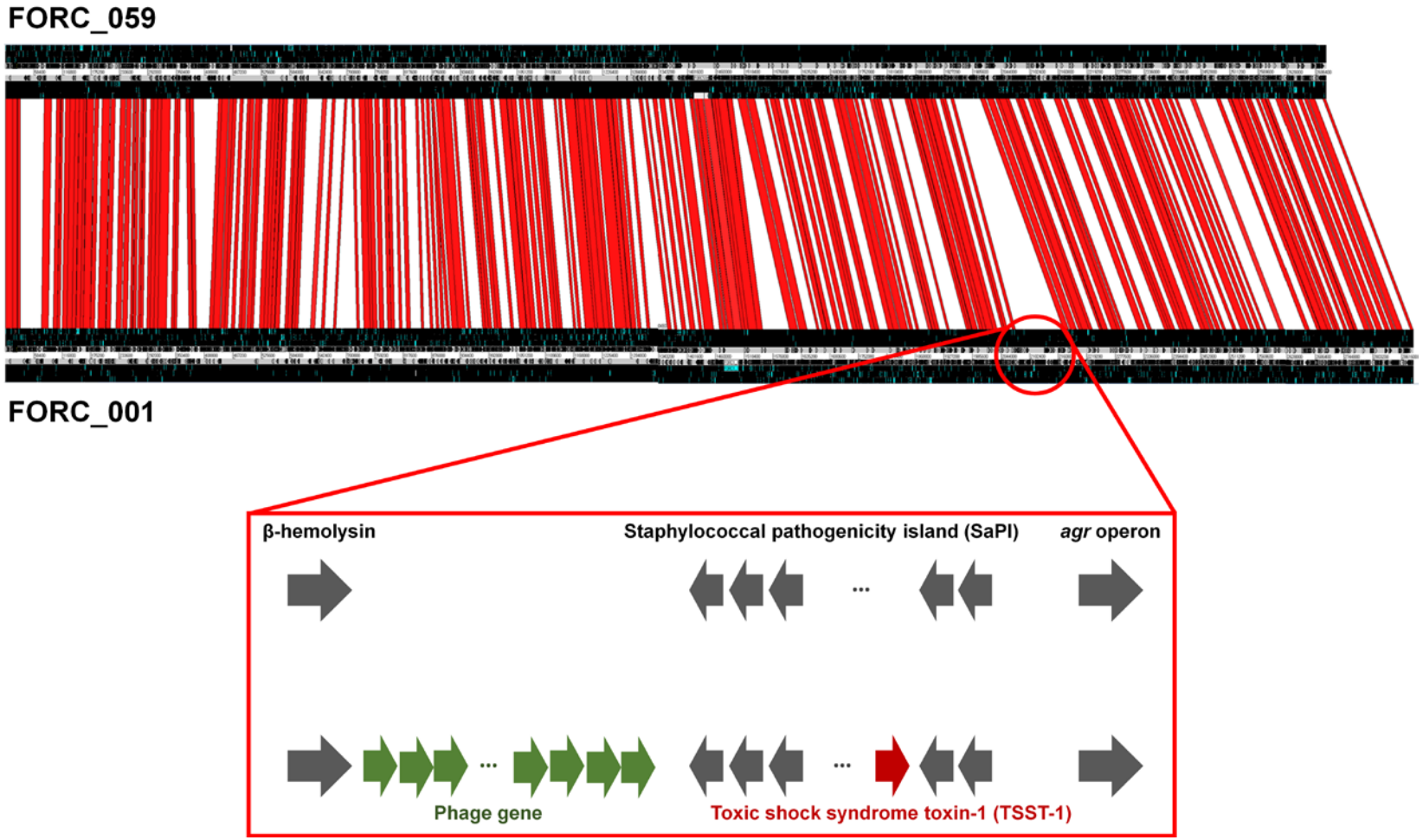
FORC_059
FORC_001
β-hemolysin
Staphylococcal pathogenicity island (SaPI)
agr operon
Phage gene
Toxic shock syndrome toxin-1 (TSST-1)

Figure II-4. Comparative genome analysis of *S. aureus* FORC_059 and FORC_001.

The chromosomes of two completely sequenced *S. aureus* isolates were compared by Artemis comparison tool (ACT). The region of significant difference was highlighted with red circle. The conserved genes were depicted as gray arrows, regarding the location on positive or negative strand. Genes of phage lysogen were represented by green arrows, and toxic shock syndrome toxin-1 was represented by dark red arrow.

Chapter III.

Development of a novel endolysin expression platform by utilizing yeast surface display system

III.1. Introduction

Since the discovery of penicillin, a wide variety of antibiotics have been developed to fight against pathogenic bacteria, and become the most successful and common antibacterial tool (Ventola, 2015). However, some of the pathogens could acquire or build up antibiotic resistance (Julian Davies & Davies, 2010; Ventola, 2015). Eventually, the rapid evolution, transmission, and persistence of resistance have made it much more challenging to control such pathogens (J. Davies, 1994; Levy & Marshall, 2004). However, the introduction of new antibiotics have been dwindled because of various scientific and structural difficulties in discovering new antibiotics (Zorzet, 2014). As a consequence, the demand for alternative antibacterial agents is growing (Wittebole, De Roock, & Opal, 2014). Recently, researches on endolysins, phage-encoded peptidoglycan hydrolases employed to lyse the peptidoglycan of the bacterial cell wall, have been actively conducted to develop alternative antibacterial agents (Fernández-Ruiz, Coutinho, & Rodriguez-Valera, 2018; N.-H. Kim et al., 2018; Schmelcher et al., 2012). Peptidoglycan serves an essential role as a building block of the bacterial cell wall, whose disruption results in rapid cell lysis. Due to the indispensable nature of peptidoglycan, it is extremely unlikely for bacteria to develop resistance against endolysins (Vincent A. Fischetti, 2005). Therefore, endolysins have been widely applied to control various Gram-positive

bacteria with high efficiency and specificity (Bai, Yang, Chang, & Ryu, 2019).

To date, production of recombinant proteins has been most frequently studied in prokaryotes, specifically Escherichia coli expression system (Rosano & Ceccarelli, 2014) due to several benefits: i) fast growth kinetics, ii) ease of obtaining high cell density culture, and iii) ease of transformation with recombinant DNA. Despite the beneficial aspects, some of its biological properties could be hurdles for further applications of endolysins. The presence of lipopolysaccharide (LPS) in *E. coli* host is detrimental for recombinant proteins produced for therapeutic purposes (Petsch & Anspach, 2000). Due to its high toxicity, recombinant therapeutic proteins have to be purified to become endotoxin-free. In addition, protein production itself can be problematic in *E. coli* system (Rosano & Ceccarelli, 2014). Accumulation of recombinant protein in the cytoplasm may lead to increased instability and formation of inclusion bodies (IBs) (Carrió & Villaverde, 2002). Even if the final product is in a soluble form, the polypeptide contents may lack proper activity due to improper folding (Martínez-Alonso et al., 2008). Finally, successfully produced soluble and active proteins have to undergo complicated and labor-intensive processes to be prepared in a purified and concentrated form.

Being the most well-established eukaryotic expression host with broad utility, yeast (*S. cerevisiae*) can offer solutions to aforementioned issues. Among several eukaryotic host systems, yeast could excel others by

combining the advantages of unicellular organisms with the capability of eukaryotes to carry out protein processing (protein folding, assembly, and post-translational modifications) (Porro et al., 2005). Moreover, the eukaryotic nature allows quality control of polypeptides in cellular organelles, preventing the production of misfolded polypeptides (C. L. Young & Robinson, 2014). Recently, it was reported that yeast *S. cerevisiae* could intracellularly express and utilize a prokaryotic protein called encapsulin (Humphries et al., 2018).

Among several yeast expression systems, yeast surface display (YSD) system has been widely utilized as a platform for recombinant protein production and engineering in various ways (Mattanovich et al., 2012). Originally, YSD was designed to facilitate antibody engineering, especially for the screening and sorting of antibodies with enhanced binding affinity or augmented specificity (Boder & Wittrup, 1997; Gai & Wittrup, 2007). Recently, YSD system has been widely utilized for the engineering and construction of whole-cell biocatalyst for several purposes, including advancements in protein stability, biomass turnover, or bioadsorption (Gai & Wittrup, 2007; Kuroda & Ueda, 2013; Shusta et al., 1999). Specifically, it has been reported that immobilization of a metabolic enzyme by YSD could greatly improve protein stability and reusability (Parthasarathy et al., 2005).

In the YSD system, recombinant proteins are expressed and extracellularly displayed by anchor proteins. Among several anchors, a-

agglutinin mating protein subunits, Aga1p and Aga2p, can be employed in *Saccharomyces cerevisiae* host (Cherf & Cochran, 2015). Regarding the activity domain, protein of interest can be fused to the N- or C- terminus of Aga2p, which forms two disulfide bonds with β 1,6-glucan-anchored Aga1p subunit embedded in the cell wall, and surface-displayed upon expression. Subsequently, displayed proteins can be detected by incorporated epitope tags, and examined for the activity. Throughout the procedures, properly folded products are secreted and displayed, hence protein aggregation due to excessive accumulation in the cytoplasm is less likely to occur. Most importantly, the immobilization of active protein on the cell surface makes it unnecessary to further purify and concentrate proteins for further applications.

Therefore, we hypothesized that, by adopting the YSD system, a catalytically active and stable endolysin could be obtained without further purification steps and be readily utilized in its cell-bound state. In the current research, we developed a novel endolysin expression platform using YSD technique, and the potential applicability of this platform as a novel antibacterial agent was evaluated. For this, endolysin LysSA11, which is isolated from a staphylococcal phage SA11, was selected and displayed on the surface of *S. cerevisiae* EBY100 strain (Chang et al., 2017). The expression pattern of endolysin LysSA11 was examined in regards to the induction period, and the efficiency of the protein display was assessed. Eventually, antibacterial activity and stability of yeast-displayed LysSA11

were compared with those properties of LysSA11 purified from *E. coli* expression system. This is the first study demonstrating an application of the YSD platform for endolysin expression. Our findings suggest that YSD can be exploited as a promising methodology for endolysin expression and further contribute to its applications as an alternative to antibiotics.

III.2. Materials and Methods

III.2.1. Strains, culture media, and growth conditions

Escherichia coli DH5α, BL21* (DE3), and Stellar™ (*E. coli HST08 strain, F-, endA1, supE44, thi-1, recA1, relA1, gyrA96, phoA, Φ80d lacZΔ M15, Δ (lacZYA –argF) U169, Δ (mrr –hsdRMS –mcrBC), ΔmcrA, λ-*, TaKaRa) strains were cultivated in Luria-Bertani (LB) broth/agar (BD Difco) with aeration at 37℃, 220 rpm/static. *Staphylococcus aureus* ATCC 13301 and FORC_059 (Accession number: CP020354) strains were cultivated in tryptic soy broth/agar (TSB/TSA) (BD Difco) or Baird-Parker agar (BD Difco) with aeration at 37℃, 220 rpm/static. *Saccharomyces cerevisiae* EBY100 strain (*S. cerevisiae* Meyen ex E.C. Hansen, ATCC® MYA-4941™, MATa, *AGA1::GAL1-AGA1::URA3 ura3-52 trp1 leu2-δ200 his3-δ200 pep4::HIS3 prbd1.6R can1 GAL*) was purchased from American Type Culture Collection (ATCC), and cultivated in yeast peptone dextrose (YPD) broth/agar (BD Difco) or synthetic media (SDCAA/SGCAA) with aeration at 30℃, 250 rpm/static. The composition of each synthetic media is as follows: SDCAA, 0.67% yeast nitrogen base (BD Difco), 0.5% casamino acid (BD Difco), 2% D-glucose, 100 mM sodium phosphate buffer pH 6.4; SGCAA, D-glucose substituted with D-galactose; agar plates, 1 M sorbitol included.

III.2.2. Cloning, expression, and purification of LysSA11 with

variant His-tag orientations

To determine the optimal orientation of protein tags and LysSA11 endolysin, the coding sequence of LysSA11 (*SA11_sp172*) was amplified using the oligonucleotides listed in Table III-1. The PCR product was cloned into pET28a for the expression of N-His or N,C-His fusion protein and pET29b for C-His fusion protein. Each vector was introduced to competent *E. coli* DH5 α and BL21* (DE3) strains by heat shock transformation for plasmid replication and protein expression, respectively. *E. coli* BL21* (DE3) with pET28a-LysSA11 (N-His/N,C-His) or pET29b-LysSA11 (C-His) were cultivated in LB broth/agar (BD Difco) supplemented with 50 μg/mL kanamycin. Single colonies formed on agar plate were inoculated in 3 mL of LB/Km broth for 12 h at 37℃, 220 rpm. The overnight cultures were sub-inoculated in 100 mL of LB/Km broth (initial OD_{600} = 0.1) for 2 h at 37℃, 220 rpm until early exponential phase (OD_{600} = 0.6 ~ 0.8). Subsequently, the cultures were induced with 0.5 mM isopropyl β-D-1-thiogalactopyranoside (IPTG) for 20 h at 18℃, 180 rpm. Afterwards, induced *E. coli* culture was pelleted and re-suspended in lysis buffer (100 mM sodium phosphate, 200 mM sodium chloride, pH 8.0) and disrupted by sonication at a duty cycle of 20% amplitude with 10 sec pulse, for 20 min (Vibra cell 500 Watt ultrasonic processor, Sonics & Materials, INC). Cell lysates were centrifuged at 20,000 × *g* for 30 min at 4℃, and the supernatant including the soluble fraction of the total protein was purified by Ni-NTA Superflow (QIAGEN) according to

the manufacturer's instructions. Eventually, the buffer was changed to storage buffer (100 mM sodium phosphate, 200 mM sodium chloride, 30% glycerol, pH 8.0) using PD Miditrap G-25 (GE healthcare), and the purified protein was concentrated by Amicon® Ultra-4 10K (Merck Millipore) and stored at -80℃ for further experiments.

III.2.3. Lytic activity test of purified LysSA11

Each His-tagged LysSA11 prepared in storage buffer (100 mM phosphate, 200 mM NaCl, 30% glycerol, pH 8.0) was diluted to 0.5 μM. Overnight culture of *S. aureus* ATCC 13301 was sub-inoculated in tryptic soy broth (BD Difco) for 2 h at 37℃, 220 rpm until mid-exponential phase (1×10^8 CFU/mL). For lysis assay, 100 μL of *S. aureus* ATCC 13301 inoculum in 5 mL of 0.4% TSB soft agar was overlaid on tryptic soy agar plate, and 10 μL of each His-tagged LysSA11 sample was spotted, followed by overnight incubation at 37℃, static.

III.2.4. Recombinant yeast construction for surface display of LysSA11

In order to have LysSA11 be surface displayed by C-terminal anchor protein, an *E. coli - S. cerevisiae* shuttle vector was constructed using plasmid pYD5. LysSA11 insert sequence was PCR amplified with oligonucleotides listed in Table III-1. Initially, the linearized vector and LysSA11 insert were

assembled and introduced to Stellar™ competent cells (*E. coli HST08 strain, F-, endA1, supE44, thi-1, recA1, relA1, gyrA96, phoA, Φ80d lacZΔ M15, Δ (lacZYA –argF) U169, Δ (mrr –hsdRMS –mcrBC), ΔmcrA, λ-*, TaKaRa) by homologous recombination, mediated by In-Fusion® HD Cloning Kit (TaKaRa Bio USA, Inc.). As a negative control, pYD5 without any insert sequence was transformed into the *E. coli* host. Recombinant *E. coli* strains were selected on LB agar with 50 μg/mL carbenicillin and single colonies were verified by PCR and nucleotide sequencing. Confirmed plasmids were then transformed to competent *Saccharomyces cerevisiae* EBY100 cells by S. c. EasyComp™ Transformation Kit (Invitrogen™) according to manufacturer's instructions. Recombinant yeast strains carrying pYD5 or pYD5-LysSA11 shuttle vectors were selected on SDCAA agar containing 25 μg/mL kanamycin. Yeast single colonies were treated with Zymolyase™ (Zymo Research Corp.) and verified by PCR and nucleotide sequencing.

III.2.5. Expression of yeast-displayed LysSA11

S. cerevisiae EBY100 carrying pYD5 or pYD5-LysSA11 were streaked on SDCAA agar (synthetic media, tryptophan auxotrophic, 2% D-glucose, 1 M sorbitol, pH 6.40, 25 μg/mL kanamycin) and incubated at 30℃ for 3 days. Single colonies were inoculated in 5 mL of SDCAA media for 24 h (final OD_{600} = 7.0 ~ 8.0) at 30℃, 250 rpm. At primary passage, each inoculum was sub-cultured in 20 mL of SDCAA (initial OD_{600} = 1.0) for 10

h (final OD_{600} = 7.0 ~ 8.0), followed by secondary passage in 50 mL of SDCAA (initial OD_{600} = 1.0) for 12 h (final OD_{600} = 8.0). At each passage, SDCAA media was supplemented with 25 μg/mL of kanamycin. Prior to induction, each yeast culture was centrifuged at 6,000 × *g* for 5 min at 25℃ and washed for twice with 15 mL of Dulbecco's phosphate buffered saline (Sigma-Aldrich) to remove extracellular glucose. Washed cell pellets were re-suspended in 50 mL of SGCAA (synthetic media, tryptophan auxotrophic, 2% D-galactose, pH 6.75, 25 μg/mL kanamycin) to an initial OD_{600} = 1.0 and cultivated for up to 40 h at 30℃, 250 rpm (Chao et al., 2006). The overall procedure is represented in Figure III-1.

III.2.6. Analyzing physiological properties of recombinant yeast during LysSA11 expression

The patterns of growth and galactose consumption were analyzed during LysSA11 expression. Three replicate batches of LysSA11 expressing yeast (EBY100 pYD5-LysSA11) and a negative control group (EBY100 pYD5) in SGCAA media were prepared. For the growth curve, cultures were sampled every 2 h and the OD_{600} value was measured by spectrophotometer (Amersham Biosciences). Galactose utilization behavior was analyzed by measuring residual galactose of yeast cultures in every 4 h with Galactose assay kit (ab83382, abcam®). According to the manufacturer's protocol, fluorometric assay of yeast cultures was conducted in 96-well black plate with

clear bottom (BD Falcon) by SpectraMax® i3x plate reader (Molecular Devices). The excitation wavelength and emission wavelength were 535 nm and 587 nm, respectively, and the resulting data set was generated by SoftMax Pro 7.0 software (Molecular Devices). Taken together, the behavior of recombinant yeast strains in SGCAA media was visualized by GraphPad Prism 5.01 software (GraphPad Software).

III.2.7. Immunoblot assay of LysSA11-Aga2p fusion protein

One milliliter of yeast cultures grown in glucose or galactose media were harvested at early- (OD_{600} = 6) and late-exponential phase (OD_{600} = 13). Each yeast culture was centrifuged at 15,000 × *g* for 3 min at 4℃, and the supernatant and pellets were separated. Each pellet was re-suspended in 50 μL of Y-PER ™ Yeast Protein Extraction Reagent (Thermo Scientific™) and mixed vigorously by Multi Mixer (MyLab #SLRM-3, SeouLin Bioscience) at 25℃, mode 15, 80 rpm, for 20 min. The resulting cell lysates were centrifuged at 15,000 × *g* for 3 min at 4℃, and the supernatant including the soluble fraction of total protein was collected. Subsequently, the protein concentration of each supernatant was measured by Bradford assay. From each supernatant, 40 μg of soluble protein was diluted with distilled water and mixed with Laemmli Sample buffer (4×) (GenDepot) to a final concentration of 1 μg/μL, and heat-denatured at 95℃ for 10 min. Ten microliter of each protein sample (10 μg) was loaded to 12% polyacrylamide gels for size

discrimination by SDS-PAGE (Bio-Rad) with constant voltage setting at 80 V for stacking and 160 V for separating. Resulting protein bands were further transferred onto a nitrocellulose membrane by Trans-Blot® Turbo™ Transfer System (Bio-Rad) with StandardSD setting (25 V, 1.0 A, 30 min). V5 tag Monoclonal Antibody (R960-25, Invitrogen™) was used for the detection of LysSA11-Aga2p complex. For positive control, Anti-PGK1 antibody 22C5D8 (ab113687, abcam®) was used. The blot was blocked with 5% bovine serum albumin fraction V in TBST (10 mM Tris-HCl, 150 mM NaCl, 0.05% Tween-20) at 25℃ for 1 h, and subsequently labeled with 10 mL of 1:5,000 anti-V5 or 1:10,000 anti-PGK1 antibody in BSA-TBST at 4℃ for overnight. Later on, it was labeled with 10 mL of 1:5,000 goat-anti-mouse-IgG-(H+L)-HRP antibody (GenDepot) at 25℃ for 1 h. After each labeling process, excess antibodies were washed out with 10 mL of TBST for 3 times by rocking for 5 min. Labeled endolysin samples were detected by ECL™ Prime Western Blotting System (GE Healthcare), using ChemiDoc™ Imaging System (Bio-Rad).

III.2.8. Glycosylation analysis of LysSA11-Aga2p fusion protein

Yeast cultures were harvested at late-exponential phase (OD_{600} = 13), and the protein samples were prepared to a final concentration of 1 μg/μL as mentioned above. For deglycosylation, 50 μg of soluble protein from each cell lysate was treated with PNGaseF (Promega). Fifty microgram of the

soluble protein was prepared in 0.5 M sodium phosphate buffer (pH 7.5) to a final volume of 12 μL, to which 1 μL each of 5% SDS and 1 M DL-dithiothreitol (DTT) was added. The sample mixture was heat-denatured at 95 for 5 min, and cooled at 25℃ for another 5 min. Then, 2 μL each of 0.5 M sodium phosphate buffer (pH 7.5), 10% Triton® X-100, and recombinant PNGaseF were added, and the mixture was incubated at 37℃ for 3 h. After deglycosylation, the sample was diluted with distilled water and then mixed with Laemmli Sample buffer (4×) (GenDepot) to a final concentration of 1 μg/μL, and heat-denatured at 95℃ for 10 min. Additionally, supernatant of yeast cultures was collected after centrifugation, and 30 μL of each supernatant was mixed with 10 μL of Laemmli Sample buffer (4×) (GenDepot), and heat-denatured at 95℃ for 10 min. As a control, fetuin (Promega), an N- and O-linked glycoprotein, was prepared in the same procedure to yield both glycosylated and deglycosylated samples. Ten microliter of each sample (10 μg) was loaded to 12% polyacrylamide gel for size discrimination by SDS-PAGE with the same settings mentioned above. Resulting protein gels were stained with coomassie blue staining solution at 25℃ for 10 min, and washed with destaining solution at 25℃ for overnight, and finally imaged with Gel Doc™ EZ imager (Bio-Rad). Additionally, western blot assay was performed with the protein gels by following the same procedures mentioned above.

III.2.9. Flow cytometry (FACS) analysis recombinant yeast

Yeast cultures with or without surface-displayed LysSA11 were analyzed by flow cytometry. At each time point, 1×10^7 yeast cells were collected and fixed by washing for twice with ice-cold PBSA (0.5% BSA, 2 mM EDTA in PBS). Fixed cells were labeled with primary antibody, V5 tag Monoclonal Antibody (R960-25, Invitrogen™), for 1 h at 25℃, washed with ice-cold PBSA for twice, and finally labeled with secondary antibody, Goat anti-Mouse IgG2a Fc γ Cross-adsorbed Secondary Antibody, APC (31634, Invitrogen™) for 1 h at 4℃ in the dark. Four different types of samples were prepared; unlabeled cells, cells labeled with either primary or secondary antibodies, and cells labeled with both antibodies. Each sample was analyzed by Navios flow cytometer (Beckman Coulter), and the resulting data was further analyzed with Kaluza flow cytometry analysis v1.2 (Beckman Coulter). Each dataset was gated according to FSC (forward scatter, indicating cell size) and SSC (side scatter, indicating granularity) values, and the fluorescence intensity data of each yeast cell within a given population was plotted in a graph.

III.2.10. Antibacterial activity analysis of yeast-displayed LysSA11

The activity of LysSA11 displayed on yeast surface was examined by combining yeast cells and *S. aureus* cells in reaction buffer (100 mM

phosphate, 200 mM NaCl, pH 7.4 or pH 4.54). After induction, (3.62 ± 0.51) × 10^8 yeast cells (OD_{600} = 200) carrying pYD5-LysSA11 or pYD5 were harvested at early- (OD_{600} = 6), mid- (OD_{600} = 9), or late-exponential (OD_{600} = 13) phase, and centrifuged at 6,000 × *g* for 5 min at 25℃. Yeast pellets were washed for once with 15 mL of reaction buffer and centrifuged again, which were re-suspended with 900 μL of the buffer in 1.75 mL microcentrifuge tube. Meanwhile, 1 mL of *S. aureus* cells in early exponential stage (at OD_{600} = 1.0, 1.15 × 10^8 CFU/mL for *S. aureus* ATCC 13301 and 2.20 × 10^8 CFU/mL for *S. aureus* FORC_059) were collected and washed with 1 mL of the buffer for three times. Washed *S. aureus* cells were serially diluted (10^{-2}), and 100 μL of diluted cells (10^6 CFU/mL) were combined with prepared yeast cells. The final concentration of *S. aureus* in the mixture was 10^5 CFU/mL. As a negative control, *S. aureus*-only samples (10^5 CFU/mL) were prepared in the buffer. All of the reaction samples were triplicated. Yeast and *S. aureus* cells were mixed by Multi Mixer (MyLab #SLRM-3, SeouLin Bioscience) at 25℃, channel F1, 20 rpm. For every 1 h, 50 μL of the mixture was collected and serially diluted (10^{-2}), and 100 μL of the serially diluted samples (10^{-1} and 10^{-2}) were spread on Baird-Parker agar plate and incubated for overnight at 37℃. The resulting colonies of *S. aureus* were enumerated with a detection limit of 2-log CFU.

III.2.11. Stability analysis of yeast-displayed and purified

LysSA11 in storage condition

Protein stability of both surface-displayed and purified LysSA11 was compared by analyzing the antibacterial activity against *S. aureus* after storage at 4℃. Triplicates of LysSA11-displaying yeast cells harvested from late-exponential phase (OD_{600} = 13) were prepared in the reaction buffer (100 mM phosphate, 200 mM NaCl, pH 7.4) in a final volume of 900 μL. Also, triplicates of LysSA11 (C-His) purified from *E. coli* was prepared in the reaction buffer in a final concentration of 2.5 μM. The samples were stored at 4℃ for 0, 7, and 14 days, while samples from 0^{th} day were shortly stored for 1 h prior to the encounter with *S. aureus* cells. *S. aureus* cultures were harvested at early exponential phase and prepared in the buffer in a final concentration of 10^6 CFU/mL, from which 100 μL were combined with stored LysSA11 samples. Yeast and *S. aureus* cells were mixed by Multi Mixer (MyLab #SLRM-3, SeouLin Bioscience) at 25℃, channel F1, 20 rpm. For every 30 min, 100 μL of the original or serially diluted samples (10^{-1} and 10^{-2}) were spread on Baird-Parker agar plate and incubated for overnight at 37℃. The resulting colonies of *S. aureus* were enumerated with a detection limit of 1-log CFU.

III.2.12 Antibacterial activity analysis of surface-displayed LysSA11 in cryo-lysed yeast

Activity of surface-displayed LysSA11 in dead yeast cells was

analyzed by cryo-lysis. Late-exponentially cultivated yeast cells (induced/un-induced) were harvested and frozen in liquid nitrogen (-196℃) and mechanically disrupted by sterilized pestle and mortar. Cryo-lysed yeast powder was collected and re-suspended with buffer (100 mM sodium phosphate, 200 mM sodium chloride, pH 7.31) to a final concentration of (OD_{600} = 200). The viable population of cryo-lysed yeast was decreased by 96.4%, leaving (1.30 ± 0.23) × 10^7 CFU/mL. *S. aureus* cultures were harvested at early exponential phase and prepared in the buffer in a final concentration of 10^6 CFU/mL, from which 100 μL were combined with stored LysSA11 samples. Yeast and *S. aureus* cells were mixed by Multi Mixer (MyLab #SLRM-3, SeouLin Bioscience) at 25℃, channel F1, 20 rpm. For every 30 min, 100 μL of the original or serially diluted samples (10^{-1} and 10^{-2}) were spread on Baird-Parker agar plate and incubated for overnight at 37℃. The resulting colonies of *S. aureus* were enumerated with a detection limit of 1-log CFU.

III.2.13. Statistical analysis

Statistical analysis of lytic activity tests was conducted with GraphPad Prism 5.01 software for Windows (GraphPad Software, San Diego, CA, USA). Each data point was presented as the mean values with standard errors of the *S. aureus* population. For the data in Figure III-8 and III-10, the CFUs of *S. aureus* at each time point were analyzed by one-way analysis of variance

(ANOVA) followed by Tukey's multiple comparison test (95% confidence interval). For the data in Figure III-9., the CFUs of *S. aureus* at each time point between each experimental group were analyzed by two-way analysis of variance (ANOVA) followed by Bonferroni post-tests to compare replicate means of each group to that of pYD5-LysSA11 (induced). A *P*-value smaller than 0.05 was considered statistically significant.

Table III-1. Plasmids and primers used in this chapter.

Plasmids		
Name	**Description**	**Reference**
pET28a	Kan^r, T7 promoter, His-tagged expression vector	Novagen, Wisconsin, SA
pET29b	Kan^r, T7 promoter, His-tagged expression vector	
pET28a-LysSA11 (N-His)	pET28a with LysSA11, N-terminal His-tag	
pET28a-LysSA11 (N,C-His)	pET28a with LysSA11, N and C-terminal His-tags	This study
pET29b-LysSA11 (C-His)	pET29b with LysSA11, C-terminal His-tag	
pYD5	*E. coli – S. cerevisiae* shuttle vector, Amp^r, TRP1, GAL1 promoter, V5-tag, yeast surface display vector for C-terminal anchor	
pYD5-LysSA11	pYD5 with LysSA11	This study
Primers (5'→3')		
Name	**Sequence[a]**	**Reference**
LysSA11_F	AAGGAGTGAAAACATATGAAAGCATCGATG	This study
LysSA11_R_nostop	AAAATTCCCTAGTCTCGAGTTTCCAGTTAATA	This study
LysSA11_R_stop	AAAATTCTCGAGTACATTATTTCCAGTTAATA	This study
pYD5_LysSA11_F	GCTAGCGTTTTAGCAATGAAAGCATCGATGAC	This study
pYD5_LysSA11_R	TAGGCTTACCGAATTCTTTCCAGTTAATACGAC	This study

a Restriction recognition sites are indicated with underlines.

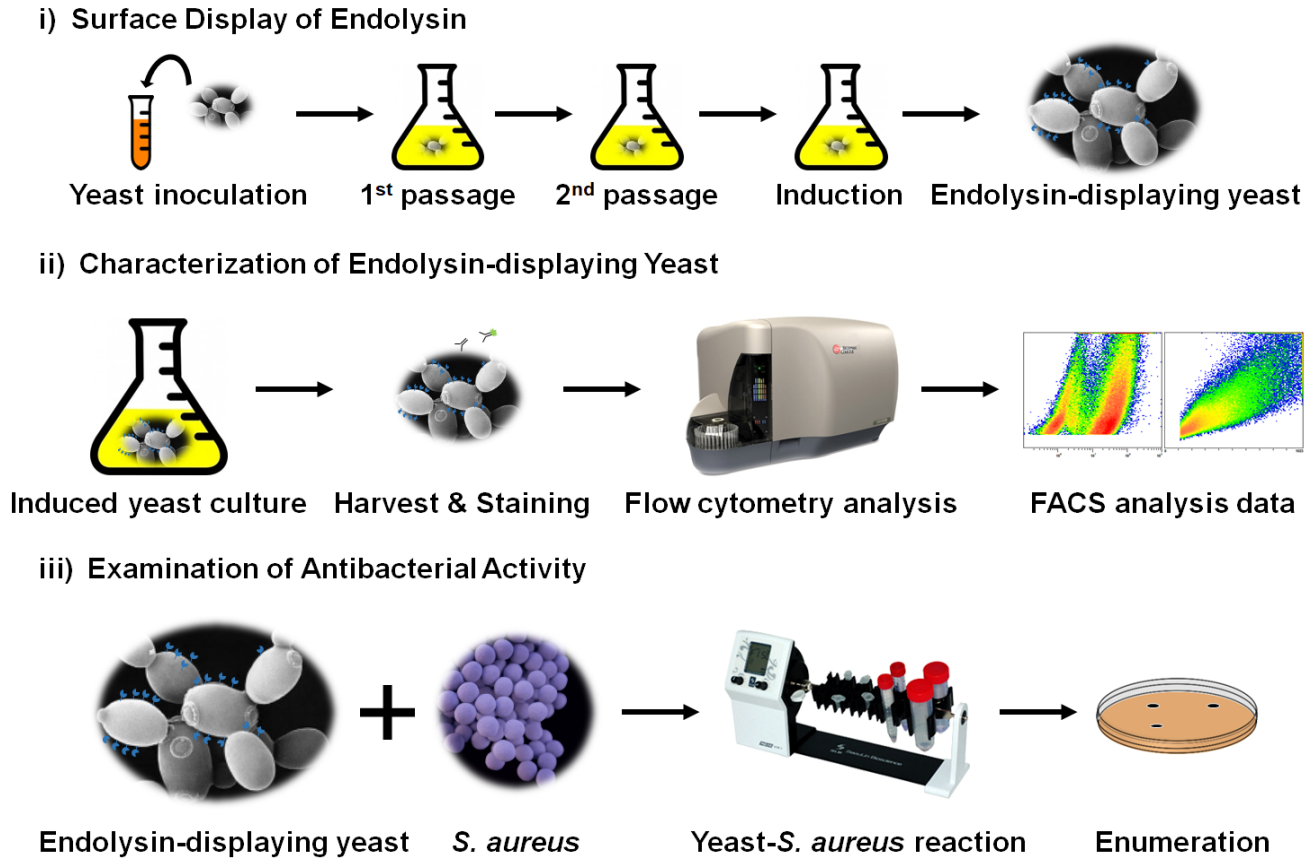

Figure III-1. Overview of YSD-based novel endolysin expression platform.

III.3. Results and Discussion

III.3.1. Determination of optimal orientation for LysSA11 fusion protein

According to a previous study, treatment of purified LysSA11 could efficiently inhibit *Staphylococcus aureus* (Chang et al., 2017). LysSA11 consists of two domains; N-terminal enzymatic activity domain (EAD) and C-terminal cell wall binding domain (CBD) (Chang et al., 2017). In general, the location of tags may affect the tertiary structure and the activity of the fusion protein (Terpe, 2003). In order to determine the optimal orientation for LysSA11 to be fused with Aga2p subunit, three different designs of His_6-tagged LysSA11 endolysin were generated (Figure III-2A). Each His_6-tagged LysSA11 was isolated from *E. coli* host, and the purified proteins migrated to predicted molecular masses in SDS-PAGE analysis (Figure III-2B). Spotting assay of each purified protein against the host strain *S. aureus* ATCC 13301 revealed that LysSA11 carrying C-terminal His_6-tag exhibited the strongest lytic activity (Figure III-2C). In regard to the N-terminal location of CHAP domain, it could be assumed that N-terminal protein conjugation may cause hindrance to the lytic activity of LysSA11.

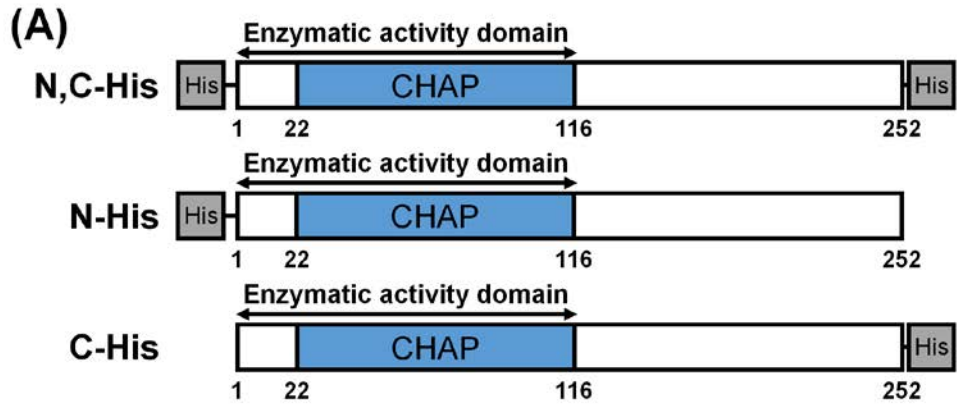
(A)
Enzymatic activity domain
N,C-His
His
CHAP
His
1
22
116
252
Enzymatic activity domain
N-His
His
CHAP
1
22
116
252
Enzymatic activity domain
C-His
CHAP
His
1
22
116
252

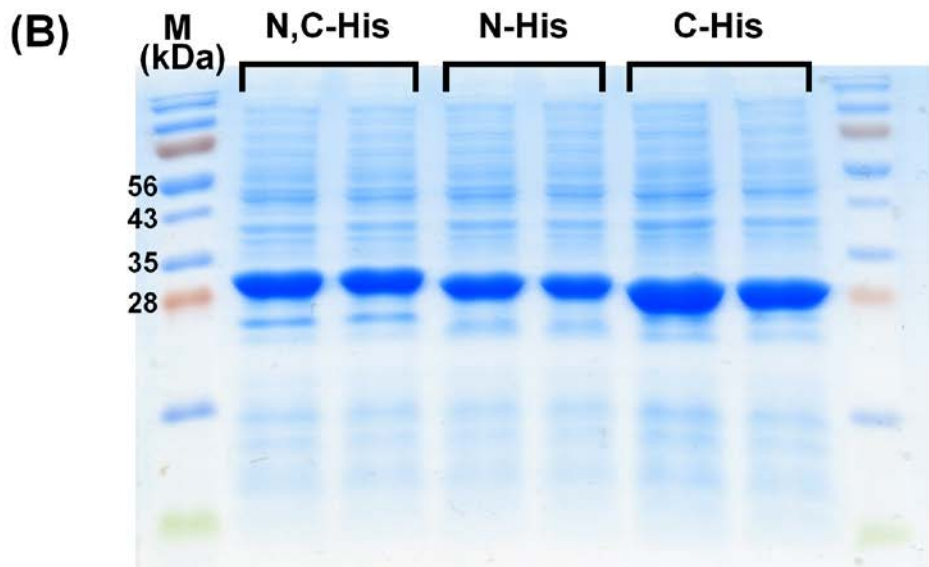
(B)
M
(kDa)
N,C-His
N-His
C-His
56
43
35
28

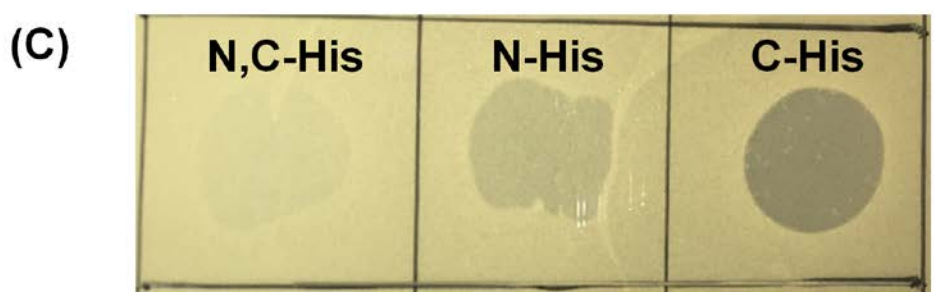
(C)
N,C-His
N-His
C-His

Figure III-2. Evaluation of LysSA11 fusion protein with divergent orientations for optimal bactericidal activity.

(A) Schematic representation of three different constructs of His-tagged LysSA11. (B) Coomassie blue stained bands of each His6-tagged LysSA11 product within soluble fraction of proteins from E. coli host. The expected size of LysSA11-(N,C-His), LysSA11-(N-His), and LysSA11-(C-His) are 31.7 kDa, 30.6 kDa, and 29.9 kDa, respectively. Each sample was duplicated. (C) Spotting assay of each His6-tagged LysSA11 against *S. aureus* ATCC 13301. Each His6-tagged LysSA11 was diluted to 0.5 μM, and 10 μL of each was spotted on the lawn of *S. aureus* ATCC 13301.

III.3.2. Construction of recombinant *S. cerevisiae* strains

Based on the spotting assay data, we constructed a recombinant *E. coli* strain with pYD5 shuttle vector in which LysSA11 coding sequence was introduced between the sequences of signal peptide and mature peptide of Aga2p subunit (Wang, Mathias, Stavrou, & Neville, 2005) (Figure III-3A). At the downstream of LysSA11 sequence, V5 epitope is inserted for the detection of fusion protein in immunoblot assay and flow cytometry analysis (Figure III-3B). Since the mature peptide of Aga2p subunit and V5 epitope are located at the C-terminal region of LysSA11 and the signal peptide of Aga2p subunit is cleaved during secretion, we expected that the polypeptide sequences would have no significant effect on LysSA11 activity. Finally, pYD5 vector expressing LysSA11 (pYD5-LysSA11) was transformed into *S. cerevisiae* EBY100 host for further experiments. Yeast strain containing empty vector (pYD5) was used as a control in growth, galactose consumption, and antibacterial activity assays.

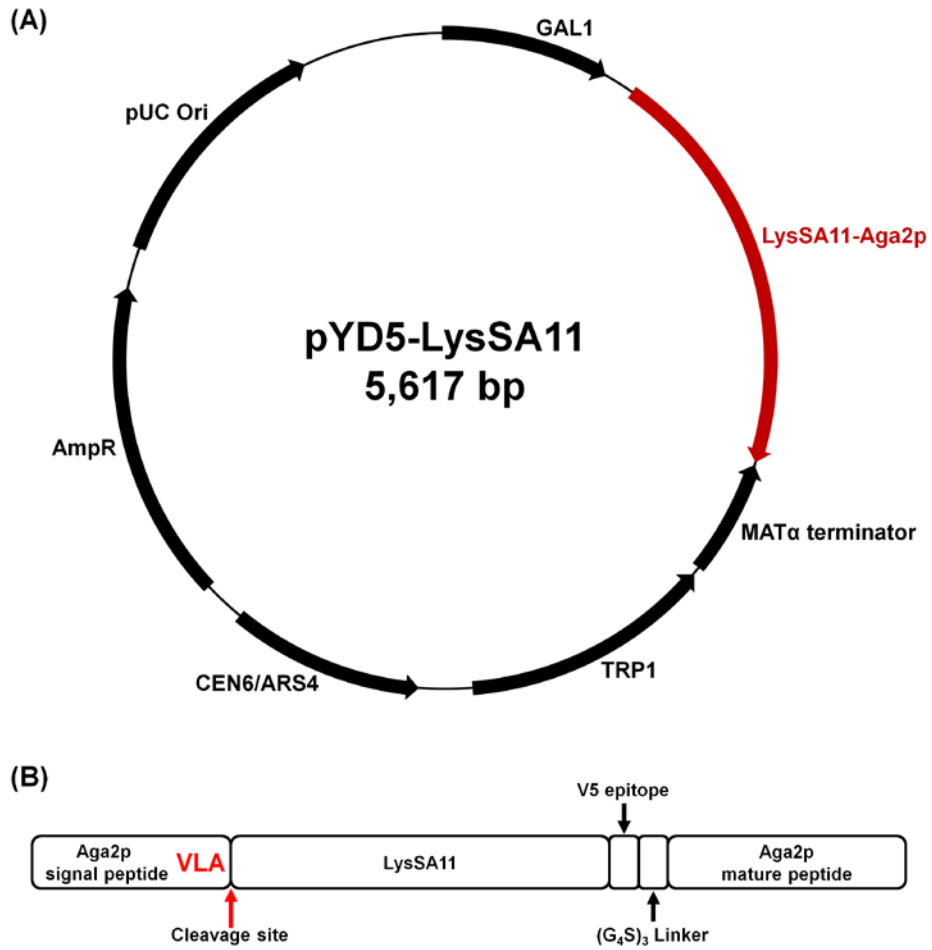

Figure III-3. Schematic diagram of pYD5-LysSA11 shuttle vector and LysSA11-Aga2p fusion protein.

Schematic diagram of (A) pYD5-LysSA11 shuttle vector construct and (B) LysSA11-Aga2p fusion protein. LysSA11 sequence was inserted between Aga2p signal peptide and Aga2p mature peptide. Ampicillin resistant marker (Amp^R) and tryptophan auxotrophic marker (TRP1) are for selection in *E. coli* and *S. cerevisiae*, respectively. Cleavage site of Aga2p signal peptide and the recognition sequence VLA are indicated with red arrow.

III.3.3. Physiological traits of the recombinant yeast during LysSA11 induction

Optimizing the growth and induction conditions for recombinant yeast is one of key determinants of cell-surface display efficiency (Tanaka & Kondo, 2015). In order to optimize the protein expression condition, physiological properties of the recombinant yeast strains, EBY100/pYD5 or EBY100/pYD5-LysSA11, were examined. First of all, the optical density (OD_{600}) of each strain in glucose (SDCAA) media was plotted to investigate the growth pattern (Figure III-4A). Compared to EBY100/pYD5, no significant growth defect was observed from EBY100/pYD5-LysSA11, and both strains were exponentially replicating at 8 h (OD_{600} = 7.68). In order to maximize the proportion of young and viable cells, yeast cultures were harvested at OD_{600} = 7 ~ 8 for induction. In pYD5 vector system, expression of endolysin-anchor protein complex is regulated by GAL1 promoter, which is induced by galactose, and strictly repressed in the presence of glucose (Wang et al., 2005; Weinhandl, Winkler, Glieder, & Camattari, 2014b). Since the recombinant yeast strain is cultivated in synthetic media with glucose (SDCAA) prior to induction in synthetic media with galactose (SGCAA), it would take certain period of time to switch to galactose consumption (van den Brink et al., 2009). The growth in SGCAA media was plotted, and the initial arrest in growth was observed to last for about 12 h (Figure III-4B). As the cells grow, the concentration of galactose in SGCAA will gradually

decrease, hence the inducing effect would not last upon its depletion (Weinhandl et al., 2014b; Whang et al., 2009). Therefore, taken together with the growth curve, the pattern of galactose consumption was observed to determine the optimal expression condition (Figure III-4B). *S. cerevisiae* EBY100/pYD5 and EBY100/pYD5-LysSA11 were separately cultivated in SDCAA for two passages, and equivalent population of each culture in exponential phase (OD_{600} = 7 ~ 8) was washed and transferred to SGCAA (initial optical density, OD_{600} = 1), cultivated for 40 hours until stationary phase. During the first 20 hours, EBY100/pYD5-LysSA11 consumed only 9.00% of the galactose, but soon after, the cells entered early-exponential phase and the galactose consumption was accelerated. Yeast culture reached stationary phase at 34 h post-induction, at which the amount of galactose decreased by over 80%, which eventually got depleted at 40 h (Figure III-4B). The overall growth and galactose consumption pattern were observed similar in the case of the negative control (EBY100/pYD5). The expression and surface display of LysSA11 were analyzed at 24 and 32 h post-induction, which represent early- and late-exponential phase, respectively. The galactose usages at each time were 33.86% and 76.70%, while the OD_{600} values were 6.23 and 13.13, respectively (Figure III-4). Based on the physiological traits during galactose induction, LysSA11-Aga2p fusion protein was expected to be expressed and surface-displayed in a greater extent in the late-exponential phase than the early one.

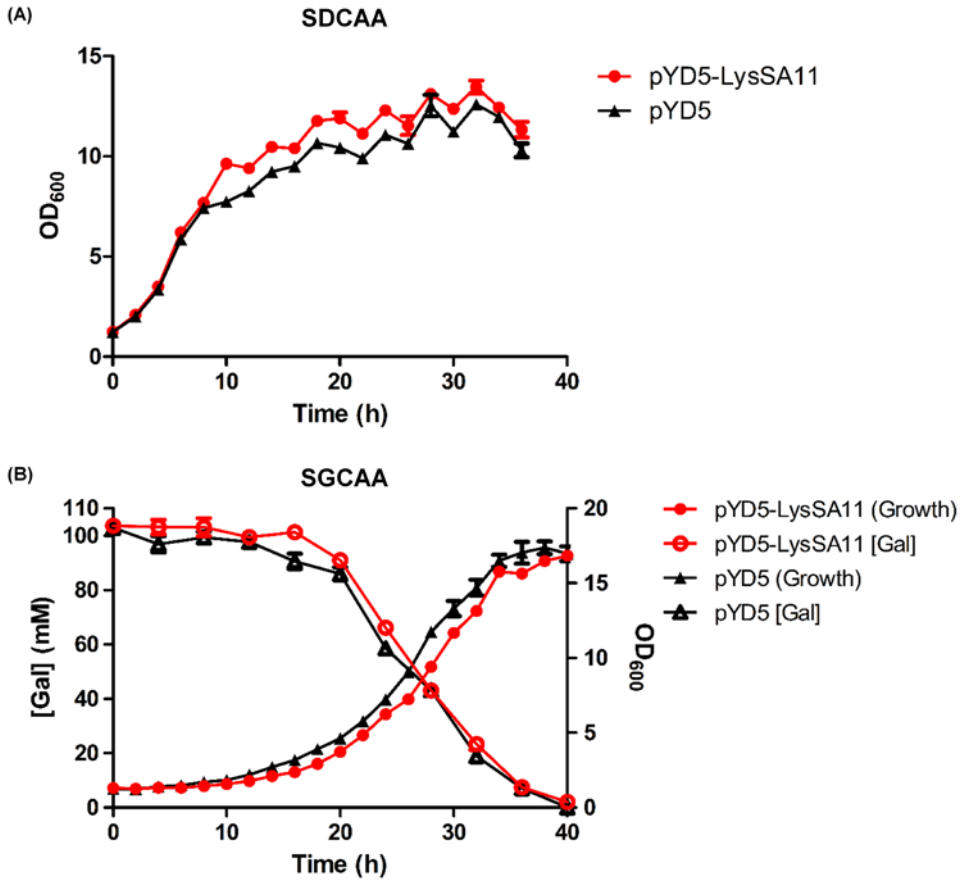

Figure III-4. Physiological behaviors of recombinant *S. cerevisiae* EBY100 strains in glucose and galactose media.

Physiological behavior of each recombinant yeast strain in each culture media was visualized. (A) Growth of *S. cerevisiae* EBY100/pYD5 and EBY100/pYD5-LysSA11 on glucose were plotted. (B) Growth of *S. cerevisiae* EBY100/pYD5 and EBY100/pYD5-LysSA11 on galactose, and their consumption pattern were plotted. Sampling of each culture was conducted every 2 h for culture turbidity and 4 h for galactose content,

respectively. Curves with filled symbols represent growth pattern of recombinant yeast strains. Curves with empty symbols represent galactose consumption pattern of recombinant yeast strains. Each growth curve starts from optical density value (OD_{600}) of 1.0. Initial concentration of galactose in SGCAA media is 100 mM. All experiments were done triplicates.

III.3.4. Expression of LysSA11-Aga2p fusion protein in the recombinant yeast

The intracellular expression of LysSA11-Aga2p fusion protein product was evaluated by immunoblot assay (Figure III-5). As a positive control, phosphoglycerate kinase (PGK1, 45 kDa), one of constitutively expressed proteins, was used (Figure III-5B). In Figure III-5A, it was confirmed that LysSA11-Aga2p fusion protein was well expressed in induced yeast cells harvested at both early- and late-exponential phases. Meanwhile, nothing was detected from the un-induced yeast samples, implying that the expression was tightly inhibited due to catabolite repression (Gancedo, 1998). PGK1 was identified from both induced and un-induced yeast cultures, confirming that all of the cultures were viable.

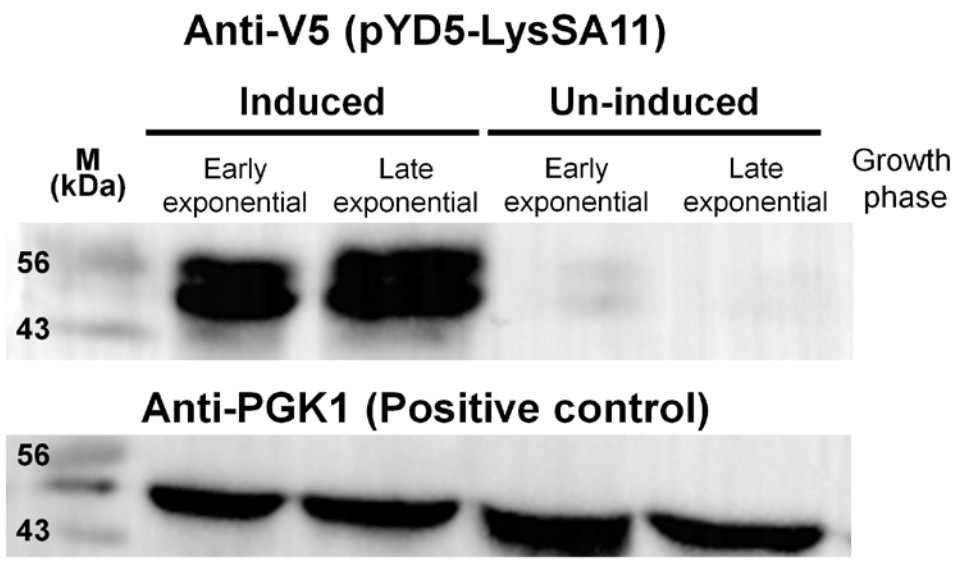

Figure III-5. Expression of LysSA11-Aga2p fusion protein.

Expression of the fusion protein was confirmed by western blot assay. Western blot data of yeast cell lysates labeled with (A) anti-V5 antibody and (B) anti-PGK1 antibody were visualized. Induced or un-induced *S. cerevisiae* EBY100/pYD5-LysSA11 cultures were collected at early- and late-exponential growth phases.

III.3.5. Glycosylation of LysSA11-Aga2p fusion protein

Interestingly, there were protein bands with two different molecular weights detected from induced yeast cells, which are ~50 kDa and 56 kDa (Figure III-5A). In fact, the predicted molecular weight of the fusion protein was 38.9 kDa, which is much smaller than the detected bands. The main reason for the increased molecular weight of the fusion protein is supposed to be glycosylation of the protein product at N or O linkages (Kukuruzinska, Bergh, & Jackson, 1987) and the bands of two different sizes might have been resulting from trimming of oligosaccharide (Shahinian et al., 1998). To investigate whether the fusion protein is glycosylated, protein samples were treated with peptide:N-glycosidase F (PNGase F). Induced and un-induced cultures were harvested at late-exponential phase (OD_{600} = 13), and the soluble proteins from cell lysate were prepared in groups with or without PNGase F treatment. Culture supernatant was also prepared to check if there is any LysSA11-Aga2p fusion protein that have failed to be displayed. As a positive control for PNGase F activity, fetuin was used. Each sample was examined by SDS-PAGE, and visualized by coomassie blue staining and western blotting (Figure III-6). From coomassie blue stained gel (Figure III-6A), size shift of fetuin from 64 kDa to 43 kDa was confirmed, but such difference was not observed between yeast cell lysates. However, in western blot data, glycosylation of LysSA11-Aga2p fusion protein was apparently verified (Figure III-6B). Molecular weight of one of the two bands identified

from untreated cell lysate has changed from 56 kDa to nearly 35 kDa, while that of the other band was conserved as 50 kDa. Since PNGase F can only remove N-glycosidic bonds, the unchanged protein band might have been modified with O-linked glycosylation.

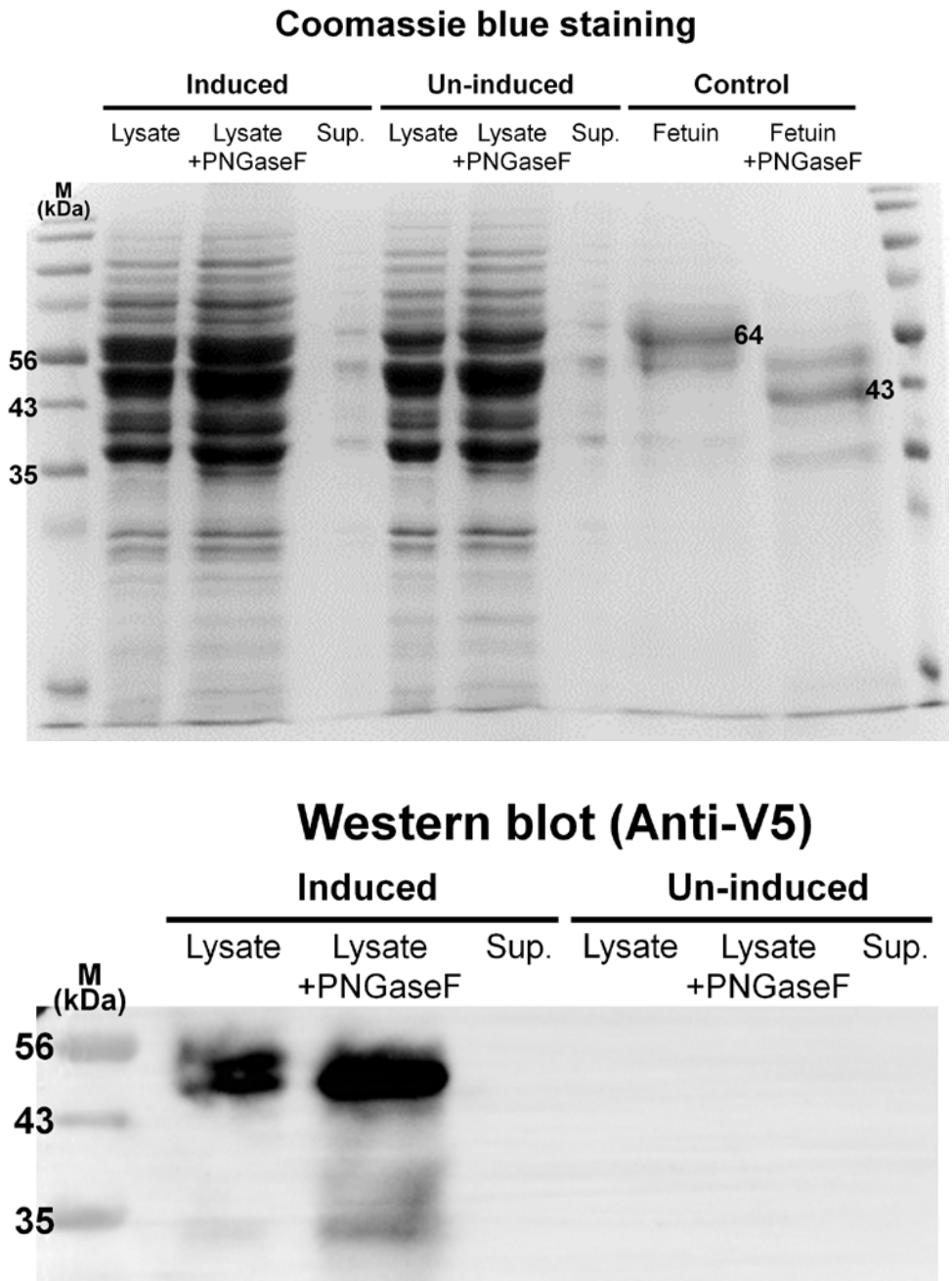

Figure III-6. Glycosylation of LysSA11-Aga2p fusion protein.

N-linked glycosylation of LysSA11-Aga2p fusion protein was examined. Protein samples from induced or un-induced yeast cell lysates and their

culture supernatants were examined by SDS-PAGE. Size separation of each protein band was visualized by (A) coomassie blue staining and (B) western blot assay. The size of deglycosylated fusion protein is indicated with red arrow.

According to the previous studies, glycosylation may affect the production or the activity of heterologous protein (Han & Yu, 2015; Hoshida, Fujita, Cha-aim, & Akada, 2013; Luong, Lam, Chen, & Levitz, 2007). In this study, LysSA11-Aga2p fusion protein from yeast lysate turned out to be obviously glycosylated. Hence, additional examinations were conducted to verify whether the glycosylated fusion protein was successfully displayed and retained bactericidal activity.

III.3.6. Characterization of surface-displayed LysSA11 in the recombinant yeast

Recombinant yeast strains were analyzed by flow cytometry to determine the functionality and efficiency of the fusion protein to be displayed on the surface (Figure III-7). A primary antibody recognizing V5 epitope was used together with a fluorescent secondary antibody to detect and label the fusion protein. In the flow cytometry data, the area below the peaks represents the population of gated cells, and the fluorescence (FL) intensity reflects the amount of fluorescence labels on a single cell, which in this case represents the relative density of surface-displayed LysSA11 (Figure III-7). The proportion of LysSA11-displaying yeast cells in a given population was confirmed to be nearly identical in both early- (Figure III-7A) and late-exponential (Figure III-7B) stages, accounting for 71.13% and 70.21%, respectively. On the other hand, the fluorescent (FL) intensity increased by 13.68% in the late-exponential phase when compared to the early-exponential phase, indicating that the amount of surface-displayed endolysin have increased over time (Figure III-7). Therefore, it was hypothesized that, although the population of LysSA11-displaying cells has slightly decreased, since the overall surface-display efficiency of a single cell was greater, the maximal antibacterial activity could be expected from yeast cultures harvested at late-exponential phase.

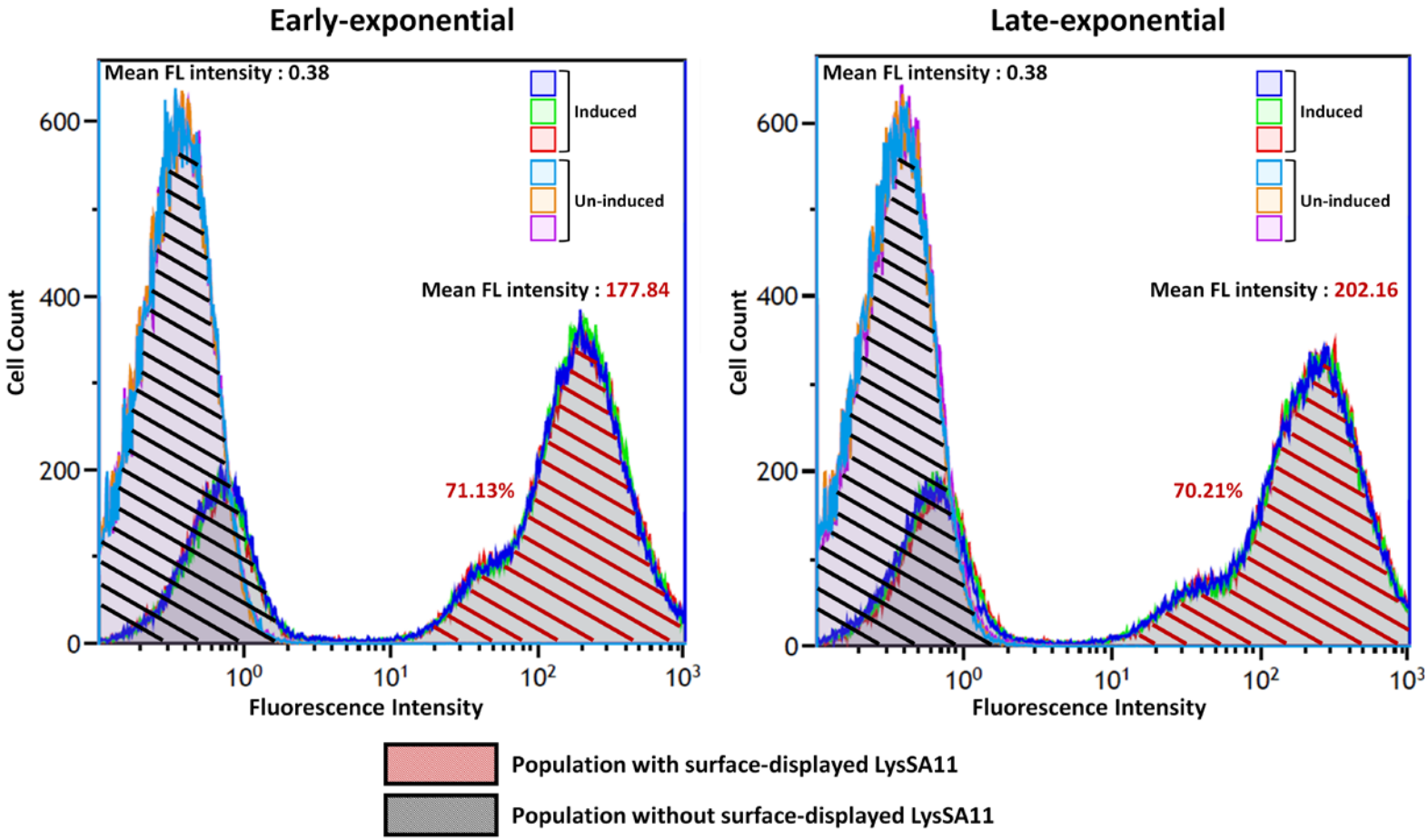
Early-exponential
Mean FL intensity : 0.38
Induced
Un-induced
Mean FL intensity : 177.84
71.13%
Cell Count
Fluorescence Intensity
Late-exponential
Mean FL intensity : 0.38
Induced
Un-induced
Mean FL intensity : 202.16
70.21%
Cell Count
Fluorescence Intensity
Population with surface-displayed LysSA11
Population without surface-displayed LysSA11

Figure III-7. Characteristics of yeast cells with surface-displayed LysSA11.

Flow cytometry (FACS) analysis of induced and un-induced *S. cerevisiae* EBY100 containing pYD5-LysSA11 harvested at (A) early-exponential phase and (B) late-exponential phase, respectively. The proportions of LysSA11-displaying yeast cells in a given population were indicated as %. Mean fluorescent (FL) intensity represents the strength of fluorescence label in each sample, which is the density of surface displayed LysSA11 in induced cells or the autofluorescence of un-induced cells. Flow cytometry analysis was done triplicates.

III.3.7. Antibacterial activity of yeast-displayed LysSA11 against *S. aureus* ATCC 13301

Previous studies revealed that a variety of enzymes such as catalase, cellulose, and amylase were successfully expressed by yeast surface-display with desired functions (Tanaka & Kondo, 2015; K. Zhang, Bhuripanyo, Wang, & Yin, 2015). Regarding the bactericidal function of native LysSA11 against *S. aureus* (Chang et al., 2017), we expected its surface-displayed version would also demonstrate strong antimicrobial activity. The activity of surface-displayed LysSA11 was examined by treating 3 ~ 4 × 10^8 CFU/mL of LysSA11-displaying yeast, which was harvested at early- (OD_{600} = 6), mid- (OD_{600} = 9) or late-exponential (OD_{600} = 13) phase, to 1 × 10^5 CFU/mL of *S. aureus* ATCC 13301 in the reaction buffer (pH 7.4). The yeast from early-exponential stage (OD_{600} = 6) achieved 1.08 log and 2.69 log reduction in bacterial number at 4 h and 6 h, respectively (Figure III-8A). No viable *S. aureus* was detected after treatment for 7 h (Figure III-8A). Yeast cells at mid-exponential phase (OD_{600} = 9) reduced 0.90 log CFU of staphylococcal population at 4 h, which then decreased below detection limit (2-log CFU) at 6 h (Figure III-8B). By treating late-exponentially grown yeast cell (OD_{600} = 13), we could inhibit the pathogen in even faster and more efficient manner (Figure III-8C). The population of viable *S. aureus* diminished by 1.00 log only in 1 h, which dropped below the detection limit after 2 h of treatment. Moreover, the regrowth of *S. aureus* was not observed until 10 h post initial

encounter, curtailing the possibilities of having persistent population. In all the cases, surface-displayed LysSA11 could successfully elicit lytic activity by simply transferring induced yeast cultures to the reaction buffer (pH 7.4). Overall, the population of *S. aureus* ATCC 13301 was reduced by 5-log units, and remained undetected until 10 h (Figure III-8). On the other hand, no significant reduction of *S. aureus* was observed when the bacteria were exposed to yeast cells without LysSA11 (EBY100/pYD5 from SGCAA culture or EBY100/pYD5-LysSA11 from SDCAA culture) or the reaction buffer (Figure III-8, Figure III-9).

Additionally, antibacterial activity of surface-displayed LysSA11 was tested in an acidic environment, since it has been reported that *S. aureus* not only survive but could also grow at pH 4.5 (Valero et al., 2009). Regarding the fact that the pH of many foods can be as low as pH 4.5, it could be assumed that *S. aureus* may also contaminate mildly acidic food products. In the given experimental condition, the surface-displayed LysSA11 turned out to maintain the activity, achieving 5 log reduction within 5 h, exhibiting not much delay during the reaction (Figure III-10). Hence, it could be expected that the immobilization effect contributed to the increased stability of the displayed endolysin at lower pH.

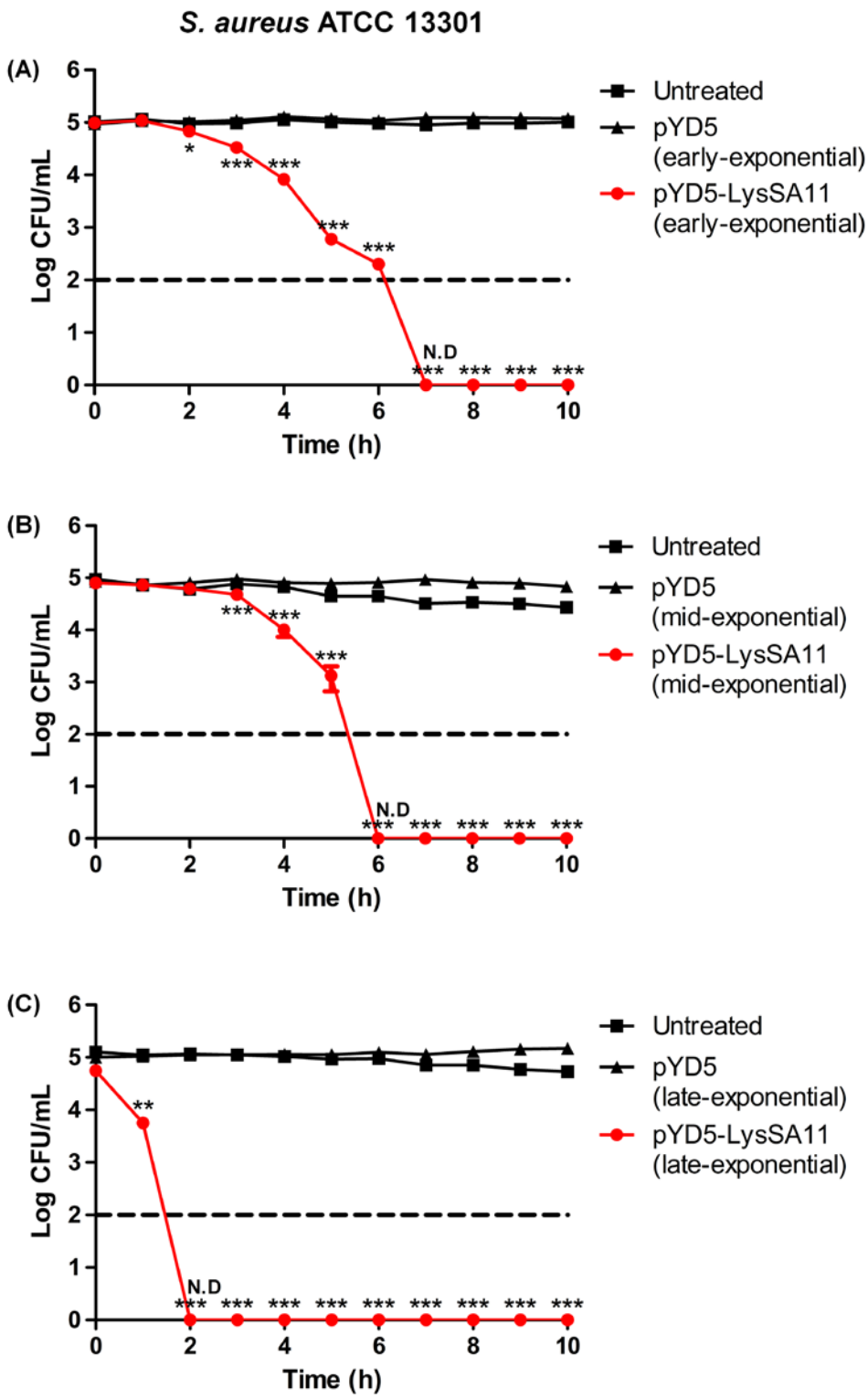
S. aureus ATCC 13301
(A)
Log CFU/mL
Time (h)
Untreated
pYD5
(early-exponential)
pYD5-LysSA11
(early-exponential)
N.D
(B)
Log CFU/mL
Time (h)
Untreated
pYD5
(mid-exponential)
pYD5-LysSA11
(mid-exponential)
N.D
(C)
Log CFU/mL
Time (h)
Untreated
pYD5
(late-exponential)
pYD5-LysSA11
(late-exponential)
N.D

Figure III-8. Antibacterial activity of yeast-displayed LysSA11 from different growth stages against *S. aureus* ATCC 13301.

Antibacterial activity of yeast-displayed LysSA11 from yeast harvested at (A) early-exponential stage, (B) mid-exponential stage, and (C) late-exponential stage were analyzed against *S. aureus* ATCC 13301. The untreated group of *S. aureus* cells were exposed to the reaction buffer. Yeast strain (EBY100/pYD5) cultivated in SGCAA was used as a control. Dashed lines denote the limit of detection (N.D, not detected). Asterisks indicate the significance of variances (***, $P < 0.0001$; **, $P < 0.001$; *, $P < 0.05$). All experiments were done triplicates.

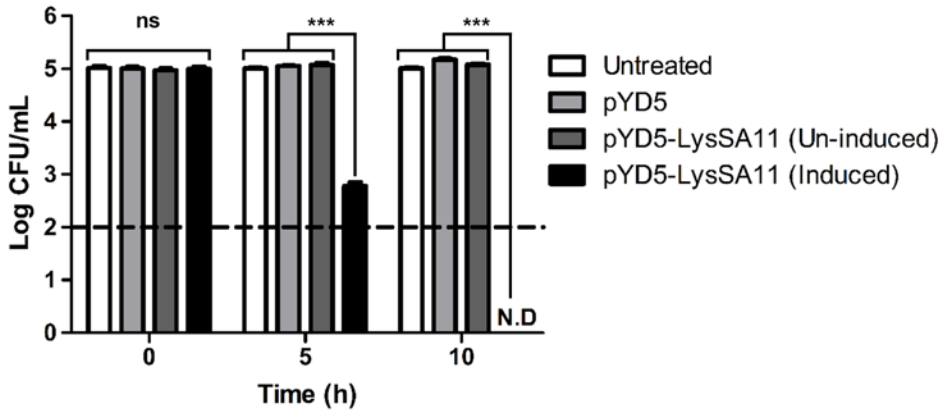

Figure III-9. Population variation of *S. aureus* ATCC 13301 upon treatment of divergent recombinant yeast strains.

The influence of recombinant yeast strains toward *S. aureus* ATCC 13301 was tested. *S. aureus* cells were treated with early-exponentially grown *S. cerevisiae* EBY100/pYD5-LysSA11 or EBY100/pYD5 strains. The former was cultivated in SDCAA or SGCAA to repress or induce the expression of LysSA11-Aga2p fusion protein, and the latter was cultivated in SGCAA to induce the expression of Aga2p anchor protein only. The untreated group of *S. aureus* ATCC 13301 cells were exposed to the reaction buffer. Dashed lines denote the limit of detection (N.D, not detected). Asterisks indicate the significance of variances (***, $P < 0.0001$; NS, not significant). All experiments were done triplicates.

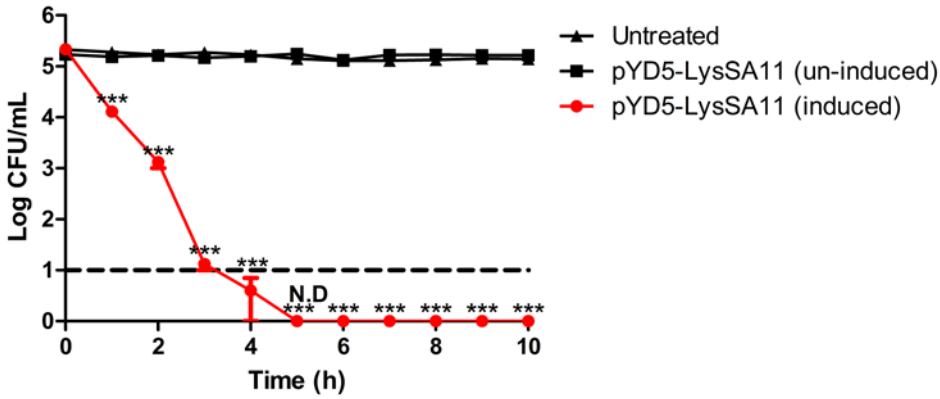

Figure III-10. Antibacterial activity of yeast-displayed LysSA11 against *S. aureus* ATCC 13301 in acidic environment.

Lytic activity of surface-displayed LysSA11 from yeast harvested at late-exponential stage against *S. aureus* ATCC 13301 in an acidic environment (pH 4.54) was examined by CFU reduction assay. The untreated group of *S. aureus* cells were exposed to the reaction buffer. Yeast strain (EBY100/pYD5-LysSA11) cultivated in SDCAA was used as a control. Dashed lines denote the limit of detection (N.D, not detected). Asterisks indicate the significance of variances (***, $P < 0.0001$). All experiments were done triplicates.

Consequently, it was learned that yeast cultures harvested at late-exponential phase (32 ~ 36 h post-induction, OD_{600} = 13), exhibited optimal antibacterial activity against *S. aureus* ATCC 13301. This could be the result of high expression and display of endolysin on the yeast cells at late-exponential phase (Figure III-7). Specifically, taking into account that the LysSA11-Aga2p fusion protein has a pI (isoelectric point) value of 8.88 and the reaction buffer has a pH value of 7.4, the surface of endolysin-displaying yeast is expected to be more positively charged at late-exponential phase (Novák & Havlíček, 2016). Although both the surfaces of yeast and *S. aureus* are known to carry net negative charge in physiological pH (Dickson & Koohmaraie, 1989; Klis, Mol, Hellingwerf, & Brul, 2002), surface-displayed endolysins might have neutralized the surface charge of yeast. Therefore, it could be assumed that the increased amount of surface-displayed LysSA11 could have eventually contributed to the accelerated reduction of *S. aureus* ATCC 13301 by endowing more chance for yeast cells to encounter the target bacteria. Such assumption can also be applied to the antimicrobial activity of surface-displayed LysSA11 at acidic pH, since the lower pH value would contribute to the increased positive charge of the displayed LysSA11, thereby mitigating the adverse effect of acidic buffer with greater chance to encounter *S. aureus* cells. In addition, it can be suggested from the antimicrobial activity data that glycosylation might have mere effect on the activity of yeast-displayed LysSA11.

III.3.8. Antibacterial activity of yeast-displayed LysSA11 against *S. aureus* FORC_059

To further verify the antibacterial activity of yeast-displayed LysSA11, induced late-exponential yeast culture was prepared and treated to a clinical isolate, *S. aureus* FORC_059 (Figure III-11). Similar to *S. aureus* ATCC 13301, the population of the clinical isolate decreased below detection limit (1-log CFU) within 4 h, and remained undetected. Although the actual number of *S. aureus* FORC_059 (2.20×10^5 CFU/mL) used in antibacterial activity test was about the twice of *S. aureus* ATCC 13301 (1.15×10^5 CFU/mL), LysSA11 could actively lyse staphylococcal cells and eliminate the whole population. Therefore, it was learned that the functionality of yeast-displayed LysSA11 was not confined to a type strain. If this finding is to be generally applicable, antibacterial activity of yeast-displayed LysSA11 should be tested against a wide range of staphylococcal strains. Nevertheless, taking into account for the broad host range of endolysin (Schmelcher et al., 2012), it can still be suggested that yeast surface display system can be potentially utilized as a universal expression and application platform of endolysin.

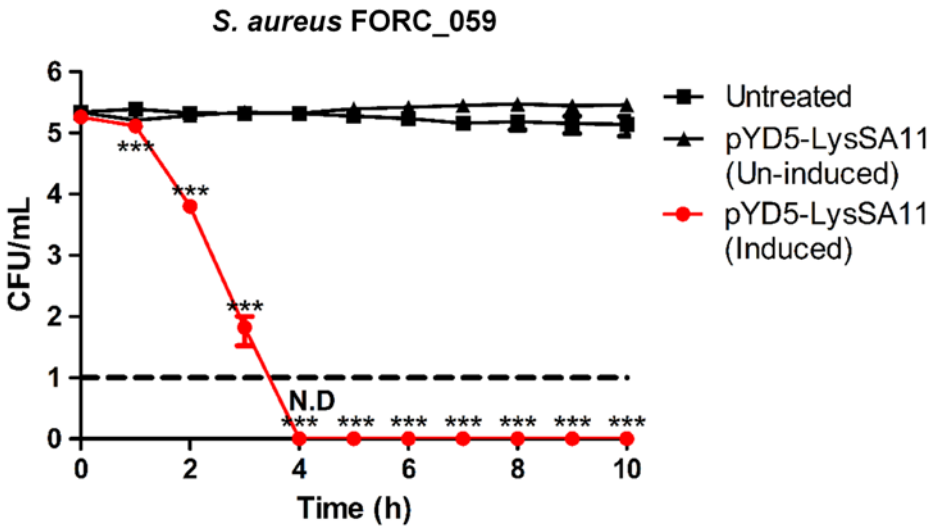

Figure III-11. Antibacterial activity of yeast-displayed LysSA11 against staphylococcal clinical isolate FORC_059.

Lytic activity of surface-displayed LysSA11 from yeast harvested at late-exponential stage against *S. aureus* FORC_059 was examined by CFU reduction assay. The untreated group of *S. aureus* cells were exposed to the reaction buffer. Yeast strain (EBY100/pYD5-LysSA11) cultivated in SDCAA was used as a control. Dashed lines denote the limit of detection (N.D, not detected). Asterisks indicate the significance of variances (***, $P < 0.0001$). All experiments were done triplicates.

III.3.9. Protein stability of yeast-displayed LysSA11

The yeast surface displayed-proteins were reported to have better thermal stability compared to the purified proteins (Parthasarathy et al., 2005; Shusta et al., 1999). In order to assess the thermal stability of surface-displayed LysSA11 endolysin, the induced yeast culture in late-exponential phase (OD_{600} = ~ 13) was collected and stored at 4℃ for 2 weeks, while its lytic activity was tested at predetermined times (Figure III-12A). In parallel, the activity of LysSA11 endolysin purified from conventional *E. coli* host was also tested under the same conditions (Figure III-12B). During the storage, the overall lytic activity of surface-displayed LysSA11 was maintained unaffected, reducing *S. aureus* CFU by 5.01 log units within 3.5 hours (Figure III-12A). In the case of purified LysSA11, 25 μM of the purified endolysin was used for each experiment, and we could achieve 5.21 log reduction in 4.5 hours on day 0, which was comparable to the activity of surface-displayed LysSA11. On the other hand, contrary to the displayed endolysin, purified LysSA11 reduced only 1.00 log-CFU of *S. aureus*, which is equivalent to 19.2% of the initial activity. Finally, the antibacterial activity shrunk to 11.5% in the second week, ending up with only 0.6 log reduction in 5 hours of reaction (Figure III-12B).

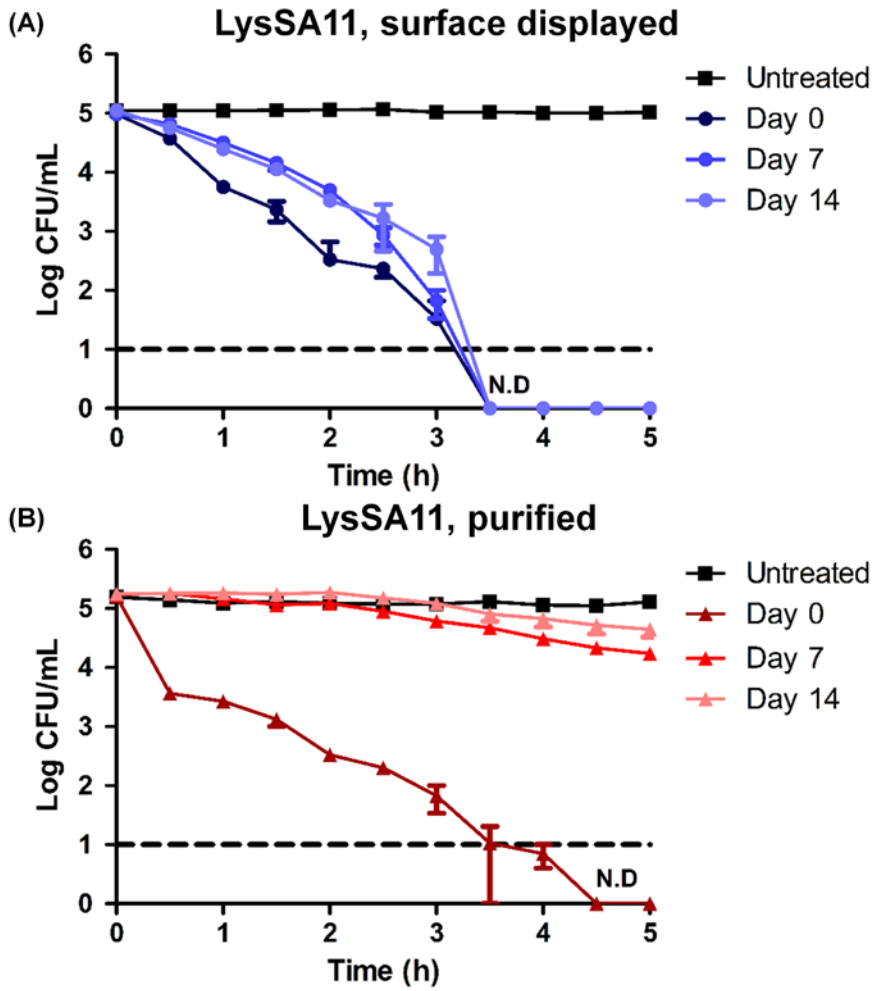

Figure III-12. Antibacterial activity of yeast-displayed and purified LysSA11 after refrigerated storage.

Antibacterial activity of (A) yeast-displayed LysSA11 and (B) purified LysSA11 against *S. aureus* ATCC 13301 during 2 weeks of storage at 4℃. Yeast-displayed or purified LysSA11 were stored at 4℃ for 1 h prior to contact with *S. aureus* at Day 0. Dashed lines denote the limit of detection (N.D, not detected). All experiments were done triplicates.

After confirming the enhanced stability of surface-displayed LysSA11 at refrigerated condition, we wanted to know if the endolysin could still be active even when the yeast cells are not viable anymore. In order to minimize the potential stress upon displayed endolysin molecules during yeast cell lysis, we decided to snap-freeze the yeast cells by using liquid nitrogen prior to mechanical lysis (cryo-lysis) (Choi & Bischof, 2010). The viability of cryo-lysed yeast was decreased by 96.4% as the viable population changed from $(3.62 \pm 0.51) \times 10^8$ CFU/mL to $(1.30 \pm 0.23) \times 10^7$ CFU/mL after the lysis. The cryo-lysed yeast was treated to *S. aureus* ATCC 13301, and it turned out that it could still reduce 5 log CFU within 5 h, implying that there was no severe downfall to the activity of endolysin related to loss of viability of the expression host (Figure III-13).

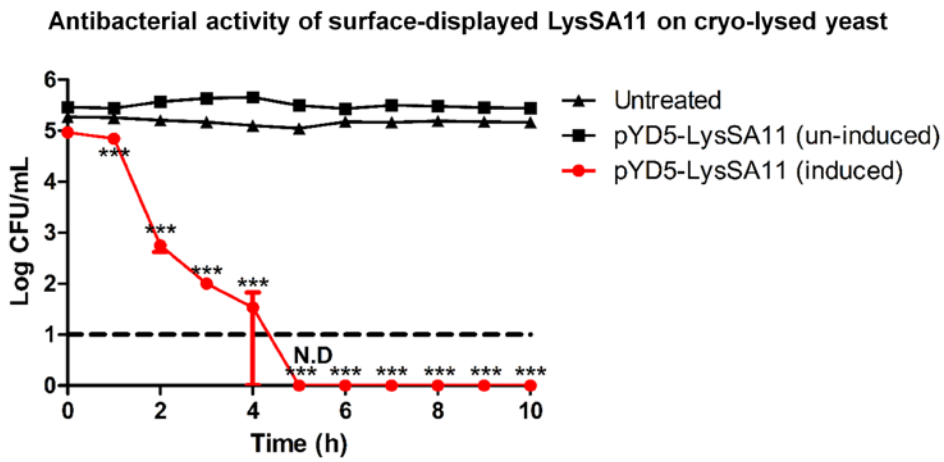

Figure III-13. Antibacterial activity of yeast-displayed LysSA11 in cryo-lysed yeast.

Antibacterial activity of yeast-displayed LysSA11 in cryo-lysed yeast against *S. aureus* ATCC 13301. Yeast with or without displayed LysSA11 were frozen in liquid nitrogen and disrupted. Dashed lines denote the limit of detection (N.D, not detected). Asterisks indicate the significance of variances (***, $P < 0.0001$). All experiments were done triplicates.

According to the previous studies, endolysin or other purified protein products can be stabilized by supplementing osmolyte stabilizers, such as glycerol, to the storage buffer (Love, Bhandari, Dobson, & Billington, 2018; Simpson, 2010). In this study, surface-displayed LysSA11 and purified LysSA11 were stored in reaction buffer void of any stabilizing agent. Thus the contribution of yeast display to the thermal stability of endolysin could be solely determined. Accordingly, it could be assumed that extended period of storage at low temperature without any protective agent, such as glycerol, has severely deteriorated the functionality of purified LysSA11. This assumption is consistent with the data in a previous report, which showed the relative lytic activity of LysSA11 after incubation at an array of specific temperature (Chang et al., 2017). It has been confirmed that the maximal activity was observed when incubated at 37℃. However, incubation at 4℃ significantly impaired the lytic activity, which dropped by nearly 70%. On the other hand, the surface-displayed LysSA11 was barely affected in storage settings, suggesting that immobilization of endolysin on yeast surface could dramatically improve protein stability with minimal defect in lytic performances. The activity of LysSA11 in cryo-lysed yeast further emphasizes the stabilizing effect of surface-display, which was not severely affected even when majority of the expression host, the yeast cells, lost the viability. Furthermore, it is suggested from this data that surface-displayed endolysins can be industrially applied by yeast cryo-lysis, since it is

unavailable to utilize genetically modified organisms (GMOs) directly in food industry. Regarding the fact that the cryo-lysis method implemented in this experiment is only resembling the actual cryogenic lysis or cryomill process, the viability of yeast cells could be thoroughly removed by using proper instruments whose efficacy has been confirmed in numerous industrial settings (Tridib Kumar, 2010). Taken altogether, the results demonstrated in this chapter strongly suggest that the YSD-based endolysin expression platform is an efficient, effective, and applicable antibacterial strategy, and we expect its contribution to the industry in near future.

Chapter IV.

Development of a novel endolysin expression platform by utilizing yeast secretion system

IV.1. Introduction

In the notion of application as an antimicrobial agent, endolysin is a highly competent candidate to substitute conventional antibiotics, regarding its biological properties (Schmelcher et al., 2012). The extensive use of broad-range antibiotics has accelerated the dissemination of resistance genes within bacterial community, due to their non-specific activity to target pathogens and commensal bacteria. However, endolysins is capable of acting on bacteria within a certain genus or species, due to its target-specific nature (Nelson et al., 2012). Moreover, the relatively low structural diversity and extracellularly exposed nature of peptidoglycans in Gram-positive bacteria have made it unfavorable for bacterial cells to develop resistance against endolysins (Vincent A. Fischetti, 2005). Although there were some reports about resistance to peptidoglycan hydrolases other than endolysins, such as a few *S. aureus* strains being resistant to lysostaphin (Gründling et al., 2006), no resistance mechanisms have been observed for phage endolysins so far. Most importantly, despite the fact that antibodies against endolysins can be raised, no adverse side effect or anaphylaxis nor any severe interference with endolysin activity *in vivo* was reported (Vincent A. Fischetti, 2010; Rashel et al., 2007).

To date, the advances in endolysin research have led to the development of a commercial endoysin-based therapeutic agent for the

biocontrol of *S. aureus*, SAL200 (Jun et al., 2013). Preclinical tests (good laboratory practice (GLP)-compliant safety evaluation) of SAL200 in rat and dog models have yielded favorable results (Jun et al., 2014), and a further study has been conducted in monkeys to analyze its pharmacokinetics (Jun et al., 2016), in which no significant adverse effect was observed. Recently, research of SAL200 was conducted as a part of the first in-human phase 1 study of endolysin-based therapeutic agent for intravenous administration (Jun et al., 2017). Despite the favorable results, a few issues must be resolved. Repeated exposure to SAL200 in rats and dogs for over 10 days triggered immune response, which is doubted to be due to residual lipopolysaccharide endotoxin originating from the bacterial expression host (Jun et al., 2014). Also, comparable to other proteins, SAL200 has low half-life in human blood plasma ranging from 0.04 to 0.38 h (Jun et al., 2017), implying that a lot more improvements are required for efficient uses.

Being the most well-established eukaryotic expression host with broad utility, yeast can offer solutions to aforementioned issues. Among several eukaryotic host systems, yeast could excel others by combining the advantages of unicellular organisms with the capability of eukaryotes to carry out protein processing (protein folding, assembly, and post-translational modifications) (Porro et al., 2005). Its ability to quality control the production of polypeptides in cellular organelles can help preventing the formation of misfolded polypeptides (C. L. Young & Robinson, 2014). Recently,

production of fully humanized sialylated glycoproteins have become available, thanks to the breakthroughs in glycoengineering of the yeast *Pichia pastoris* (Hamilton & Gerngross, 2007). Moreover, *Saccharomyces cerevisiae* is classified as generally regarded as safe (GRAS) organism by U.S. Food and Drug Administration (FDA), thereby ensuring endotoxin-free production of desired proteins. In addition, it was confirmed that yeast is capable of intracellularly producing or secreting endolysin LysA2 in a functionally active form (Khatibi et al., 2014; J.-S. Kim, M. A. Daum, et al., 2018).

Yeast secretion system has also been developed and optimized for the production of heterologous proteins (Porro et al., 2005). Many yeast systems have been exploited for protein production for pharmaceutical, food, and other industries (Vieira Gomes et al., 2018). In respect to pharmaceutical proteins, *S. cerevisiae* has been engineered for the production of insulin, insulin analogs, human serum albumin, hepatitis vaccines (Martínez et al., 2012). The advantage of yeast over bacterial system in pharmaceutical protein production rooted from the ability to do post-translational processing and secrete proteins in functionally active forms. The rapid growth and high-density fermentation of yeast in chemically defined media also facilitated industrial applications.

In *S. cerevisiae* and other yeast strains, protein of interest can be secreted by adding appropriate secretion signal sequence. One of the most

commonly used signal peptide is the *S. cerevisiae* α-mating factor (α-MF). It has been reported that the use of entire processing sequence of prepro α-MF could achieve high secretion level of target protein in both nonmethylotrophic and methylotrophic yeasts (*S. cerevisiae*, *K. lactis*, and *P. pastoris*) (Porro et al., 2005). Upon expression, nascent protein is further processed in endoplasmic reticulum (ER) and Golgi, such as signal peptide cleavage, or glycosylation (Banfield, 2011; Walker & Lively, 2013). If unfolded proteins accumulate in the ER, unfolded protein response (UPR) is induced, and the proteins may be rescued or degraded. Through such modification and quality control mechanisms, heterologous proteins can be successfully secreted in an active form for further applications.

IV.2. Materials and Methods

IV.2.1. Strains, culture media, and growth conditions

Escherichia coli DH5α, BL21* (DE3), and Stellar™ (*E. coli HST08 strain, F-, endA1, supE44, thi-1, recA1, relA1, gyrA96, phoA, Φ80d lacZΔ M15, Δ (lacZYA –argF) U169, Δ (mrr –hsdRMS –mcrBC), ΔmcrA, λ-*, TaKaRa) strains were cultivated in Luria-Bertani (LB) broth/agar (BD Difco) with aeration at 37℃, 220 rpm/static. *Staphylococcus aureus* ATCC 13301 strain was cultivated in tryptic soy broth/agar (TSB/TSA) (BD Difco) or Baird-Parker agar (BD Difco) with aeration at 37℃, 220 rpm/static. *Saccharomyces cerevisiae* YVH10 strain (*S. cerevisiae* Meyen ex E.C. Hansen, ATCC® MYA-4940™, MATα, *PDI1::GAPDH-PDI1::LEU2 ura3- 52 trp1 leu2-δ200 his3-δ200 pep4::HIS3 prbd1.6R can1 GAL*) was provided by Prof. Yong-Sung Kim (Ajou University, Korea), and *Saccharomyces cerevisiae* EBY100 strain (*S. cerevisiae* Meyen ex E.C. Hansen, ATCC® MYA-4941TM, MATa, *AGA1::GAL1-AGA1::URA3 ura3-52 trp1 leu2-δ200 his3-δ200 pep4::HIS3 prbd1.6R can1 GAL*) was purchased from American Type Culture Collection (ATCC). Yeast strains were cultivated in yeast peptone dextrose (YPD) broth/agar (BD Difco) or synthetic media (SDCAAT/SGCAAT for *S. cerevisiae* YVH10 and its recombinants and SDCAA/SGCAA for *S. cerevisiae* EBY100 and its recombinants) with aeration at 30℃, 250 rpm/static. The composition of each synthetic media is as follows:

SDCAA/SGCAA, 0.67% yeast nitrogen base (BD Difco), 0.5% casamino acid (BD Difco), 2% D-glucose/D-galactose, 100 mM sodium phosphate buffer pH 6.4; SDCAAT/SGCAAT, 80 mg/L tryptophan (Pronk, 2002) supplemented; agar plates, 1 M sorbitol included.

IV.2.2. Recombinant yeast construction for inducible secretion of LysSA11

Inducible yeast secretion plasmid of LysSA11 was constructed by modifying an *E. coli - S. cerevisiae* shuttle vector pYDS-K (Kim, 2014). LysSA11-His insert sequence was PCR amplified with oligonucleotides listed in Table IV-1. Originally, pYDS-K vector was constructed by inserting VL gene library with CL to pRS416 at the downstream of signal sequence (Kim, 2014). In this research, pYDS-K vector was digested with *NheI* and *XhoI* to remove previously inserted antibody gene and the flag-tag sequence. The linearized plasmid backbone was separated from the antibody and flat-tag sequence fragment by gel electrophoresis. Subsequently, the linearized backbone sequence was salvaged from the agarose gel by Wizard® SV Gel and PCR Clean-up system (Promega). The purified LysSA11-His insert sequence and linearized plasmid backbone sequence were introduced to Stellar™ competent cells (*E. coli HST08 strain, F-, endA1, supE44, thi-1, recA1, relA1, gyrA96, phoA, Φ80d lacZΔ M15, Δ (lacZYA –argF) U169, Δ (mrr –hsdRMS –mcrBC), ΔmcrA, λ-*, TaKaRa) for assembly by homologous

recombination, mediated by In-Fusion® HD Cloning Kit (TaKaRa Bio USA, Inc.). Recombinant *E. coli* strains were selected on LB agar with 50 μg/mL carbenicillin and single colonies were verified by PCR and nucleotide sequencing. Confirmed plasmids were then transformed to competent *S. cerevisiae* YVH10 cells by S. c. EasyComp™ Transformation Kit (Invitrogen™) according to manufacturer's instructions. As a negative control, original *S. cerevisiae* YVH10/pYDS-K strain was used. Recombinant yeast strain *S. cerevisiae* YVH10/pYDS-K-LysSA11 was selected on SDCAAT agar with 25 μg/mL kanamycin supplement. Yeast single colonies were treated with Zymolyase™ (Zymo Research Corp.) for colony PCR and nucleotide sequencing.

IV.2.3. Recombinant yeast construction for constitutive secretion of LysSA11

Constitutive yeast secretion plasmid of LysSA11 was constructed by inserting Aga2p signal peptide-LysSA11-His or Aga2p signal peptide-LysSA11 sequence into p404TEF1 plasmid originated from pRS404 (Sikorski & Hieter, 1989). The sequences of Aga2p signal peptide-LysSA11-His and Aga2p signal peptide-LysSA11 fusion protein were PCR amplified with oligonucleotides listed in Table IV-1. Plasmid p404TEF1 was digested with *BamHI* and *XhoI*, and the linearized plasmid backbone was isolated by gel electrophoresis and further purified by Wizard® SV Gel and PCR Clean-

up system (Promega). The purified insert DNA sequences and linearized plasmid backbone sequence were introduced to Stellar^{TM} competent cells as previously described. By following the same procedures, plasmid construct was confirmed and transformed to competent *S. cerevisiae* EBY100 cells, yielding *S. cerevisiae* EBY100/p404TEF1-LysSA11, a false negative control EBY100/p404TEF1-LysSA11-noHis, and a true negative control EBY100/p404TEF1. Each recombinant strain was selected and confirmed as previously described.

IV.2.4. Galactose-induced expression of yeast-secreted LysSA11 from low-density population

S. cerevisiae YVH10/pYDS-K-LysSA11 or YVH10/pYDS-K were streaked on SDCAAT agar (synthetic media, tryptophan supplemented, 2% D-glucose, 1 M sorbitol, pH 6.40, 25 μg/mL kanamycin) and incubated at 30℃ for 3 days. Single colonies were inoculated in 5 mL of SDCAAT media for 24 h (final OD_{600} = 7.0 ~ 8.0) at 30℃, 250 rpm. At primary passage, each inoculum was sub-cultured in 20 mL of SDCAAT (initial OD_{600} = 1.0) for 12 h (final OD_{600} = 7.0 ~ 8.0), followed by secondary passage in 50 mL of SDCAAT (initial OD_{600} = 1.0) for 9 h (final OD_{600} = 7.0). At each passage, SDCAAT media was supplemented with 25 μg/mL of kanamycin. Prior to induction, each yeast culture was centrifuged at 6,000 × *g* for 5 min at 25℃ and washed for twice with 15 mL of Dulbecco's phosphate buffered saline

(Sigma-Aldrich) to remove extracellular glucose. Washed cell pellets were re-suspended in 50 mL of SGCAAT (synthetic media, tryptophan supplemented, 2% D-galactose, pH 6.75, 25 μg/mL kanamycin) to diluted initial OD_{600} of 1.0. Prepared culture flasks were cultivated at 20℃ or 30℃, 250 rpm for up to 62 h or 50 h, respectively. The overall procedure is represented in Figure IV-1.

IV.2.5. Galactose-induced expression of yeast-secreted LysSA11 from high-density population

S. cerevisiae YVH10/pYDS-K-LysSA11 or YVH10/pYDS-K strains were prepared by the same procedures in IV.2.4. In contrast to the low cell density induction, *S. cerevisiae* cultures were cultivated for 7 h in the secondary passage (final OD_{600} = 5.0 ~ 6.0). The entire cultures were then centrifuged at 6,000 × *g* for 5 min at 25℃, washed with Dulbecco's phosphate buffered saline (Sigma-Aldrich), and re-suspended in 50 mL of SGCAAT (synthetic media, tryptophan supplemented, 2% D-galactose, pH 6.75, 25 μg/mL kanamycin) without any dilution process. Therefore, the induction of each yeast culture could be started with much larger population (initial OD_{600} = 5.0 ~ 6.0). Prepared culture flasks were cultivated at 20℃ or 30℃, 250 rpm for up to 64 h or 36 h. The overall procedure is represented in Figure IV-1.

IV.2.6. Constitutive expression of yeast-secreted LysSA11 from

low-density population

S. cerevisiae EBY100/p404TEF1-LysSA11, EBY100/p404TEF1-LysSA11-noHis, and EBY100/p404TEF1 strains were separately streaked on SDCAA agar and incubated at 30℃ for 3 days. Single colonies were inoculated in 5 mL of SDCAA media for 24 h (final OD_{600} = 8.0 ~ 9.0) at 30℃, 250 rpm. The inoculum was passed for once in 20 mL of SDCAA (initial OD_{600} = 1.0) for 8 h (final OD_{600} = 8.0) and then scaled-up to 50 mL culture of SDCAA (initial OD_{600} = 1.0), which was cultivated for 8 h (final OD_{600} = 10.0). At each passage, SDCAA media was supplemented with 25 μg/mL of kanamycin.

IV.2.7. Analyzing physiological properties of recombinant yeast during LysSA11 expression

The patterns of growth and galactose consumption of YVH10/pYDS-K-LysSA11 and YVH10/pYDS-K strains were analyzed during LysSA11 expression. Three replicate batches of each strain in SGCAAT media were prepared. For the growth curve of low cell density culture at 30℃, cultures were sampled every 2 h and the optical density at 600 nm (OD_{600}) was measured by spectrophotometer (Amersham Biosciences). Galactose utilization behavior was analyzed by measuring residual galactose of yeast cultures in every 4 h with Galactose assay kit (ab83382, abcam®). According to the manufacturer's protocol, fluorometric assay of yeast cultures was

conducted in 96-well black plate with clear bottom (BD Falcon) by SpectraMax® i3x plate reader (Molecular Devices). The excitation wavelength and emission wavelength were 535 nm and 587 nm, respectively, and the resulting data set was generated by SoftMax Pro 7.0 software (Molecular Devices). Taken together, the behavior of recombinant yeast strains in SGCAA media was visualized by GraphPad Prism 5.01 software (GraphPad Software). Meanwhile, the growth of high cell density cultures at 20℃ and 30℃ was visualized by measuring OD_{600} of the cultures in every 4 h. Likewise, growth and galactose consumption pattern of each sample were visualized.

For EBY100/p404TEF1-LysSA11 and EBY100/p404TEF1 strains, growth in SDCAA media was plotted by measuring the optical density (OD_{600}) of culture at every 2 h.

IV.2.8. Harvesting and concentrating secreted LysSA11 in yeast culture

Secreted LysSA11 in yeast culture supernatants from different expression conditions (promoter, cell density and induction temperature) were harvested and concentrated. Entire cultures from three replicate batches were collected in 50 mL conical tubes (BD Falcon) and centrifuged at 6,000 × *g* for 10 min at 4℃. The supernatants were transferred to new 50 mL conical tubes and centrifuged again at 6,000 × *g* for 10 min at 4℃ to minimize

residual cells in the supernatant. Collected supernatants (total of 150 mL) were gently mixed with equal amount of chilled LysSA11 storage buffer (50 mM sodium phosphate buffer, 200 mM sodium chloride, 30% glycerol, pH 8.0) to a final volume of 300 mL. For concentrating supernatant-buffer mixture, Amicon® Ultra-15 10K (Merck Millipore) centrifugal filters were prepared by equilibration with 3 mL of LysSA11 storage buffer for at 1 h in advance. Pre-equilibrated membranes were washed by centrifugation at 5,000 × *g* for 20 min at 4℃. Then, 12 mL of supernatant-buffer mixtures were introduced to the filter unit at a time, centrifuged at 5,000 × *g* for 20 min at 4℃, and the resulting concentrates were carefully collected to a new 50 mL conical tube on ice. When the entire amount of supernatant-buffer mixtures was concentrated for a single round, the protein concentration was measured by Bradford assay. Then the collected concentrated mixtures were concentrated for subsequent rounds, until the final products are concentrated by over 100 times. In order to prevent proteins from aggregating, centrifugation duration was adjusted to 5 min at a time.

IV.2.9. Immunoblot assay of intracellular or secreted LysSA11 from yeast

Yeast cell pellets in each 50 mL conical tube from IV.2.8. were re-suspended by 1 mL of LysSA11 reaction buffer (50 mM sodium phosphate, 200 mM sodium chloride, pH 8.0). Two hundred microliter of each cell

suspension was transferred to a 1.75 mL microcentrifuge tube and the cells were pelleted by centrifuging at 15,000 × *g* for 5 min at 4℃. After discarding the supernatant, each cell pellet was re-suspended in 200 μL of Y-PER ™ Yeast Protein Extraction Reagent (Thermo Scientific™), and mixed vigorously by Multi Mixer (MyLab #SLRM-3, SeouLin Bioscience) at 25℃, mode 15, 80 rpm, for 20 min. The resulting cell lysates were centrifuged at 15,000 × *g* for 5 min at 4℃, and the supernatant harboring the soluble fraction of total protein was collected. Subsequently, the protein concentration of each cell lysate was measured by Bradford assay. Cell lysates were used for analyzing intracellularly expressed LysSA11. Meanwhile, concentrated culture supernatants were used for the analysis of secreted LysSA11. Based on the Bradford assay data, 40 μg of each soluble protein was diluted with distilled water and mixed with Laemmli Sample buffer (4×) (GenDepot) to a final concentration of 1 μg/μL, and heat-denatured at 95℃ for 10 min. Ten microliter of each protein sample (10 μg) was loaded to 12% polyacrylamide gels for size discrimination by SDS-PAGE (Bio-Rad) with constant voltage setting at 80 V for stacking and 160 V for separating. Resulting protein bands were stained with coomassie blue staining solution at 25℃ for 10 min, and washed with destaining solution at 25℃ for overnight, and finally imaged with Gel Doc™ EZ imager (Bio-Rad). Also, the protein bands were further transferred onto a nitrocellulose membrane by Trans-Blot® Turbo™ Transfer System (Bio-Rad) with StandardSD setting (25 V, 1.0 A, 30 min). For the

detection of LysSA11-His in cell lysates or supernatant concentrates, 6x-His tag monoclonal antibody (HIS.H8) (MA1-21315, Invitrogen™) was used. For positive control, Anti-PGK1 antibody 22C5D8 (ab113687, abcam®) was used. The blot was blocked with 5% bovine serum albumin fraction V in TBST (10 mM Tris-HCl, 150 mM NaCl, 0.05% Tween-20) at 25℃ for 1 h, and subsequently labeled with 10 mL of 1:3,000 anti-His or 1:10,000 anti-PGK1 antibody in BSA-TBST at 4℃ for overnight. Later on, it was labeled with 10 mL of 1:5,000 goat-anti-mouse-IgG-(H+L)-HRP antibody (GenDepot) at 25℃ for 1 h. After each labeling process, excess antibodies were washed out with 10 mL of TBST for 3 times by rocking for 5 min. Labeled endolysin samples were detected by ECL™ Prime Western Blotting System (GE Healthcare), using ChemiDoc™ Imaging System (Bio-Rad).

IV.2.10. Glycosylation analysis of yeast-secreted LysSA11

Yeast cell lysates or supernatant concentrates were prepared to a final concentration of 1 μg/μL as mentioned above. For deglycosylation, 50 μg of soluble protein from each cell lysate or supernatant concentrate was treated with PNGaseF (Promega). Fifty microgram of the soluble protein was prepared in 0.5 M sodium phosphate buffer (pH 7.5) to a final volume of 12 μL, to which 1 μL each of 5% SDS and 1 M DL-dithiothreitol (DTT) was added. The sample mixture was heat-denatured at 95 for 5 min, and cooled at 25℃ for another 5 min. Then, 2 μL each of 0.5 M sodium phosphate buffer

(pH 7.5), 10% Triton® X-100, and recombinant PNGaseF were added, and the mixture was incubated at 37℃ for 3 h. After deglycosylation, the sample was diluted with distilled water and then mixed with Laemmli Sample buffer (4×) (GenDepot) to a final concentration of 1 μg/μL, and heat-denatured at 95℃ for 10 min. Additionally, supernatant of yeast cultures was collected after centrifugation, and 30 μL of each supernatant was mixed with 10 μL of Laemmli Sample buffer (4×) (GenDepot), and heat-denatured at 95℃ for 10 min. As a control, fetuin (Promega), an N- and O-linked glycoprotein, was prepared in the same procedure to yield both glycosylated and deglycosylated samples. Ten microliter of each sample (10 μg) was loaded to 12% polyacrylamide gel for size discrimination by SDS-PAGE with the same settings mentioned above. Resulting protein gels were visualized by coomassie blue staining assay or western blot assay as mentioned above.

IV.2.11. Zymography of yeast-secreted LysSA11

Yeast supernatant concentrates and purified LysSA11 from *E. coli* host were prepared. Yeast supernatants were concentrated by 130×. For zymography, *S. aureus* ATCC 13301 was cultivated to early-exponential phase and autoclaved, washed for once with PBS, and finally concentrated by 200× in buffer (50 mM sodium phosphate, 200 mM sodium chloride, pH 8.0). Subsequently, 600 μL of autoclaved *S. aureus* was added to acrylamide gel. After electrophoresis, zymogram gel was washed for twice with DW for 15

min at 25℃, and soaked in renaturation buffer (50 mM sodium phosphate, 200 mM sodium chloride, 0.1% Triton X-100, pH 8.0) at 37℃ for overnight. The peptidoglycan of zymogram gel was stained with staining solution (0.1% methylene blue, 0.001% methanol) for 1 h at 25℃ and washed with DW for 1 day at 25℃.

IV.2.12. Antibacterial activity analysis of yeast-secreted LysSA11

The antibacterial activity of extracellularly secreted LysSA11 was examined by combining the concentrated mixture of culture supernatant and buffer (50 mM sodium phosphate, 200 mM sodium chloride, 30% glycerol, pH 8.0) with *S. aureus* ATCC 13301 cells. Each mixture of culture supernatant and buffer was concentrated to a smaller volume with concentration factors higher than 100×. From each concentrate, 900 μL was transferred to a 1.75 mL microcentrifuge tube. Meanwhile, 1 mL of *S. aureus* ATCC 13301 culture in early exponential stage (at OD_{600} = 1.0, 1.15×10^8 CFU/mL) was collected and washed with 1 mL of LysSA11 lysis buffer (50 mM sodium phosphate, 200 mM sodium chloride, pH 8.0) for three times. Washed *S. aureus* cells were serially diluted (10^{-3}), and 100 μL of diluted cells (10^5 CFU/mL) were added to the culture supernatant concentrate prepared in 1.75 mL microcentrifuge tube. The final concentration of *S. aureus* in the mixture was 10^4 CFU/mL. As a negative control, *S. aureus*-only samples (10^4 CFU/mL) were prepared in the buffer. All of the reaction samples were triplicated. Each

microcentrifuge tube was mixed by Multi Mixer (MyLab #SLRM-3, SeouLin Bioscience) at 25℃, channel F1, 20 rpm. For every 1 h, 50 μL of the mixture was collected and diluted (10^{-1}), and 100 μL of the diluted samples or the original mixture were spread on Baird-Parker agar plate and incubated for overnight at 37℃. The resulting colonies of *S. aureus* were enumerated with a detection limit of 2-log or 1-log CFU.

IV.2.13. Antibacterial activity assessment of LysSA11-secreting yeast

The antibacterial activity of LysSA11-expressing yeast cells was verified by bacteria overlay assay. *S. cerevisiae* YVH10/pYDS-K-LysSA11 and YVH10/pYDS-K were cultivated in SDCAAT and induced in SGCAAT as previously explained. *S. cerevisiae* EBY100/p404TEF1-LysSA11, EBY100/p404TEF1-LysSA11-noHis, and EBY100/p404TEF1 were cultivated in SDCAA as previously explained. After separating the culture supernatant and yeast cells by centrifugation, cell pellets were re-suspended in LysSA11 reaction buffer (50 mM sodium phosphate, 200 mM sodium chloride, pH 8.0). The concentration of each yeast cell suspension was adjusted to have the amount of yeast cells equivalent to OD_{600} = 200 in a volume of 1 mL. Then, 50 μL of *S. cerevisiae* YVH10/pYDS-K-LysSA11 or YVH10/pYDS-K cell suspensions were dotted on SGCAAT agar plate, and 50 μL of *S. cerevisiae* EBY100/p404TEF1-LysSA11, EBY100/p404TEF1-

LysSA11-noHis, or EBY100/p404TEF1 cell suspensions were dotted on SDCAA agar plate. Spotted cells were dried at 25℃ for 15 min in a sterile environment, and incubated at 30℃, static for 24 h. In the meantime, *S. aureus* ATCC 13301 was inoculated and cultivated in 3 mL of TSB media at 37℃, 220 rpm for overnight, subsequently sub-inoculated in the same volume of TSB and cultivated at the same condition for 2 h until early-exponential phase (OD_{600} = 1.0). Then, culture equivalent to OD_{600} = 1.0 in 1 mL was collected and washed with LysSA11 reaction buffer for three times. From the washed *S. aureus* ATCC 13301 cells, 100 μL was mixed with 5 mL of 0.4% distilled water-based soft agar by vortex mixer, and gently poured over the prepared SGCAAT or SDCAA agar plates with spotted yeast cells. The overlay plates were dried at 25℃ for 20 min in a sterile environment, and incubated at 37℃, static for 24 h. The antibacterial activity of LysSA11-secreting yeast cells could be confirmed by inhibited growth of adjacent *S. aureus* ATCC 13301.

IV.2.14. Statistical analysis

Statistical analysis of lytic activity tests was conducted with GraphPad Prism 5.01 software for Windows (GraphPad Software, San Diego, CA, USA). Each data point was presented as the mean values with standard errors of the *S. aureus* population. The CFUs of *S. aureus* at each time point were analyzed by one-way analysis of variance (ANOVA) followed by Tukey's multiple

comparison test (95% confidence interval). A *P*-value smaller than 0.05 was considered statistically significant.

Table IV-1. Plasmids and primers used in this chapter.

Plasmids		
Name	**Description**	**Reference**
pYDS-K	*E. coli – S. cerevisiae* shuttle vector, Amp^r, URA3, GAL1 promoter, flag-tag, yeast secretion vector	(Kim, 2014)
pYDS-K-LysSA11	pYDS-K with LysSA11, flag-tag substituted with C-terminal His-tag	This study
p404TEF1	*E. coli – S. cerevisiae* shuttle vector, Amp^r, TRP1, TEF1 promoter	Unpublished
p404TEF1-LysSA11	p404TEF1 with LysSA11, Aga2p signal peptide, His-tag	This study
P404TEF1-LysSA11-noHis	p404TEF1 with LysSA11, Aga2p signal peptide	This study
Primers (5'→3')		
Name	**Sequence[a]**	**Reference**
LysSA11_sec_confirm_F	GAAGGGGATTTCGATGCTGCTGCTTTGCCACTATCC	This study
LysSA11_sec_confirm_R	TCTAACTCCTTCCTTTTCGGTTAGAGCGGATGTGGG	This study
sig_LysSA11_insert_BamHI_F	TTTTCTAGAACTAGTGGATCCATGCAGTTACTTCGC	This study
sig_LysSA11_His_insert_XhoI_R	TAACTAATTACATGACTCGAGGTGATGATGATGATGATG	This study
sig_LysSA11_noHis_insert_XhoI_R	AATTACATGACTCGAGTTTCCAGTTAATACGACCCCAA	This study

a Restriction recognition sites are indicated with underlines.

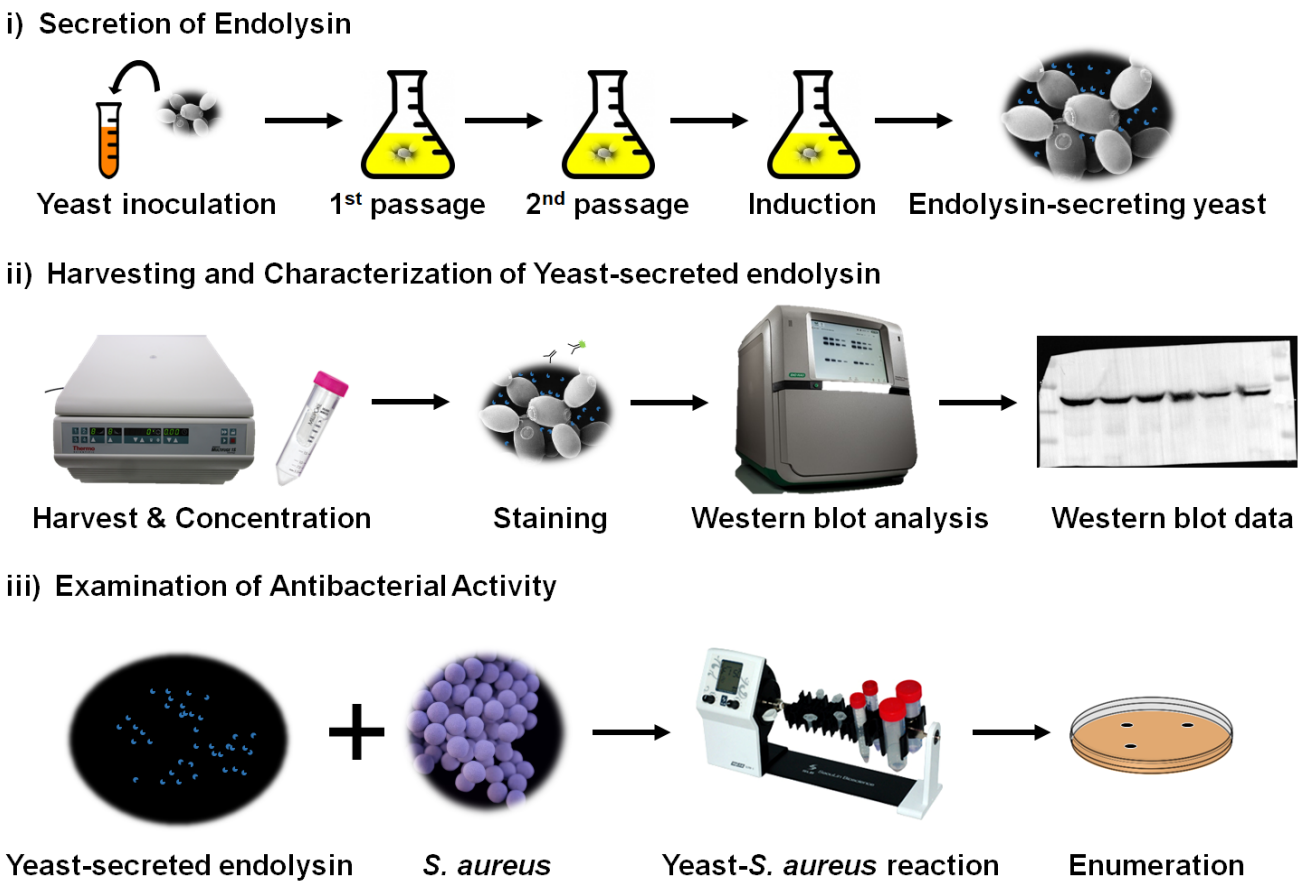

Figure IV-1. Overview of yeast secretion-based endolysin expression platform

IV.3. Results and Discussion

IV.3.1. Determination of optimal expression system for LysSA11 secretion

There have been two studies to produce phage endolysin from yeast systems (Khatibi et al., 2014; J.-S. Kim, M. Daum, Y.-S. Jin, & M. J. V. Miller, 2018). In both cases, the goal was to produce endolysin LysA2 (Ribelles, Rodríguez, & Suárez, 2012) from yeast system to control bacterial contamination by *Lactobacillus* during bioethanol fermentation. As expression hosts, *Pichia pastoris* and *Saccharomyces cerevisiae* were used in previous studies, which are two of the most widely used yeast strains in biofuel fermentation industry (Buijs, Siewers, & Nielsen, 2013; Siripong et al., 2018). Although *P. pastoris* has been renowned for the high yield during secretion of heterologous proteins (Damasceno, Huang, Batt, & biotechnology, 2012), since the most well established AOX1 promoter system is induced by methanol (Cereghino & Cregg, 2000), it seemed inappropriate for the production of endolysin as a therapeutic or food additive agent.

As a result, *S. cerevisiae* was selected as the expression host for LysSA11 secretion. In order to make the most productive secretion platform, two different promoter systems were considered: an inducible promoter or a constitutive promoter. It is perceived that simple and relatively constant expression level of target protein is expected from constitutive promoters,

while inducible promoters are preferred when it is desirable to separate protein production from growth of the host cells (Vieira Gomes et al., 2018). Among various *S. cerevisiae* promoter systems, GAL1 promoter was selected for inducible promoter, and TEF1 promoter was selected for constitutive promoter, regarding each of their activation level during induction or cultivation (Mumberg, Müller, & Funk, 1994; Partow, Siewers, Bjørn, Nielsen, & Maury, 2010; Weinhandl, Winkler, Glieder, & Camattari, 2014a).

IV.3.2. Construction of recombinant *S. cerevisiae* strains

Based on the promoter system, two different types of recombinant *S. cerevisiae* strains were constructed. For the inducible GAL1 promoter, recombinant *E. coli* strains were constructed by introducing pYDS-K shuttle vector with or without LysSA11 coding sequence at the downstream of signal peptide sequence (Kim, 2014) (Figure IV-2A). Specifically, the signal peptide sequence was derived from yeast pheromone MFα-1 (mating factor) (S Caplan, Green, Rocco, & Kurjan, 1991; Shari Caplan & Kurjan, 1991). At the downstream of LysSA11 sequence, 6His was inserted for the detection and purification of secreted endolysin by immunoblot assay and affinity chromatography, respectively (Figure IV-2B). After selecting of successfully transformed *E. coli* strains, the vector was replicated, isolated, and eventually introduced to *S. cerevisiae* YVH10 strain (MATα, *ura3*, *trp1*) for further experiments. As a negative control, pYDS-K without LysSA11 sequence was introduced to YVH10.

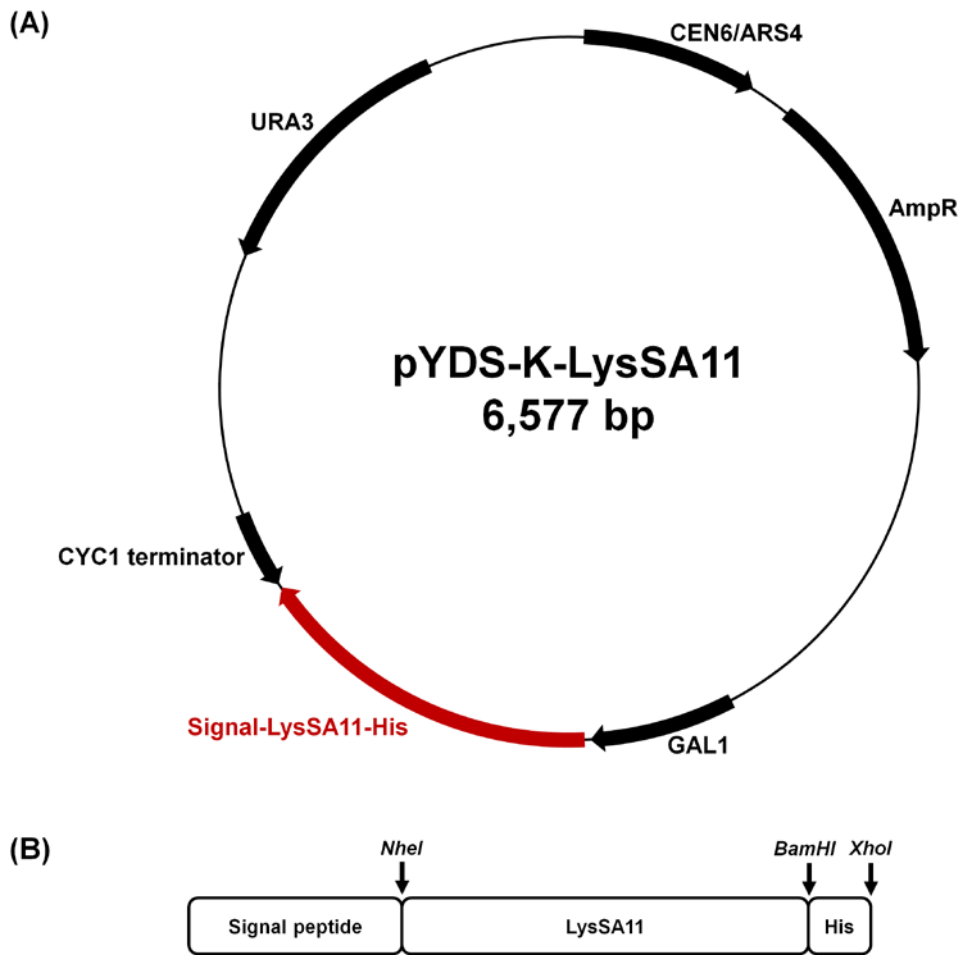

Figure IV-2. Schematic diagram of pYDS-K-LysSA11 shuttle vector and LysSA11 secretion cassette.

Schematic diagram of (A) pYDS-K-LysSA11 shuttle vector construct and (B) LysSA11 secretion cassette. LysSA11 sequence was inserted between the downstream of signal peptide and the upstream of CYC1 terminator at *NheI* and *XhoI* sites. Ampicillin resistant marker (Amp^R) and uracil auxotrophic marker (URA3) are for selection in *E. coli* and *S. cerevisiae*, respectively.

In terms of constitutive TEF1 promoter, recombinant *E. coli* strains were constructed by introducing p404TEF1 shuttle vector (backbone: pRS404) with or without LysSA11 coding sequence at the downstream of TEF1 promoter region (Sikorski & Hieter, 1989) (Figure IV-3A). In this case, the a-agglutinin (AGA2p) signal peptide sequence (Mori et al., 2015) was inserted at the upstream of LysSA11 sequence (Figure IV3-B). Similar to pYDS-K-LysSA11, 6His was inserted at the downstream of LysSA11 sequence. Likewise, positive *E. coli* strains were selected, and p404TEF1-LysSA11 was introduced to *S. cerevisiae* EBY100 strain (MATa, *ura3*) for further experiments. As a negative control, p404TEF1 empty vector was introduced to EBY100.

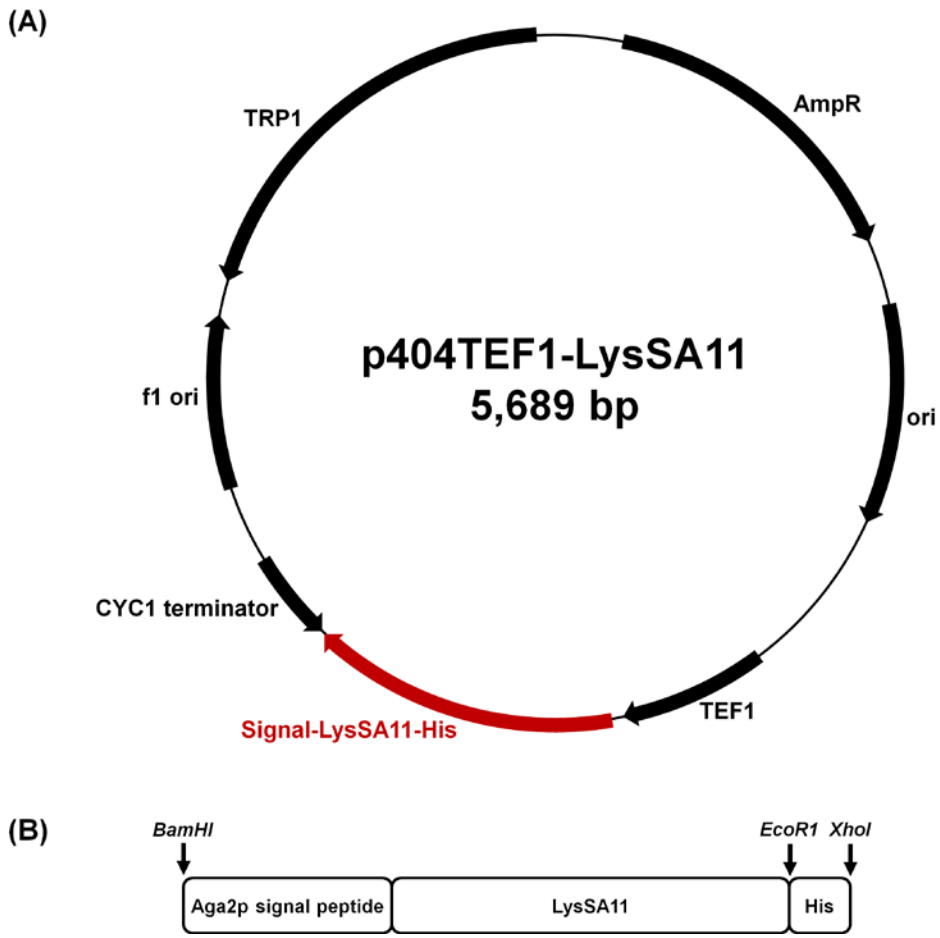

Figure IV-3. Schematic diagram of p404TEF1-LysSA11 shuttle vector and LysSA11 secretion cassette.

Schematic diagram of (A) p404TEF1-LysSA11 shuttle vector construct and (B) LysSA11 secretion cassette. LysSA11 sequence was inserted between the downstream of TEF1 promoter region and the upstream of CYC1 terminator at *BamHI* and *XhoI* sites. Ampicillin resistant marker (Amp^R) and tryptophan auxotrophic marker (TRP1) are for selection in *E. coli* and *S. cerevisiae*, respectively.

IV.3.3. Physiological traits of the recombinant yeast with inducible expression system

In order to determine the most appropriate conditions for heterologous protein production, it was necessary to characterize the physiological properties of each host system (M. Huang, Bao, Hallström, Petranovic, & Nielsen, 2017). For the case of inducible GAL1 promoter system, the growth of *S. cerevisiae* YVH10/pYDS-K and YVH10/pYDS-K-LysSA11 strains at 30℃ in SDCAAT media, and their growth and galactose consumption in SGCAAT media were investigated (Figure IV-4). Each recombinant strain exhibited similar growth pattern in both carbon sources. In SDCAAT media, both strains were exponentially grown at 8 h (OD_{600} = 7.53 for YVH10/pYDS-K, and OD_{600} = 7.80 for YVH10/pYDS-K-LysSA11) (Figure IV-4A). To make sure the culture is rich in young and viable cells, it was decided to harvest the cultures for induction at 7 ~ 8 h after inoculation in each passage. After secondary passage, yeast cells were washed and transferred to SGCAAT (initial OD_{600} = 1) for induction. Similar to the yeast surface display system developed in this study (Figure III-4B), it took about 12 h for the cells for adaptation in galactose media and restart growth (Figure IV-4B) (van den Brink et al., 2009). As previously mentioned in III.3.3., the inducing effect of galactose is expected to be turned off after depletion (Weinhandl et al., 2014a; Whang et al., 2009). Thus, the concentration of galactose in each culture was measured and visualized on a graph together

with growth curve (Figure IV-4B). For the case of YVH10/pYDS-K-LysSA11, 20%, 65%, 85% of galactose was consumed at 24 h, 32 h, 40 h post induction. At 50 h, it could be considered to be depleted, since over 97% of total galactose was gone. Meanwhile, the growth phase at 24 h, 32 h, 40 h could be regarded as early- (OD_{600} = 5), mid- (OD_{600} = 11), and late-exponential or early-stationary (OD_{600} = 16). Again, the physiological behavior of YVH10/pYDS-K was similar to YVH10/pYDS-K-LysSA11 in galactose. In regard to the growth and galactose consumption, induced cultures were harvested at early- (24 h) and late-exponential (40 h) phases to examine intracellular expression, secretion, and antibacterial activity of LysSA11.

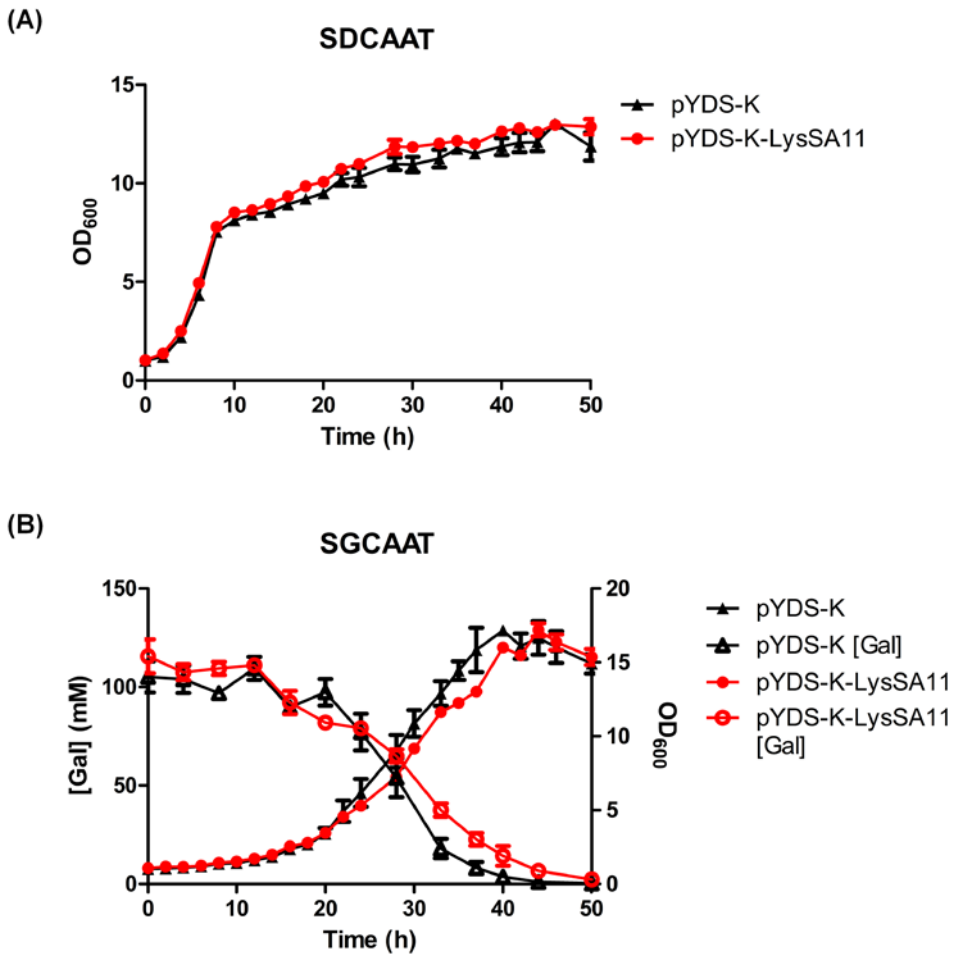

Figure IV-4. Physiological behaviors of recombinant *S. cerevisiae* YVH10 strains in glucose and galactose media at 30°C.

Behavior of each recombinant YVH10 strain in glucose or galactose media was visualized. (A) Growth of *S. cerevisiae* YVH10/pYDS-K and YVH10/pYDS-K-LysSA11 on glucose. (B) Growth of *S. cerevisiae* YVH10/pYDS-K and YVH10/pYDS-K-LysSA11 on galactose, and galactose concentration change were plotted. Each culture was sampled at every 2 h for

turbidity and 4 h for galactose content, respectively. Curves with filled symbols represent growth pattern of recombinant yeast strains. Curves with empty symbols represent galactose consumption pattern of recombinant yeast strains. Each growth curve starts from optical density value (OD_{600}) of 1.0. Initial concentration of galactose in SGCAA media is 100 mM. All experiments were done triplicates.

IV.3.4. Physiological traits of the recombinant yeast with constitutive expression system

In contrast to inducible expression system, TEF1 (translation elongation factor-1A) promoter is known to be capable of strong and constitutive expression of target protein without any induction process (Partow et al., 2010). According to a previous study, TEF1 promoter was revealed to be merely affected by variant glucose level (Vieira Gomes et al., 2018). Nevertheless, yeast cells enter diauxic shift when deprived of primary carbon source, which is glucose in most of the case, while growth rate decreases and the cells start to utilize ethanol as a result of switch in metabolism (Galdieri, Mehrotra, Yu, & Vancura, 2010). Eventually, the culture will face stationary phase and the cellular physiology will significantly change, (Werner-Washburne, Braun, Johnston, & Singer, 1993), thus the fate of intracellular LysSA11 molecules will dramatically differ from those in exponential phase. Interestingly, in a previous study, secretion of heterologous protein was increased by feeding *S. cerevisiae* cultures with extra amount of nitrogen source before entering stationary phase (D. Huang, Gore, & Shusta, 2008). Taking into account for such findings, it was decided to harvest yeast cells and secreted LysSA11 ahead of stationary phase, thus the expression of intracellular and secreted LysSA11 was tested at 4 h, 6 h, 8 h, and 10 h after inoculation in the last passage.

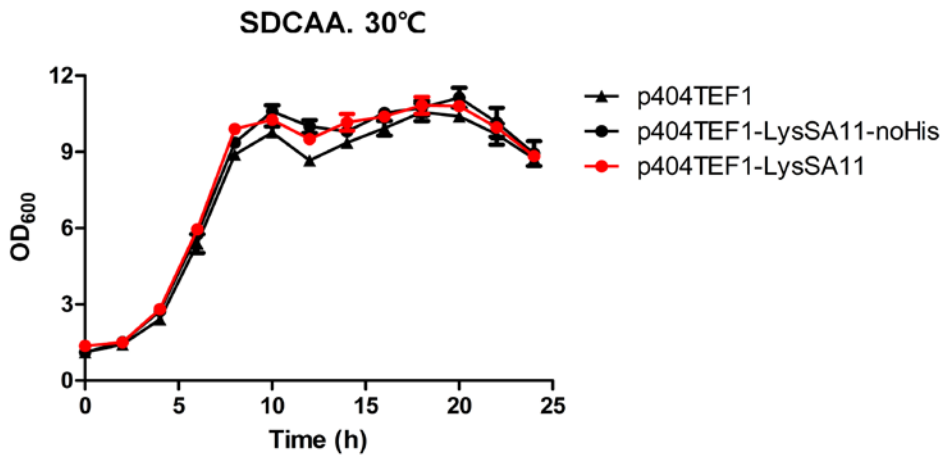

Figure IV-5. Growth of recombinant *S. cerevisiae* EBY100 strains in glucose media at 30°C.

Growth pattern of EBY100/p404TEF1, EBY100/p404TEF1-LysSA11-noHis, and EBY100/p404TEF1-LysSA11 strain in glucose media was visualized. Each culture was sampled at every 2 h to measure optical density. Each growth curve starts at OD_{600} = 1.0. All experiments were done triplicates.

IV.3.5. Confirming the expression of LysSA11 in inducible system

Expression of LysSA11 in *S. cerevisiae* YVH10/pYDS-K-LysSA11 was confirmed by analyzing intracellular proteins and concentrated culture supernatant at early- and late-exponential phase (Figure IV-6). Regarding the fact that 10 μg of each protein sample was loaded, the difference in band intensity between early- and late-exponential phase makes it obvious that secretion of target protein could be largely impaired when the culture approaches stationary phase. In fact, the adverse effect of cell starvation toward recombinant protein secretion has been reported (D. Huang et al., 2008), hence such decrease in protein product could be avoided by adjusting the harvesting time. Originally, the molecular weight of secreted LysSA11 was predicted as approximately 28 kDa. From intracellular protein samples, dense protein bands were detected at 28 kDa and 40 kDa region, thus it can be assumed that nascent LysSA11 products are accumulated in the cell interior. According to a previous study, such accumulation of newly synthesized protein could be caused by fusing the α-factor signal peptide, but not the full-length secretion signal (Fitzgerald & Glick, 2014), and it may explain the accumulation of LysSA11 in this case as well. However, from the concentrated culture supernatant, the signal at 28 kDa region has become much weaker than that from cell lysate. Taking into account for the intense band at 40 kDa region from supernatant concentrate, it could be hypothesized that LysSA11 is post-translationally glycosylated during secretion.

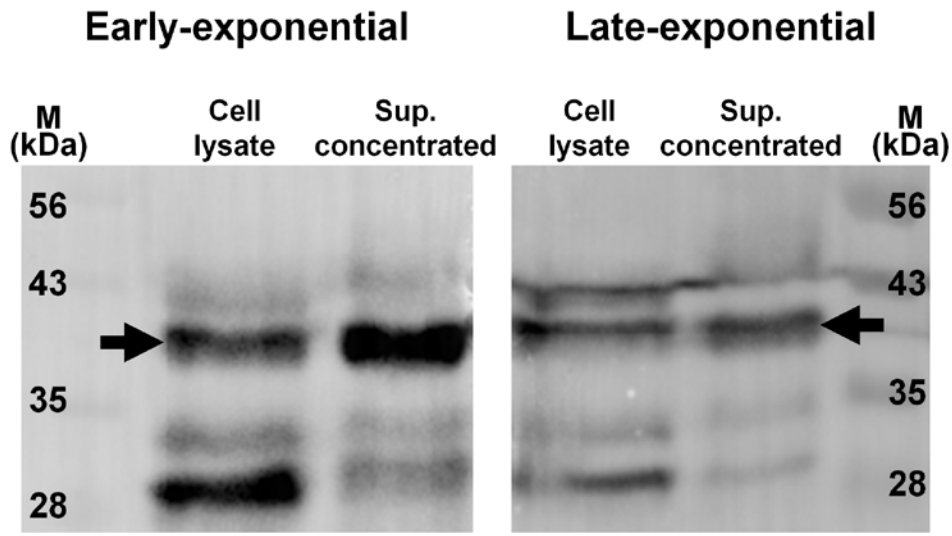

Figure IV-6. Expression of LysSA11 in *S. cerevisiae* YVH10/pYDS-K-LysSA11 at 30℃.

Western blot data of intracellularly expressed and extracellularly secreted LysSA11 from *S. cerevisiae* YVH10/pYDS-K-LysSA11 induced at 30℃. Ten microgram of each protein sample was loaded to each well. Detected bands of LysSA11 are marked with black arrows.

In order to verify whether the secreted LysSA11 is glycosylated or not, protein samples were treated with PNGase F to remove N-glycosyl moieties (Figure IV-7). For deglycosylation assay, concentrated supernatant of early- and late-exponential phase cultures were used. From coomassie blue stained gel (Figure IV-7A), the putative band for LysSA11 (same size as Figure IV-6) was identified, as well as PNGase F (molecular weight: 36 kDa). Interestingly, a thin band was observed at approximately 30 kDa region in the deglycosylated supernatant concentrates of both growth phases from Figure IV-7A and B (lower red arrows), while a thin band of 50 kDa in early-exponential phase disappears after deglycosylation. However, despite the assumptions, since the major band identified from both Figure IV-6 and 7 has a molecular weight of approximately 40 kDa, it can be assumed that LysSA11 might carry O-linked glycosidic bonds. Unfortunately, due to lack of O-glycosidase activity, O-glycosylation could not be verified by PNGase F.

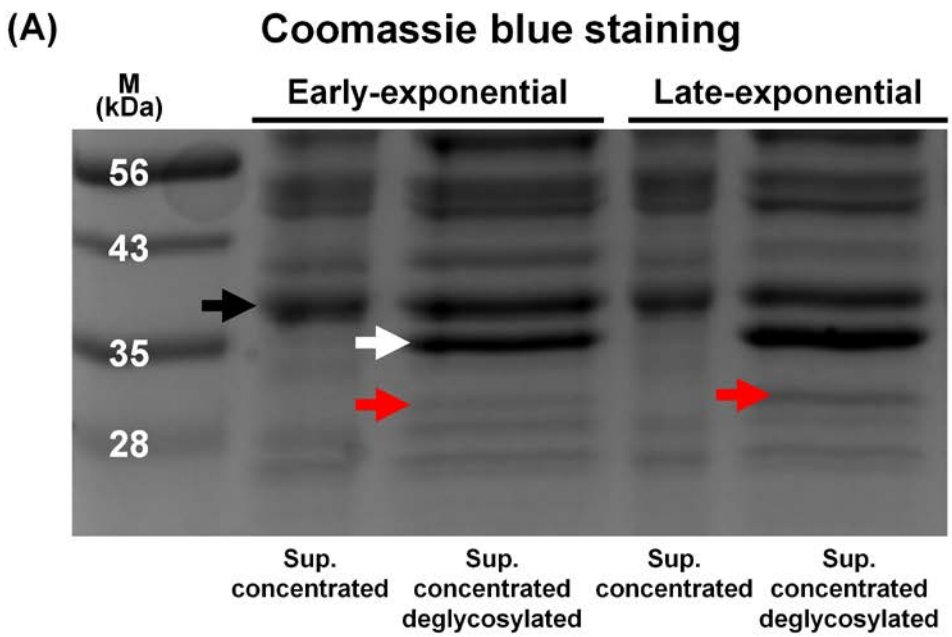
(A)
Coomassie blue staining
M (kDa)
Early-exponential
Late-exponential
56
43
35
28
Sup. concentrated
Sup. concentrated deglycosylated
Sup. concentrated
Sup. concentrated deglycosylated

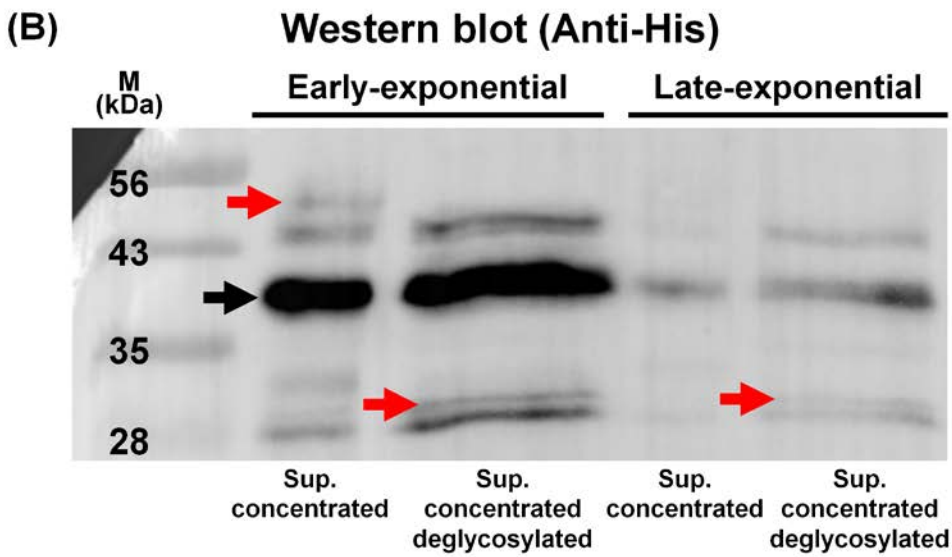
(B)
Western blot (Anti-His)
M (kDa)
Early-exponential
Late-exponential
56
43
35
28
Sup. concentrated
Sup. concentrated deglycosylated
Sup. concentrated
Sup. concentrated deglycosylated

Figure IV-7. Glycosylation of LysSA11 secreted from *S. cerevisiae* YVH10/pYDS-K-LysSA11.

Size discrimination of proteins in intact or deglycosylated supernatant concentrate from *S. cerevisiae* YVH10/pYDS-K-LysSA11 induced at 30℃ visualized by (A) coomassie blue staining and (B) western blot assay. The microgram of each protein sample was loaded to each well. Protein bands representing LysSA11, putative glycosylated/deglycosylated LysSA11, and PNGase F are marked with black, red, and white arrows, respectively.

Then, the potential activity of secreted LysSA11 was examined by conducting zymography assay. To compare the relative migration of proteins in each sample (purified LysSA11 from *E. coli*, concentrate of un-induced supernatant from *S. cerevisiae*, and concentrate of induced supernatant from *S. cerevisiae*), SDS gels were prepared along with zymogram gel (SDS gel containing autoclaved *S. aureus* as a substrate) (Figure IV-8). As a result, purified LysSA11 from *E. coli* was detected as a thick band at around 28 kDa in both coomassie blue stained gel (Figure IV-8A) and western blot image (Figure IV-8B). In the zymogram gel, it digested the peptidoglycan of the autoclaved *S. aureus*, leaving the area un-stained, making it appear as a light-blue colored band (Figure IV-8C). Likewise, thin and rather vague band appears from the concentrate of induced supernatant collected from *S. cerevisiae* in all three gel images (Figure IV-8). However, it can be learned from the thickness, which is much thinner than LysSA11 from *E. coli*, it can be assumed that the actual amount of secreted LysSA11 in the supernatant is scarce even after concentration.

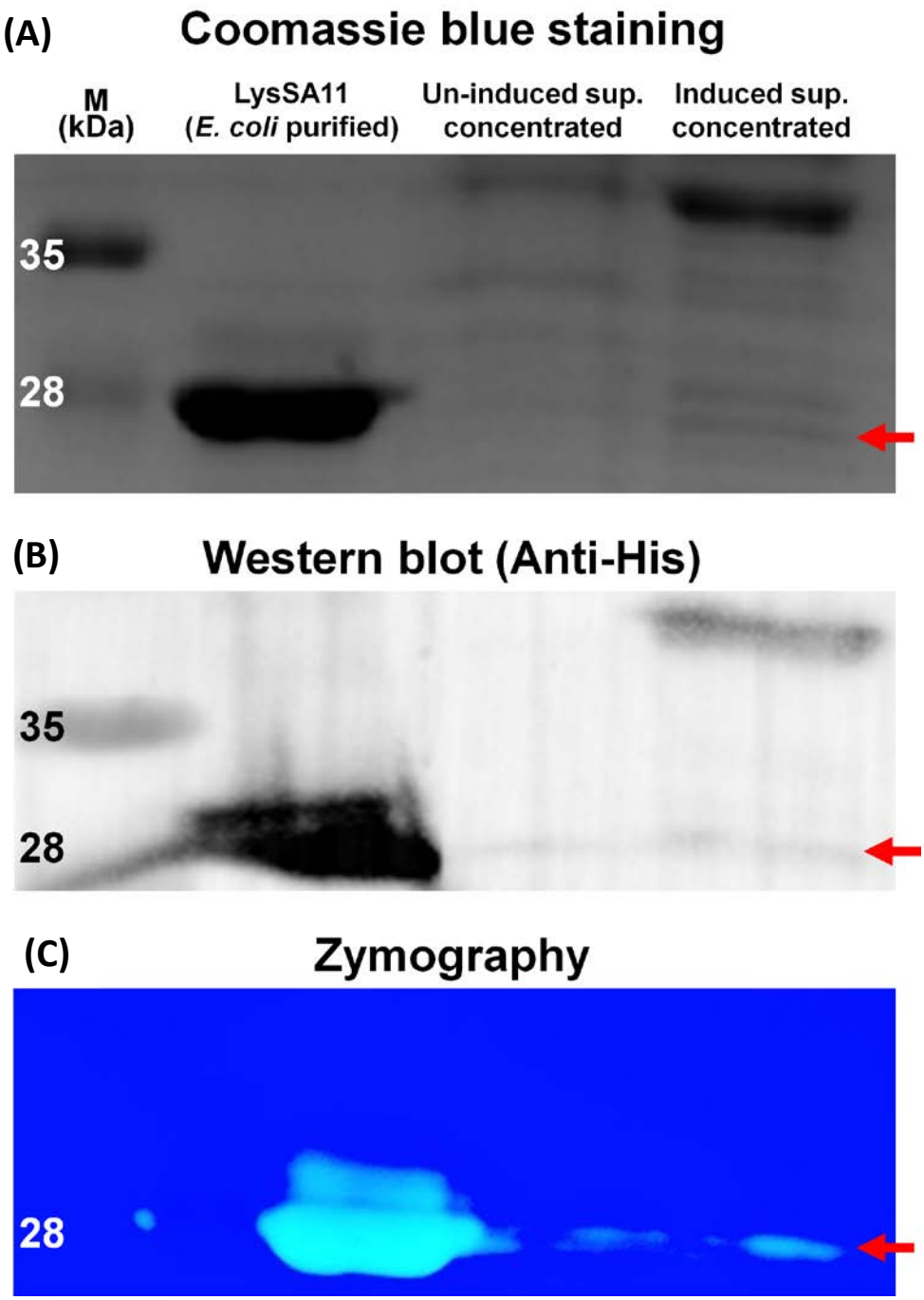
(A)
Coomassie blue staining
M
(kDa)
LysSA11
(E. coli purified)
Un-induced sup.
concentrated
Induced sup.
concentrated
35
28
(B)
Western blot (Anti-His)
35
28
(C)
Zymography
28

Figure IV-8. Zymography of LysSA11 secreted from *S. cerevisiae* YVH10/pYDS-K-LysSA11.

Size discrimination of proteins in supernatant concentrate from *S. cerevisiae* YVH10/pYDS-K-LysSA11 induced at 30℃ or LysSA11 purified from *E. coli* host were visualized by (A) coomassie blue staining and (B) western blot assay. (C) The peptidoglycan hydrolase activity was visualized by zymography.

IV.3.6. Confirming the expression of LysSA11 in constitutive system

Meanwhile, constitutive expression of LysSA11 from p404TEF1 vector system was analyzed. Since there is no inducing procedure required in this system, the recombinant yeast strains were cultivated in glucose media and harvested at 4, 6, 8, and 10 h after inoculation. In this system, p404TEF1-LysSA11-noHis was used as a false negative control for western blot assay. To be specific, since it does not carry C-terminal His-tag, it cannot be detected by anti-His antibody, but due to possible non-specific labeling, it could be puzzling to recognize the exact band for LysSA11. At this point, since the false negative control cannot have its LysSA11 to be labeled, we could distinguish the correct band for LysSA11 by comparing non-specific labels of p404TEF1-LysSA11 and the false negative control (Figure IV-9).

As expected, the bands for LysSA11 were successfully distinguished from intracellular proteins and concentrated culture supernatants. From all the cell lysates, two distinctive bands were identified at 28 kDa and 30 kDa, approximately. Moreover, those bands could also be recognized from supernatant concentrates, in which the intensity have gradually increased over time. Interestingly, a very thin band with molecular weight of 28 kDa was observed in the original supernatant at 8 and 10 h (Figure IV-9C, D). Since the predicted size of native LysSA11 is 28 kDa, it could be assumed that secreted protein in this system may not be heavily glycosylated.

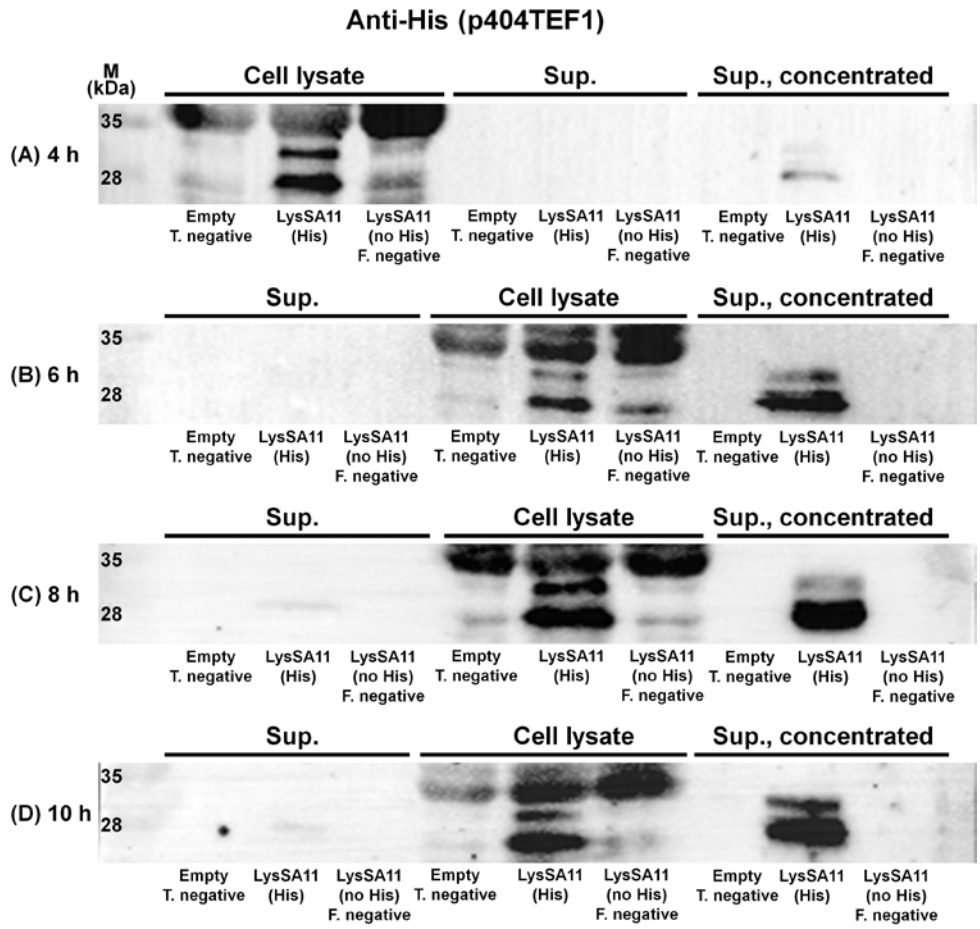

Figure IV-9. Expression of LysSA11 in *S. cerevisiae* EBY100/p404TEF1-LysSA11 at 30℃.

Western blot data of proteins in cell lysate, culture supernatant, and concentrated culture supernatant of *S. cerevisiae* EBY100/p404TEF1-LysSA11 and control groups harvested at different time points during growth in SDCAA at 30℃. Ten microgram of each protein sample was loaded to each well. Two different recombinant yeast strains were used as control groups: p404TEF1, true negative; p404TEF1-LysSA11-noHis, false negative.

IV.3.7. Antibacterial activity of yeast-secreted LysSA11 against *S. aureus* ATCC 13301

Based on the expression pattern of LysSA11 from inducible or constitutive promoter systems, culture supernatant from each strain was prepared and concentrated to an equivalent level to examine its effect on *S. aureus* ATCC 13301 (Figure IV-10). Starting from three replicative batches of 50 mL yeast culture mixed with identical volume of LysSA11 storage buffer, total of 300 mL of supernatant-buffer mixtures were concentrated to a final volume of 2 mL (150× concentration). By combining the concentrated early-exponential yeast supernatant with exponentially grown *S. aureus* ATCC 13301 in LysSA11 reaction buffer, the bacterial population was reduced by approximately 4.39-log CFU within 4 h (Figure IV-10A). On the other hand, late-exponential supernatant concentrate could only accomplish 1.73 log reduction (Figure IV-10B). Meanwhile, LysSA11 from constitutive expression system did not exhibit any inhibitory activity against LysSA11, hence it was decided to be excluded for further experiments (Figure IV-10C).

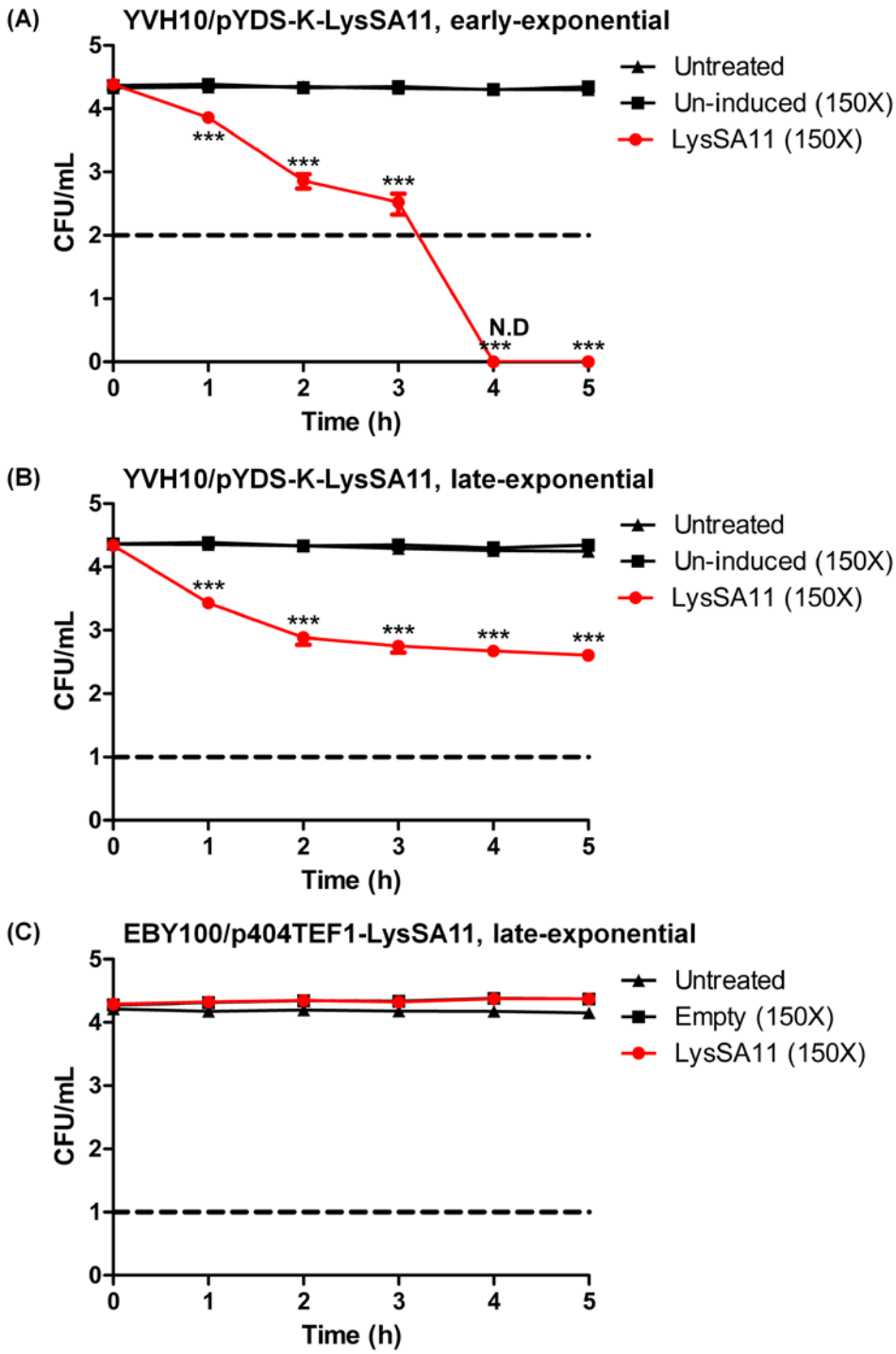
(A)
YVH10/pYDS-K-LysSA11, early-exponential
CFU/mL
Time (h)
Untreated
Un-induced (150X)
LysSA11 (150X)
***
N.D
(B)
YVH10/pYDS-K-LysSA11, late-exponential
CFU/mL
Time (h)
Untreated
Un-induced (150X)
LysSA11 (150X)
***
(C)
EBY100/p404TEF1-LysSA11, late-exponential
CFU/mL
Time (h)
Untreated
Empty (150X)
LysSA11 (150X)

Figure IV-10. Antibacterial activity of yeast-secreted LysSA11 from different hosts.

Population change of *S. aureus* ATCC 13301 upon treatment with concentrated culture supernatant of different yeast hosts (*S. cerevisiae* YVH10/pYDS-K-LysSA11 and *S. cerevisiae* EBY100/p404TEF1-LysSA11, EBY100/p404TEF1) at different growth phase (early or late-exponential) was plotted. The host strains were cultivated at 30℃, low cell density condition. Dashed lines denote the limit of detection (N.D, not detected). Asterisks indicate the significance of variances (***, $P < 0.0001$). All experiments were done triplicates.

According to the result in Figure IV-10, several different induction conditions were tested with *S. cerevisiae* YVH10/pYDS-K-LysSA11 to figure out the most favorable expression condition (Figure IV-11). Two different induction temperatures, 30℃ and 20℃ were tested, regarding to the findings reported in a previous study (D. Huang et al., 2008). In yeast system, accumulation of heterologous protein may trigger unfolded protein response (UPR), which takes part in the protein folding and degradation (Kimata, Ishiwata-Kimata, Yamada, & Kohno, 2006). Interestingly, it was reported that UPR can be minimized by conducting induction of secreted protein at 20℃ (D. Huang et al., 2008). Moreover, the density of cells to be inoculated in induction media was modified to investigate any improvements in productivity of recombinant protein. In fact, it has been stated in a review article that high cell density cultivation can be beneficial for protein productions (Shojaosadati, Varedi Kolaei, Babaeipour, & Farnoud, 2008). Therefore, I have tested the effect of dense population for the secretion of LysSA11 in an active form. As a result, it was confirmed that high cell density (initial OD_{600} = 5) in 20℃ could produce sufficient amount of active secreted LysSA11 in concentrated culture supernatant to have 4.31-log CFU of *S. aureus* ATCC 13301 to be eliminated (Figure IV-11C, F). When the high density culture was cultivated at 30℃, the secreted LysSA11 in concentrated culture supernatant could only accomplish 2.37-log reduction during 5 h (Figure IV-11B, E). This relatively impaired antibacterial action may be due

to the starved cells in stationary phase, since the culture was harvested at late-exponential or early-stationary phase (Figure IV-11B). In contrast to high density cultures, low density culture could not actually replicate to a certain extent at 20℃, hence the activity of LysSA11 in a highly concentrated culture supernatant was rather deteriorated than at 30℃. Taken together, although the activity of secreted LysSA11 could be maintained from high cell density at 20℃, since there was no significant increase in final concentration observed, more approaches would be required to improve endolysin secretion in yeast.

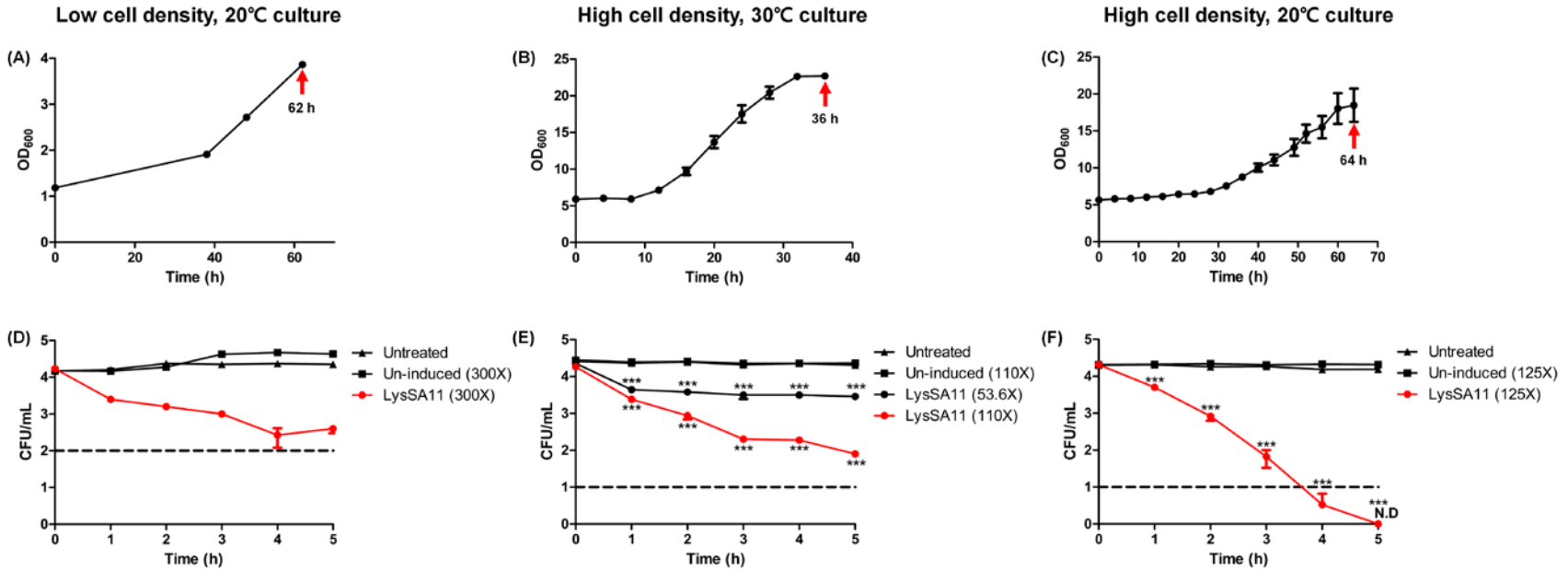
Low cell density, 20℃ culture
High cell density, 30℃ culture
High cell density, 20℃ culture
(A)
(B)
(C)
OD600
Time (h)
62 h
36 h
64 h
(D)
(E)
(F)
CFU/mL
Untreated
Un-induced (300X)
LysSA11 (300X)
Un-induced (110X)
LysSA11 (53.6X)
LysSA11 (110X)
Un-induced (125X)
LysSA11 (125X)
***
N.D

Figure IV-11. Antibacterial activity of LysSA11 secreted from inducible host with various induction conditions.

Growth of *S. cerevisiae* YVH10/pYDS-K-LysSA11 during induction and corresponding antibacterial activity of concentrated culture supernatant against *S. aureus* ATCC 13301 in (A, D) low cell density condition, 20℃, (B, E) high cell density condition, 30℃, and (C, F) high cell density condition, 20℃. The harvesting time of each culture is marked with red arrows. Dashed lines denote the limit of detection (N.D, not detected). Asterisks indicate the significance of variances (***, $P < 0.0001$). All experiments were done triplicates.

IV.3.8. Antibacterial activity of LysSA11-secreting yeast against *S. aureus* ATCC 13301

In addition to the activity of secreted LysSA11, the effect of *S. cerevisiae* harvested from induced culture upon *S. aureus* ATCC 13301 was analyzed (Figure IV-12). When the *S. aureus* cells prepared in 0.4% distilled water-based soft agar were poured over the pre-incubated yeast spots on SGCAAT (Figure IV-12A) or SDCAAT (Figure IV-12B) agar, bacterial growth was inhibited in SGCAAT, resulting in yeast spot culture with a transparent glossy surface and clear halo around it (Figure IV-12A). In contrast, on SDCAAT, yeast spot culture was thoroughly covered with *S. aureus* cells, resulting in typical yellow color of *S. aureus* colonies with turbid, matt surface (Figure IV-12B). When exponentially grown yeast cultures were spotted, the inhibitory effect was more obvious, with a larger halo and clear yeast surface (Figure IV-12C, D). When the overlay plate was incubated for an elongated period, *S. aureus* cells have synthesized more yellow pigment, staphyloxanthin (Lan, Cheng, Dunman, Missiakas, & He, 2010), but the inhibition zone appearing as clear halo was not overtaken by surrounding *S. aureus* cells (Figure IV-12D). From these data, it can be regarded that induced yeast cells would resume the expression and secretion of LysSA11 when inoculated to a fresh inducing media.

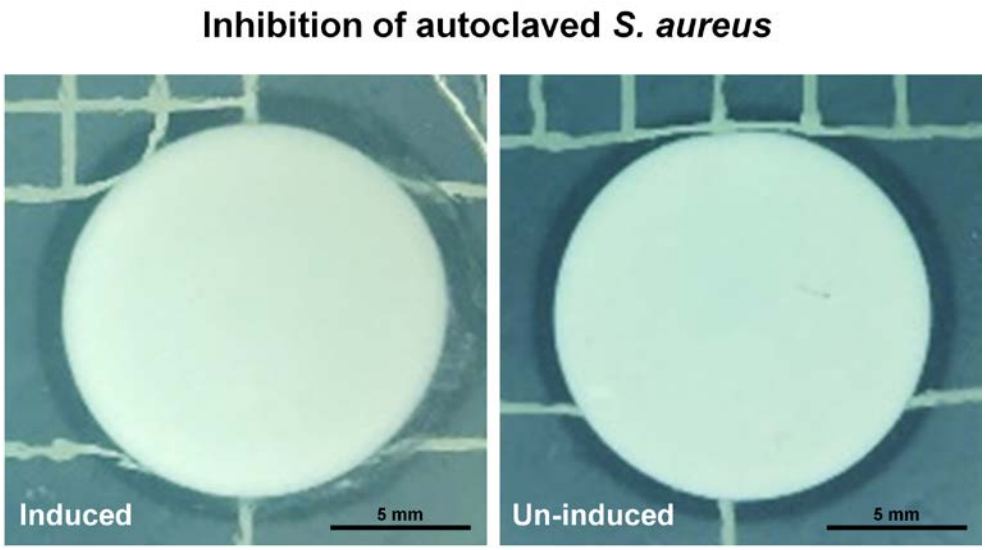

Figure IV-12. Antibacterial activity of LysSA11-secreting inducible yeast visualized on solid culture matrix.

Effect of pre-cultured *S. cerevisiae* YVH10/pYDS-K-LysSA11 spots on (A) SGCAAT or (B) SDCAAT agar media to the growth of *S. aureus* ATCC 13301 overlay culture. Growth and morphological changes in *S. aureus* ATCC 13301 culture over *S. cerevisiae* YVH10/pYDS-K-LysSA11 spots at (C) 24 h or (D) 48 h after overlay assay. Yeast was pre-cultured to early- or late-exponential phase in SGCAAT and spotted on SGCAAT agar media.

References

Ackermann, H.-W. (2006). Classification of bacteriophages. *The bacteriophages, 635*, 8-16.

Adriaenssens, E. M., Ackermann, H.-W., Anany, H., Blasdel, B., Connerton, I. F., Goulding, D., . . . Lavigne, R. (2012). A suggested new bacteriophage genus: “Viunalikevirus”. *Archives of Virology, 157*(10), 2035-2046. doi:10.1007/s00705-012-1360-5

Adriaenssens, E. M., Wittmann, J., Kuhn, J. H., Turner, D., Sullivan, M. B., Dutilh, B. E., . . . Rodney Brister, J. (2018). Taxonomy of prokaryotic viruses: 2017 update from the ICTV Bacterial and Archaeal Viruses Subcommittee. *Archives of Virology, 163*(4), 1125-1129. doi:10.1007/s00705-018-3723-z

Alisky, J., Iczkowski, K., Rapoport, A., & Troitsky, N. (1998). Bacteriophages show promise as antimicrobial agents. *Journal of Infection, 36*(1), 5-15. doi:https://doi.org/10.1016/S0163-4453(98)92874-2

Aziz, R. K., Bartels, D., Best, A. A., DeJongh, M., Disz, T., Edwards, R. A., . . . Zagnitko, O. (2008). The RAST Server: rapid annotations using subsystems technology. *BMC genomics, 9*, 75-75. doi:10.1186/1471-

2164-9-75

Bai, J., Yang, E., Chang, P.-s., & Ryu, S. (2019). Preparation and characterization of endolysin-containing liposomes and evaluation of their antimicrobial activities against Gram-negative bacteria. *Enzyme and Microbial Technology*.

Banfield, D. K. (2011). Mechanisms of protein retention in the Golgi. *Cold Spring Harbor perspectives in biology, 3*(8), a005264-a005264. doi:10.1101/cshperspect.a005264

Becker, S. C., Dong, S., Baker, J. R., Foster-Frey, J., Pritchard, D. G., & Donovan, D. M. (2009). LysK CHAP endopeptidase domain is required for lysis of live staphylococcal cells. *FEMS Microbiology Letters, 294*(1), 52-60. doi:10.1111/j.1574-6968.2009.01541.x

Becker, S. C., Foster-Frey, J., & Donovan, D. M. (2008). The phage K lytic enzyme LysK and lysostaphin act synergistically to kill MRSA. *FEMS Microbiology Letters, 287*(2), 185-191. doi:10.1111/j.1574-6968.2008.01308.x

Becker, S. C., Swift, S., Korobova, O., Schischkova, N., Kopylov, P., Donovan, D. M., & Abaev, I. (2015). Lytic activity of the staphylolytic Twort phage endolysin CHAP domain is enhanced by the SH3b cell wall binding domain. *FEMS Microbiology Letters, 362*(1), 1-8.

doi:10.1093/femsle/fnu019

Bérard, S., Chateau, A., Pompidor, N., Guertin, P., Bergeron, A., & Swenson, K. M. (2016). Aligning the unalignable: bacteriophage whole genome alignments. *BMC Bioinformatics, 17*(1), 30. doi:10.1186/s12859-015-0869-5

Berry, J., Rajaure, M., Pang, T., & Young, R. (2012). The Spanin Complex Is Essential for Lambda Lysis. *Journal of Bacteriology, 194*(20), 5667. doi:10.1128/JB.01245-12

Besemer, J., Lomsadze, A., & Borodovsky, M. (2001). GeneMarkS: a self-training method for prediction of gene starts in microbial genomes. Implications for finding sequence motifs in regulatory regions. *Nucleic Acids Research, 29*(12), 2607-2618. doi:10.1093/nar/29.12.2607

Boder, E. T., & Wittrup, K. D. (1997). Yeast surface display for screening combinatorial polypeptide libraries. *Nature Biotechnology, 15*(6), 553-557. doi:10.1038/nbt0697-553

Briers, Y., & Lavigne, R. (2015). Breaking barriers: expansion of the use of endolysins as novel antibacterials against Gram-negative bacteria. *Future microbiology, 10*(3), 377-390. doi:10.2217/fmb.15.8

Brown-Jaque, M., Calero-Cáceres, W., & Muniesa, M. (2015). Transfer of

antibiotic-resistance genes via phage-related mobile elements. *Plasmid, 79*, 1-7. doi:https://doi.org/10.1016/j.plasmid.2015.01.001

Buijs, N. A., Siewers, V., & Nielsen, J. (2013). Advanced biofuel production by the yeast Saccharomyces cerevisiae. *Current Opinion in Chemical Biology, 17*(3), 480-488. doi:https://doi.org/10.1016/j.cbpa.2013.03.036

Camacho, C., Coulouris, G., Avagyan, V., Ma, N., Papadopoulos, J., Bealer, K., & Madden, T. L. (2009). BLAST+: architecture and applications. *BMC Bioinformatics, 10*, 421-421. doi:10.1186/1471-2105-10-421

Caplan, S., Green, R., Rocco, J., & Kurjan, J. (1991). Glycosylation and structure of the yeast MF alpha 1 alpha-factor precursor is important for efficient transport through the secretory pathway. *Journal of Bacteriology, 173*(2), 627-635.

Caplan, S., & Kurjan, J. (1991). Role of alpha-factor and the MF alpha 1 alpha-factor precursor in mating in yeast. *Genetics, 127*(2), 299-307.

Carrió, M. M., & Villaverde, A. (2002). Construction and deconstruction of bacterial inclusion bodies. *Journal of Biotechnology, 96*(1), 3-12. doi:https://doi.org/10.1016/S0168-1656(02)00032-9

Carver, T., Harris, S. R., Berriman, M., Parkhill, J., & McQuillan, J. A. (2012). Artemis: an integrated platform for visualization and analysis of high-

throughput sequence-based experimental data. *Bioinformatics (Oxford, England), 28*(4), 464-469. doi:10.1093/bioinformatics/btr703

Carver, T. J., Rutherford, K. M., Berriman, M., Rajandream, M.-A., Barrell, B. G., & Parkhill, J. (2005). ACT: the Artemis comparison tool. *Bioinformatics (Oxford, England), 21*(16), 3422-3423. doi:10.1093/bioinformatics/bti553

Casjens, S. R. (2005). Comparative genomics and evolution of the tailed-bacteriophages. *Current opinion in microbiology, 8*(4), 451-458. doi:https://doi.org/10.1016/j.mib.2005.06.014

Catalão, M. J., Gil, F., Moniz-Pereira, J., São-José, C., & Pimentel, M. (2013). Diversity in bacterial lysis systems: bacteriophages show the way. *FEMS Microbiology Reviews, 37*(4), 554-571. doi:10.1111/1574-6976.12006

Cenens, W., Makumi, A., Mebrhatu, M. T., Lavigne, R., & Aertsen, A. (2013). Phage-host interactions during pseudolysogeny: Lessons from the Pid/dgo interaction. *Bacteriophage, 3*(1), e25029-e25029. doi:10.4161/bact.25029

Center for Disease, C., Prevention, Lee, M.-J., Song, K.-Y., Lee, W.-C., Chon, J.-W., . . . Seo, K.-H. (2019). Epidemiological aspects of pathogenic

microbial foodborne disease outbreaks in Korea and Japan from 2011 to 2015. *Journal of Preventive Veterinary Medicine, 43*(2), 62-67. doi:10.13041/jpvm.2019.43.2.62

Cereghino, J. L., & Cregg, J. M. (2000). Heterologous protein expression in the methylotrophic yeast Pichia pastoris. *FEMS Microbiology Reviews, 24*(1), 45-66.

Cervera-Alamar, M., Guzmán-Markevitch, K., Žiemytė, M., Ortí, L., Bernabé-Quispe, P., Pineda-Lucena, A., . . . Tormo-Mas, M. Á. (2018). Mobilisation Mechanism of Pathogenicity Islands by Endogenous Phages in Staphylococcus aureus clinical strains. *Scientific Reports, 8*(1), 16742. doi:10.1038/s41598-018-34918-2

Cha, J. O., Lee, J. K., Jung, Y. H., Yoo, J. I., Park, Y. K., Kim, B. S., & Lee, Y. S. (2006). Molecular analysis of Staphylococcus aureus isolates associated with staphylococcal food poisoning in South Korea. *Journal of Applied Microbiology, 101*(4), 864-871. doi:10.1111/j.1365-2672.2006.02957.x

Chambers, H. F., & DeLeo, F. R. (2009). Waves of resistance: Staphylococcus aureus in the antibiotic era. *Nature Reviews Microbiology, 7*, 629. doi:10.1038/nrmicro2200

Chang, Y., Kim, M., & Ryu, S. (2017). Characterization of a novel endolysin

LysSA11 and its utility as a potent biocontrol agent against Staphylococcus aureus on food and utensils. *Food Microbiology, 68*, 112-120. doi:https://doi.org/10.1016/j.fm.2017.07.004

Chao, G., Lau, W. L., Hackel, B. J., Sazinsky, S. L., Lippow, S. M., & Wittrup, K. D. (2006). Isolating and engineering human antibodies using yeast surface display. *Nature Protocols, 1*(2), 755-768. doi:10.1038/nprot.2006.94

Chen, L., Yang, J., Yu, J., Yao, Z., Sun, L., Shen, Y., & Jin, Q. (2005). VFDB: a reference database for bacterial virulence factors. *Nucleic Acids Research, 33*(Database issue), D325-D328. doi:10.1093/nar/gki008

Cherf, G. M., & Cochran, J. R. (2015). Applications of Yeast Surface Display for Protein Engineering. *Methods in molecular biology (Clifton, N.J.), 1319*, 155-175. doi:10.1007/978-1-4939-2748-7_8

Chin, C.-S., Alexander, D. H., Marks, P., Klammer, A. A., Drake, J., Heiner, C., . . . Korlach, J. (2013). Nonhybrid, finished microbial genome assemblies from long-read SMRT sequencing data. *Nature Methods, 10*, 563. doi:10.1038/nmeth.2474

Choi, J., & Bischof, J. C. (2010). Review of biomaterial thermal property measurements in the cryogenic regime and their use for prediction of equilibrium and non-equilibrium freezing applications in cryobiology.

Cryobiology, 60(1), 52-70. doi:https://doi.org/10.1016/j.cryobiol.2009.11.004

Cramton, S. E., Gerke, C., Schnell, N. F., Nichols, W. W., Götz, F. J. I., & immunity. (1999). The intercellular adhesion (ica) locus is present in Staphylococcus aureus and is required for biofilm formation. *67*(10), 5427-5433.

Damasceno, L. M., Huang, C.-J., Batt, C. A. J. A. m., & biotechnology. (2012). Protein secretion in Pichia pastoris and advances in protein production. *93*(1), 31-39.

Davies, J. (1994). Inactivation of antibiotics and the dissemination of resistance genes. *Science, 264*(5157), 375. doi:10.1126/science.8153624

Davies, J., & Davies, D. (2010). Origins and Evolution of Antibiotic Resistance. *Microbiology and Molecular Biology Reviews, 74*(3), 417. doi:10.1128/MMBR.00016-10

Delcher, A. L., Bratke, K. A., Powers, E. C., & Salzberg, S. L. (2007). Identifying bacterial genes and endosymbiont DNA with Glimmer. *Bioinformatics (Oxford, England), 23*(6), 673-679. doi:10.1093/bioinformatics/btm009

Dickson, J. S., & Koohmaraie, M. (1989). Cell surface charge characteristics

and their relationship to bacterial attachment to meat surfaces. *Applied and Environmental Microbiology, 55*(4), 832-836.

Dinges, M. M., Orwin, P. M., & Schlievert, P. M. (2000). Exotoxins of Staphylococcus aureus. *Clinical microbiology reviews, 13*(1), 16-34. doi:10.1128/cmr.13.1.16-34.2000

Dunne Jr, W. M., Pouseele, H., Monecke, S., Ehricht, R., & van Belkum, A. (2018). Epidemiology of transmissible diseases: array hybridization and next generation sequencing as universal nucleic acid-mediated typing tools. *Infection, Genetics Evolution, 63*, 332-345.

Erez, Z., Steinberger-Levy, I., Shamir, M., Doron, S., Stokar-Avihail, A., Peleg, Y., . . . Sorek, R. (2017). Communication between viruses guides lysis–lysogeny decisions. *Nature, 541*, 488. doi:10.1038/nature21049

. Family - Myoviridae. (2012). In A. M. Q. King, M. J. Adams, E. B. Carstens, & E. J. Lefkowitz (Eds.), *Virus Taxonomy* (pp. 46-62). San Diego: Elsevier.

. Family - Podoviridae. (2012). In A. M. Q. King, M. J. Adams, E. B. Carstens, & E. J. Lefkowitz (Eds.), *Virus Taxonomy* (pp. 63-85). San Diego: Elsevier.

. Family - Siphoviridae. (2012). In A. M. Q. King, M. J. Adams, E. B. Carstens,

& E. J. Lefkowitz (Eds.), *Virus Taxonomy* (pp. 86-98). San Diego: Elsevier.

Fernández-Ruiz, I., Coutinho, F. H., & Rodriguez-Valera, F. (2018). Thousands of Novel Endolysins Discovered in Uncultured Phage Genomes. *Frontiers in microbiology, 9*(1033). doi:10.3389/fmicb.2018.01033

Fernández, L., Gutiérrez, D., Rodríguez, A., & García, P. (2018). Application of Bacteriophages in the Agro-Food Sector: A Long Way Toward Approval. *Frontiers in cellular and infection microbiology, 8*, 296-296. doi:10.3389/fcimb.2018.00296

Fischetti, V. A. (2005). Bacteriophage lytic enzymes: novel anti-infectives. *Trends in Microbiology, 13*(10), 491-496. doi:https://doi.org/10.1016/j.tim.2005.08.007

Fischetti, V. A. (2008). Bacteriophage lysins as effective antibacterials. *Current opinion in microbiology, 11*(5), 393-400.

Fischetti, V. A. (2010). Bacteriophage endolysins: A novel anti-infective to control Gram-positive pathogens. *International Journal of Medical Microbiology, 300*(6), 357-362. doi:https://doi.org/10.1016/j.ijmm.2010.04.002

Fischetti, V. A. (2011). Exploiting what phage have evolved to control gram-

positive pathogens. *Bacteriophage, 1*(4), 188-194. doi:10.4161/bact.1.4.17747

Fitzgerald, I., & Glick, B. S. (2014). Secretion of a foreign protein from budding yeasts is enhanced by cotranslational translocation and by suppression of vacuolar targeting. *Microbial Cell Factories, 13*(1), 125. doi:10.1186/s12934-014-0125-0

Fortier, L.-C., & Sekulovic, O. (2013). Importance of prophages to evolution and virulence of bacterial pathogens. *Virulence, 4*(5), 354-365. doi:10.4161/viru.24498

Foster, T. J., Geoghegan, J. A., Ganesh, V. K., & Höök, M. (2013). Adhesion, invasion and evasion: the many functions of the surface proteins of Staphylococcus aureus. *Nature Reviews Microbiology, 12*, 49. doi:10.1038/nrmicro3161

Fowler Jr, V. G., Fey, P. D., Reller, L. B., Chamis, A. L., Corey, G. R., & Rupp, M. E. (2001). The intercellular adhesin locus ica is present in clinical isolates of Staphylococcus aureus from bacteremic patients with infected and uninfected prosthetic joints. *Medical microbiology immunology, 189*(3), 127-131.

Fridkin, S. K., Hageman, J. C., Morrison, M., Sanza, L. T., Como-Sabetti, K., Jernigan, J. A., . . . Farley, M. M. (2005). Methicillin-resistant

Staphylococcus aureus disease in three communities. *New England Journal of Medicine, 352*(14), 1436-1444.

Gai, S. A., & Wittrup, K. D. (2007). Yeast surface display for protein engineering and characterization. *Current opinion in structural biology, 17*(4), 467-473. doi:10.1016/j.sbi.2007.08.012

Galdieri, L., Mehrotra, S., Yu, S., & Vancura, A. (2010). Transcriptional regulation in yeast during diauxic shift and stationary phase. *Omics : a journal of integrative biology, 14*(6), 629-638. doi:10.1089/omi.2010.0069

Gancedo, J. M. (1998). Yeast Carbon Catabolite Repression. *Microbiology and Molecular Biology Reviews, 62*(2), 334.

Gordon, N., Price, J., Cole, K., Everitt, R., Morgan, M., Finney, J., . . . Wilson, D. (2014). Prediction of Staphylococcus aureus antimicrobial resistance by whole-genome sequencing. *Journal of clinical microbiology, 52*(4), 1182-1191.

Grose, J. H., & Casjens, S. R. (2014). Understanding the enormous diversity of bacteriophages: The tailed phages that infect the bacterial family Enterobacteriaceae. *Virology, 468-470*, 421-443. doi:https://doi.org/10.1016/j.virol.2014.08.024

Gründling, A., Missiakas, D. M., & Schneewind, O. (2006). Staphylococcus

aureus mutants with increased lysostaphin resistance. *Journal of Bacteriology, 188*(17), 6286-6297. doi:10.1128/JB.00457-06

Gründling, A., & Schneewind, O. (2006). Cross-Linked Peptidoglycan Mediates Lysostaphin Binding to the Cell Wall Envelope of Staphylococcus aureus. *Journal of Bacteriology, 188*(7), 2463. doi:10.1128/JB.188.7.2463-2472.2006

Hamilton, S. R., & Gerngross, T. U. (2007). Glycosylation engineering in yeast: the advent of fully humanized yeast. *Current Opinion in Biotechnology, 18*(5), 387-392. doi:https://doi.org/10.1016/j.copbio.2007.09.001

Han, M., & Yu, X. (2015). Enhanced expression of heterologous proteins in yeast cells via the modification of N-glycosylation sites. *Bioengineered, 6*(2), 115-118. doi:10.1080/21655979.2015.1011031

Harris, S. R., Feil, E. J., Holden, M. T., Quail, M. A., Nickerson, E. K., Chantratita, N., . . . Lindsay, J. A. J. S. (2010). Evolution of MRSA during hospital transmission and intercontinental spread. *327*(5964), 469-474.

Hasman, H., Moodley, A., Guardabassi, L., Stegger, M., Skov, R. L., & Aarestrup, F. M. (2010). spa type distribution in Staphylococcus aureus originating from pigs, cattle and poultry. *Veterinary*

Microbiology, 141(3), 326-331. doi:https://doi.org/10.1016/j.vetmic.2009.09.025

Hatfull, G. F. (2008). Bacteriophage genomics. *Current opinion in microbiology, 11*(5), 447-453. doi:10.1016/j.mib.2008.09.004

Hoshida, H., Fujita, T., Cha-aim, K., & Akada, R. (2013). N-glycosylation deficiency enhanced heterologous production of a Bacillus licheniformis thermostable α-amylase in Saccharomyces cerevisiae. *Applied Microbiology and Biotechnology, 97*(12), 5473-5482. doi:10.1007/s00253-012-4582-2

Huang, D., Gore, P. R., & Shusta, E. V. (2008). Increasing yeast secretion of heterologous proteins by regulating expression rates and post-secretory loss. *Biotechnology and Bioengineering, 101*(6), 1264-1275. doi:10.1002/bit.22019

Huang, M., Bao, J., Hallström, B. M., Petranovic, D., & Nielsen, J. (2017). Efficient protein production by yeast requires global tuning of metabolism. *Nature communications, 8*(1), 1131-1131. doi:10.1038/s41467-017-00999-2

Hudzicki, J. (2009). Kirby-Bauer disk diffusion susceptibility test protocol. *ASM protocols*.

Humphries, R. M., Ambler, J., Mitchell, S. L., Castanheira, M., Dingle, T.,

Hindler, J. A., . . . Standardization Working Group of the Subcommittee on Antimicrobial Susceptibility, T. (2018). CLSI Methods Development and Standardization Working Group Best Practices for Evaluation of Antimicrobial Susceptibility Tests. *Journal of clinical microbiology, 56*(4), e01934-01917. doi:10.1128/JCM.01934-17

Jamet, A., Touchon, M., Ribeiro-Gonçalves, B., Carriço, J. A., Charbit, A., Nassif, X., . . . Rocha, E. P. C. (2017). A widespread family of polymorphic toxins encoded by temperate phages. *BMC biology, 15*(1), 75-75. doi:10.1186/s12915-017-0415-1

Jun, S. Y., Jang, I. J., Yoon, S., Jang, K., Yu, K.-S., Cho, J. Y., . . . Kang, S. H. (2017). Pharmacokinetics and Tolerance of the Phage Endolysin-Based Candidate Drug SAL200 after a Single Intravenous Administration among Healthy Volunteers. *Antimicrobial Agents and Chemotherapy, 61*(6), e02629-02616. doi:10.1128/AAC.02629-16

Jun, S. Y., Jung, G. M., Yoon, S. J., Choi, Y.-J., Koh, W. S., Moon, K. S., & Kang, S. H. (2014). Preclinical Safety Evaluation of Intravenously Administered SAL200 Containing the Recombinant Phage Endolysin SAL-1 as a Pharmaceutical Ingredient. *Antimicrobial Agents and Chemotherapy, 58*(4), 2084. doi:10.1128/AAC.02232-13

Jun, S. Y., Jung, G. M., Yoon, S. J., Oh, M.-D., Choi, Y.-J., Lee, W. J., . . . Kang, S. H. (2013). Antibacterial properties of a pre-formulated recombinant phage endolysin, SAL-1. *International Journal of Antimicrobial Agents*, *41*(2), 156-161. doi:https://doi.org/10.1016/j.ijantimicag.2012.10.011

Jun, S. Y., Jung, G. M., Yoon, S. J., Youm, S. Y., Han, H.-Y., Lee, J.-H., & Kang, S. H. (2016). Pharmacokinetics of the phage endolysin-based candidate drug SAL200 in monkeys and its appropriate intravenous dosing period. *Clinical and Experimental Pharmacology and Physiology*, *43*(10), 1013-1016. doi:10.1111/1440-1681.12613

Khatibi, P. A., Roach, D. R., Donovan, D. M., Hughes, S. R., & Bischoff, K. M. (2014). Saccharomyces cerevisiae expressing bacteriophage endolysins reduce Lactobacillus contamination during fermentation. *Biotechnology for Biofuels*, *7*(1), 104. doi:10.1186/1754-6834-7-104

Kim, J.-S., Daum, M., Jin, Y.-S., & Miller, M. J. V. (2018). Yeast Derived LysA2 Can Control Bacterial Contamination in Ethanol Fermentation. *10*(6), 281.

Kim, J.-S., Daum, M. A., Jin, Y.-S., & Miller, M. J. (2018). Yeast Derived LysA2 Can Control Bacterial Contamination in Ethanol Fermentation. *Viruses*, *10*(6), 281. doi:10.3390/v10060281

Kim, N.-H., Park, W. B., Cho, J. E., Choi, Y. J., Choi, S. J., Jun, S. Y., . . . Kim, H. B. (2018). Effects of Phage Endolysin SAL200 Combined with Antibiotics on Staphylococcus aureus Infection. *Antimicrobial Agents and Chemotherapy, 62*(10), e00731-00718. doi:10.1128/AAC.00731-18

Kim, Y. S. (2014). Construction of a large synthetic human Fab antibody library on yeast cell surface by optimized yeast mating. *J Journal of microbiology & biotechnology, 24*(3), 408-420.

Kimata, Y., Ishiwata-Kimata, Y., Yamada, S., & Kohno, K. (2006). Yeast unfolded protein response pathway regulates expression of genes for anti-oxidative stress and for cell surface proteins. *Genes to Cells, 11*(1), 59-69. doi:10.1111/j.1365-2443.2005.00921.x

Klis, F. M., Mol, P., Hellingwerf, K., & Brul, S. (2002). Dynamics of cell wall structure in Saccharomyces cerevisiae. *FEMS Microbiology Reviews, 26*(3), 239-256. doi:10.1111/j.1574-6976.2002.tb00613.x

Köser, C. U., Ellington, M. J., Cartwright, E. J., Gillespie, S. H., Brown, N. M., Farrington, M., . . . Parkhill, J. (2012). Routine use of microbial whole genome sequencing in diagnostic and public health microbiology. *PLoS pathogens, 8*(8), e1002824.

Kowalski, J. M., Parekh, R. N., & Wittrup, K. D. (1998). Secretion Efficiency

in Saccharomyces cerevisiae of Bovine Pancreatic Trypsin Inhibitor Mutants Lacking Disulfide Bonds Is Correlated with Thermodynamic Stability. *Biochemistry, 37*(5), 1264-1273. doi:10.1021/bi9722397

Kukuruzinska, M. A., Bergh, M. L. E., & Jackson, B. J. (1987). PROTEIN GLYCOSYLATION IN YEAST. *Annual Review of Biochemistry, 56*(1), 915-944. doi:10.1146/annurev.bi.56.070187.004411

Kuroda, K., & Ueda, M. (2013). Arming Technology in Yeast—Novel Strategy for Whole-cell Biocatalyst and Protein Engineering. *Biomolecules, 3*(3). doi:10.3390/biom3030632

Kurtz, S., Phillippy, A., Delcher, A. L., Smoot, M., Shumway, M., Antonescu, C., & Salzberg, S. L. (2004). Versatile and open software for comparing large genomes. *Genome biology, 5*(2), R12-R12. doi:10.1186/gb-2004-5-2-r12

Labrie, S. J., Samson, J. E., & Moineau, S. (2010). Bacteriophage resistance mechanisms. *Nature Reviews Microbiology, 8*(5), 317-327. doi:10.1038/nrmicro2315

Lagesen, K., Hallin, P., Rødland, E. A., Staerfeldt, H.-H., Rognes, T., & Ussery, D. W. (2007). RNAmmer: consistent and rapid annotation of ribosomal RNA genes. *Nucleic Acids Research, 35*(9), 3100-3108. doi:10.1093/nar/gkm160

Lan, L., Cheng, A., Dunman, P. M., Missiakas, D., & He, C. (2010). Golden Pigment Production and Virulence Gene Expression Are Affected by Metabolisms in Staphylococcus aureus. *Journal of Bacteriology, 192*(12), 3068. doi:10.1128/JB.00928-09

Laslett, D., & Canback, B. (2004). ARAGORN, a program to detect tRNA genes and tmRNA genes in nucleotide sequences. *Nucleic Acids Research, 32*(1), 11-16. doi:10.1093/nar/gkh152

Lee, A. S., de Lencastre, H., Garau, J., Kluytmans, J., Malhotra-Kumar, S., Peschel, A., & Harbarth, S. (2018). Methicillin-resistant Staphylococcus aureus. *Nature Reviews Disease Primers, 4*(1), 18033. doi:10.1038/nrdp.2018.33

Levy, S. B., & Marshall, B. (2004). Antibacterial resistance worldwide: causes, challenges and responses. *Nature Medicine, 10*, S122. doi:10.1038/nm1145

Lim, S., Lee, D.-H., Kwak, W., Shin, H., Ku, H.-J., Lee, J. E., . . . Ryu, S. (2015). Comparative genomic analysis of Staphylococcus aureus FORC_001 and S. aureus MRSA252 reveals the characteristics of antibiotic resistance and virulence factors for human infection. *J. Microbiol. Biotechnol, 25*(1), 98-108.

Lin, D. M., Koskella, B., & Lin, H. C. (2017). Phage therapy: An alternative

to antibiotics in the age of multi-drug resistance. *World journal of gastrointestinal pharmacology and therapeutics, 8*(3), 162-173. doi:10.4292/wjgpt.v8.i3.162

Loc-Carrillo, C., & Abedon, S. T. (2011). Pros and cons of phage therapy. *Bacteriophage, 1*(2), 111-114. doi:10.4161/bact.1.2.14590

Loessner, M. J. (2005). Bacteriophage endolysins—current state of research and applications. *Current opinion in microbiology, 8*(4), 480-487.

Love, M. J., Bhandari, D., Dobson, R. C. J., & Billington, C. (2018). Potential for Bacteriophage Endolysins to Supplement or Replace Antibiotics in Food Production and Clinical Care. *Antibiotics (Basel, Switzerland), 7*(1), 17. doi:10.3390/antibiotics7010017

Lowder, B. V., Guinane, C. M., Ben Zakour, N. L., Weinert, L. A., Conway-Morris, A., Cartwright, R. A., . . . Fitzgerald, J. R. (2009). Recent human-to-poultry host jump, adaptation, and pandemic spread of Staphylococcus aureus. *Proceedings of the National Academy of Sciences, 106*(46), 19545. doi:10.1073/pnas.0909285106

Lowy, F. D. (1998). Staphylococcus aureus Infections. *New England Journal of Medicine, 339*(8), 520-532. doi:10.1056/NEJM199808203390806

Luong, M., Lam, J. S., Chen, J., & Levitz, S. M. (2007). Effects of fungal N- and O-linked mannosylation on the immunogenicity of model

vaccines. *Vaccine, 25*(22), 4340-4344. doi:https://doi.org/10.1016/j.vaccine.2007.03.027

Maiden, M. C., Bygraves, J. A., Feil, E., Morelli, G., Russell, J. E., Urwin, R., . . . Caugant, D. A. (1998). Multilocus sequence typing: a portable approach to the identification of clones within populations of pathogenic microorganisms. *Proceedings of the National Academy of Sciences, 95*(6), 3140-3145.

Maiques, E., Úbeda, C., Campoy, S., Salvador, N., Lasa, Í., Novick, R. P., . . . Penadés, J. R. (2006). β-Lactam Antibiotics Induce the SOS Response and Horizontal Transfer of Virulence Factors in Staphylococcus aureus. *Journal of Bacteriology, 188*(7), 2726. doi:10.1128/JB.188.7.2726-2729.2006

Marciano, D. K., Russel, M., & Simon, S. M. (1999). An Aqueous Channel for Filamentous Phage Export. *Science, 284*(5419), 1516. doi:10.1126/science.284.5419.1516

Martínez-Alonso, M., González-Montalbán, N., García-Fruitós, E., & Villaverde, A. (2008). The Functional Quality of Soluble Recombinant Polypeptides Produced in Escherichia coli Is Defined by a Wide Conformational Spectrum. *Applied and Environmental Microbiology, 74*(23), 7431. doi:10.1128/AEM.01446-08

Martínez, J. L., Liu, L., Petranovic, D., & Nielsen, J. (2012). Pharmaceutical protein production by yeast: towards production of human blood proteins by microbial fermentation. *Current Opinion in Biotechnology, 23*(6), 965-971. doi:https://doi.org/10.1016/j.copbio.2012.03.011

Mattanovich, D., Branduardi, P., Dato, L., Gasser, B., Sauer, M., & Porro, D. (2012). Recombinant Protein Production in Yeasts. In A. Lorence (Ed.), *Recombinant Gene Expression* (pp. 329-358). Totowa, NJ: Humana Press.

McCarthy, H., Rudkin, J. K., Black, N. S., Gallagher, L., O'Neill, E., & O'Gara, J. P. (2015). Methicillin resistance and the biofilm phenotype in Staphylococcus aureus. *Frontiers in cellular and infection microbiology, 5*(1). doi:10.3389/fcimb.2015.00001

Medical Microbiology. 4th Edition. (1996). University of Texas Medical Branch at Galveston.

Mori, A., Hara, S., Sugahara, T., Kojima, T., Iwasaki, Y., Kawarasaki, Y., . . . Nakano, H. (2015). Signal peptide optimization tool for the secretion of recombinant protein from Saccharomyces cerevisiae. *Journal of Bioscience and Bioengineering, 120*(5), 518-525. doi:https://doi.org/10.1016/j.jbiosc.2015.03.003

Moye, Z. D., Woolston, J., & Sulakvelidze, A. (2018). Bacteriophage

Applications for Food Production and Processing. *Viruses*, *10*(4), 205. doi:10.3390/v10040205

Mumberg, D., Müller, R., & Funk, M. (1994). Regulatable promoters of Saccharomyces cerevisiae: comparison of transcriptional activity and their use for heterologous expression. *J Nucleic acids research*, *22*(25), 5767.

Nanra, J. S., Buitrago, S. M., Crawford, S., Ng, J., Fink, P. S., Hawkins, J., . . . Anderson, A. S. (2013). Capsular polysaccharides are an important immune evasion mechanism for Staphylococcus aureus. *Human vaccines & immunotherapeutics*, *9*(3), 480-487. doi:10.4161/hv.23223

Navarre, W. W., Ton-That, H., Faull, K. F., & Schneewind, O. (1999). Multiple Enzymatic Activities of the Murein Hydrolase from Staphylococcal Phage φ11 IDENTIFICATION OF A d-ALANYL-GLYCINE ENDOPEPTIDASE ACTIVITY. *Journal of Biological Chemistry*, *274*(22), 15847-15856.

Nelson, D. C., Schmelcher, M., Rodriguez-Rubio, L., Klumpp, J., Pritchard, D. G., Dong, S., & Donovan, D. M. (2012). Chapter 7 - Endolysins as Antimicrobials. In M. Łobocka & W. Szybalski (Eds.), *Advances in Virus Research* (Vol. 83, pp. 299-365): Academic Press.

Novák, P., & Havlíček, V. (2016). 4 - Protein Extraction and Precipitation. In P. Ciborowski & J. Silberring (Eds.), *Proteomic Profiling and Analytical Chemistry (Second Edition)* (pp. 51-62). Boston: Elsevier.

Novick, R. P., Christie, G. E., & Penadés, J. R. (2010). The phage-related chromosomal islands of Gram-positive bacteria. *Nature Reviews Microbiology, 8*(8), 541-551. doi:10.1038/nrmicro2393

Oppenheim, A. B., Kobiler, O., Stavans, J., Court, D. L., & Adhya, S. (2005). Switches in Bacteriophage Lambda Development. *Annual Review of Genetics, 39*(1), 409-429. doi:10.1146/annurev.genet.39.073003.113656

Ortega, E., Abriouel, H., Lucas, R., & Gálvez, A. (2010). Multiple roles of Staphylococcus aureus enterotoxins: pathogenicity, superantigenic activity, and correlation to antibiotic resistance. *Toxins, 2*(8), 2117-2131. doi:10.3390/toxins2082117

Otto, M. (2014). Staphylococcus aureus toxins. *Current opinion in microbiology, 17*, 32-37. doi:https://doi.org/10.1016/j.mib.2013.11.004

P R, V., & M, J. (2013). A comparative analysis of community acquired and hospital acquired methicillin resistant Staphylococcus aureus. *Journal of clinical and diagnostic research : JCDR, 7*(7), 1339-1342.

doi:10.7860/JCDR/2013/5302.3139

Parthasarathy, R., Bajaj, J., & Boder, E. T. (2005). An Immobilized Biotin Ligase: Surface Display of Escherichia coli BirA on Saccharomycescerevisiae. *Biotechnology Progress, 21*(6), 1627-1631. doi:10.1021/bp050279t

Partow, S., Siewers, V., Bjørn, S., Nielsen, J., & Maury, J. (2010). Characterization of different promoters for designing a new expression vector in Saccharomyces cerevisiae. *Yeast, 27*(11), 955-964. doi:10.1002/yea.1806

Peterson, P. K., Verhoef, J., Sabath, L. D., & Quie, P. G. (1977). Effect of protein A on staphylococcal opsonization. *Infection and immunity, 15*(3), 760-764.

Petsch, D., & Anspach, F. B. (2000). Endotoxin removal from protein solutions. *Journal of Biotechnology, 76*(2), 97-119. doi:https://doi.org/10.1016/S0168-1656(99)00185-6

Porro, D., Sauer, M., Branduardi, P., & Mattanovich, D. (2005). Recombinant protein production in yeasts. *Molecular Biotechnology, 31*(3), 245-259. doi:10.1385/MB:31:3:245

Pronk, J. T. (2002). Auxotrophic Yeast Strains in Fundamental and Applied Research. *Applied and Environmental Microbiology, 68*(5), 2095.

doi:10.1128/AEM.68.5.2095-2100.2002

Quinn, P. (1994). Staphylococcus species. *J Clinical veterinary microbiology*, 118-126.

Rashel, M., Uchiyama, J., Ujihara, T., Uehara, Y., Kuramoto, S., Sugihara, S., . . . Matsuzaki, S. (2007). Efficient Elimination of Multidrug-Resistant Staphylococcus aureus by Cloned Lysin Derived from Bacteriophage ϕMR11. *The Journal of Infectious Diseases, 196*(8), 1237-1247. doi:10.1086/521305

Ribelles, P., Rodríguez, I., & Suárez, J. E. (2012). LysA2, the Lactobacillus casei bacteriophage A2 lysin is an endopeptidase active on a wide spectrum of lactic acid bacteria. *Applied microbiology biotechnology and Bioengineering, 94*(1), 101-110.

Rice, K., Peralta, R., Bast, D., de Azavedo, J., & McGavin, M. J. (2001). Description of staphylococcus serine protease (ssp) operon in Staphylococcus aureus and nonpolar inactivation of sspA-encoded serine protease. *Infection and immunity, 69*(1), 159-169. doi:10.1128/IAI.69.1.159-169.2001

Rohde, H., Knobloch, J. K., Horstkotte, M. A., & Mack, D. (2001). Correlation of Staphylococcus aureus icaADBCgenotype and biofilm expression phenotype. *Journal of clinical microbiology, 39*(12), 4595-

4596.

Rosano, G. L., & Ceccarelli, E. A. (2014). Recombinant protein expression in Escherichia coli: advances and challenges. *Frontiers in microbiology, 5*, 172-172. doi:10.3389/fmicb.2014.00172

Sabat, A., Budimir, A., Nashev, D., Sá-Leão, R., Van Dijl, J., Laurent, F., . . . Markers, E. S. G. o. E. (2013). Overview of molecular typing methods for outbreak detection and epidemiological surveillance. *European Centre for Disease Prevention & Control, 18*(4), 20380.

Sakoulas, G., Gold, H. S., Venkataraman, L., DeGirolami, P. C., Eliopoulos, G. M., & Qian, Q. (2001). Methicillin-resistant Staphylococcus aureus: comparison of susceptibility testing methods and analysis of mecA-positive susceptible strains. *Journal of clinical microbiology, 39*(11), 3946-3951.

Salipante, S. J., SenGupta, D. J., Cummings, L. A., Land, T. A., Hoogestraat, D. R., & Cookson, B. T. (2015). Application of whole-genome sequencing for bacterial strain typing in molecular epidemiology. *Journal of clinical microbiology, 53*(4), 1072-1079.

Sanz-Gaitero, M., Keary, R., Garcia-Doval, C., Coffey, A., & van Raaij, M. J. (2014). Crystal structure of the lytic CHAPK domain of the endolysin LysK from Staphylococcus aureus bacteriophage K. *Virology Journal*,

11(1), 133. doi:10.1186/1743-422X-11-133

São-José, C., Parreira, R., Vieira, G., & Santos, M. A. (2000). The N-Terminal Region of the Oenococcus oeniBacteriophage fOg44 Lysin Behaves as a Bona Fide Signal Peptide inEscherichia coli and as a cis-Inhibitory Element, Preventing Lytic Activity on Oenococcal Cells. *Journal of Bacteriology, 182*(20), 5823-5831.

Schmelcher, M., Donovan, D. M., & Loessner, M. J. (2012). Bacteriophage endolysins as novel antimicrobials. *Future microbiology, 7*(10), 1147-1171. doi:10.2217/fmb.12.97

Schmelcher, M., Powell, A. M., Camp, M. J., Pohl, C. S., & Donovan, D. M. (2015). Synergistic streptococcal phage λSA2 and B30 endolysins kill streptococci in cow milk and in a mouse model of mastitis. *Applied Microbiology and Biotechnology, 99*(20), 8475-8486. doi:10.1007/s00253-015-6579-0

Schmelcher, M., Shen, Y., Nelson, D. C., Eugster, M. R., Eichenseher, F., Hanke, D. C., . . . Donovan, D. M. (2015). Evolutionarily distinct bacteriophage endolysins featuring conserved peptidoglycan cleavage sites protect mice from MRSA infection. *Journal of Antimicrobial Chemotherapy, 70*(5), 1453-1465. doi:10.1093/jac/dku552

Schwartz, D. C., & Cantor, C. R. (1984). Separation of yeast chromosome-

sized DNAs by pulsed field gradient gel electrophoresis. *Cell, 37*(1), 67-75.

Shahinian, S., Dijkgraaf, G. J. P., Sdicu, A.-M., Thomas, D. Y., Jakob, C. A., Aebi, M., & Bussey, H. (1998). Involvement of Protein N-Glycosyl Chain Glucosylation and Processing in the Biosynthesis of Cell Wall β-1,6-Glucan of Saccharomyces cerevisiae. *Genetics, 149*(2), 843.

Sharma, M. (2013). Lytic bacteriophages: Potential interventions against enteric bacterial pathogens on produce. *Bacteriophage, 3*(2), e25518-e25518. doi:10.4161/bact.25518

Shojaosadati, S. A., Varedi Kolaei, S. M., Babaeipour, V., & Farnoud, A. M. (2008). Recent Advances in High Cell Density Cultivation for Production of Recombinant Protein. *Iranian Journal of Biotechnology, 6*(2), 63-84.

Shusta, E. V., Kieke, M. C., Parke, E., Kranz, D. M., & Wittrup, K. D. (1999). Yeast polypeptide fusion surface display levels predict thermal stability and soluble secretion efficiency11Edited by J. A. Wells. *Journal of Molecular Biology, 292*(5), 949-956. doi:https://doi.org/10.1006/jmbi.1999.3130

Sikorski, R. S., & Hieter, P. (1989). A system of shuttle vectors and yeast host strains designed for efficient manipulation of DNA in Saccharomyces

cerevisiae. *Genetics, 122*(1), 19-27.

Silpe, J. E., & Bassler, B. L. (2019). A Host-Produced Quorum-Sensing Autoinducer Controls a Phage Lysis-Lysogeny Decision. *Cell, 176*(1), 268-280.e213. doi:https://doi.org/10.1016/j.cell.2018.10.059

Simpson, R. J. (2010). Stabilization of Proteins for Storage. *Cold Spring Harbor Protocols, 2010*(5), pdb.top79. doi:10.1101/pdb.top79

Siripong, W., Wolf, P., Kusumoputri, T. P., Downes, J. J., Kocharin, K., Tanapongpipat, S., & Runguphan, W. (2018). Metabolic engineering of Pichia pastoris for production of isobutanol and isobutyl acetate. *Biotechnology for Biofuels, 11*(1), 1. doi:10.1186/s13068-017-1003-x

Squires, R. A. (2018). Bacteriophage therapy for management of bacterial infections in veterinary practice: what was once old is new again. *New Zealand Veterinary Journal, 66*(5), 229-235. doi:10.1080/00480169.2018.1491348

Srinivasan, R., Karaoz, U., Volegova, M., MacKichan, J., Kato-Maeda, M., Miller, S., . . . Lynch, S. V. (2015). Use of 16S rRNA Gene for Identification of a Broad Range of Clinically Relevant Bacterial Pathogens. *PLOS ONE, 10*(2), e0117617. doi:10.1371/journal.pone.0117617

Stone, E., Campbell, K., Grant, I., & McAuliffe, O. (2019). Understanding

and Exploiting Phage-Host Interactions. *Viruses, 11*(6), 567. doi:10.3390/v11060567

Sulakvelidze, A. (2013). Using lytic bacteriophages to eliminate or significantly reduce contamination of food by foodborne bacterial pathogens. *Journal of the Science of Food and Agriculture, 93*(13), 3137-3146. doi:10.1002/jsfa.6222

Svircev, A., Roach, D., & Castle, A. (2018). Framing the Future with Bacteriophages in Agriculture. *Viruses, 10*(5), 218. doi:10.3390/v10050218

Tanaka, T., & Kondo, A. (2015). Cell-surface display of enzymes by the yeast Saccharomyces cerevisiae for synthetic biology. *FEMS Yeast Res, 15*(1), 1-9. doi:10.1111/1567-1364.12212

Tatusov, R. L., Galperin, M. Y., Natale, D. A., & Koonin, E. V. (2000). The COG database: a tool for genome-scale analysis of protein functions and evolution. *Nucleic Acids Research, 28*(1), 33-36. doi:10.1093/nar/28.1.33

Terpe, K. (2003). Overview of tag protein fusions: from molecular and biochemical fundamentals to commercial systems. *Appl Microbiol Biotechnol, 60*(5), 523-533. doi:10.1007/s00253-002-1158-6

Tridib Kumar, G. (2010). Role of Cryogenics in Food Processing and

Preservation. *International Journal of Food Engineering, 6*(1). doi:https://doi.org/10.2202/1556-3758.1771

Valero, A., Pérez-Rodríguez, F., Carrasco, E., Fuentes-Alventosa, J. M., García-Gimeno, R. M., & Zurera, G. (2009). Modelling the growth boundaries of Staphylococcus aureus: Effect of temperature, pH and water activity. *International Journal of Food Microbiology, 133*(1), 186-194. doi:https://doi.org/10.1016/j.ijfoodmicro.2009.05.023

van Belkum, A. (2003). High-throughput epidemiologic typing in clinical microbiology. *Clinical microbiology infection and immunity, 9*(2), 86-100.

van den Brink, J., Akeroyd, M., van der Hoeven, R., Pronk, J. T., de Winde, J. H., & Daran-Lapujade, P. (2009). Energetic limits to metabolic flexibility: responses of Saccharomyces cerevisiae to glucose–galactose transitions. *Microbiology Society, 155*(4), 1340-1350. doi:doi:10.1099/mic.0.025775-0

Ventola, C. L. (2015). The antibiotic resistance crisis: part 1: causes and threats. *P & T : a peer-reviewed journal for formulary management, 40*(4), 277-283.

Vieira Gomes, A. M., Souza Carmo, T., Silva Carvalho, L., Mendonça Bahia, F., & Parachin, N. S. (2018). Comparison of Yeasts as Hosts for

Recombinant Protein Production. *Microorganisms, 6*(2), 38. doi:10.3390/microorganisms6020038

Voss, A., Loeffen, F., Bakker, J., Klaassen, C., & Wulf, M. (2005). Methicillin-resistant Staphylococcus aureus in pig farming. *Emerging infectious diseases, 11*(12), 1965-1966. doi:10.3201/eid1112.050428

Walker, S. J., & Lively, M. O. (2013). Chapter 778 - Signal Peptidase (Eukaryote). In N. D. Rawlings & G. Salvesen (Eds.), *Handbook of Proteolytic Enzymes (Third Edition)* (pp. 3512-3517): Academic Press.

Walmagh, M., Boczkowska, B., Grymonprez, B., Briers, Y., Drulis-Kawa, Z., & Lavigne, R. (2013). Characterization of five novel endolysins from Gram-negative infecting bacteriophages. *Applied microbiology biotechnology and Bioengineering, 97*(10), 4369-4375.

Wang, Z., Mathias, A., Stavrou, S., & Neville, D. M., Jr. (2005). A new yeast display vector permitting free scFv amino termini can augment ligand binding affinities. *Protein Engineering, Design and Selection, 18*(7), 337-343. doi:10.1093/protein/gzi036

Weinbauer, M. G. (2004). Ecology of prokaryotic viruses. *FEMS Microbiology Reviews, 28*(2), 127-181. doi:10.1016/j.femsre.2003.08.001

Weinhandl, K., Winkler, M., Glieder, A., & Camattari, A. (2014a). Carbon

source dependent promoters in yeasts. *Microbial Cell Factories, 13*(1), 5. doi:10.1186/1475-2859-13-5

Weinhandl, K., Winkler, M., Glieder, A., & Camattari, A. (2014b). Carbon source dependent promoters in yeasts. *Microbial cell factories, 13*, 5-5. doi:10.1186/1475-2859-13-5

Werner-Washburne, M., Braun, E., Johnston, G. C., & Singer, R. A. (1993). Stationary phase in the yeast Saccharomyces cerevisiae. *Microbiological reviews, 57*(2), 383-401.

Whang, J., Ahn, J., Chun, C.-S., Son, Y.-J., Lee, H., & Choi, E.-S. (2009). Efficient, galactose-free production of Candida antarctica lipase B by GAL10 promoter in Δgal80 mutant of Saccharomyces cerevisiae. *Process Biochemistry, 44*(10), 1190-1192. doi:https://doi.org/10.1016/j.procbio.2009.06.009

Withey, S., Cartmell, E., Avery, L. M., & Stephenson, T. (2005). Bacteriophages—potential for application in wastewater treatment processes. *Science of The Total Environment, 339*(1), 1-18. doi:https://doi.org/10.1016/j.scitotenv.2004.09.021

Wittebole, X., De Roock, S., & Opal, S. M. (2014). A historical overview of bacteriophage therapy as an alternative to antibiotics for the treatment of bacterial pathogens. *Virulence, 5*(1), 226-235.

doi:10.4161/viru.25991

Xu, M., Struck, D. K., Deaton, J., Wang, N., & Young, R. (2004). A signal-arrest-release sequence mediates export and control of the phage P1 endolysin. *Proceedings of the National Academy of Sciences, 101*(17), 6415-6420.

Young, C. L., & Robinson, A. S. (2014). Protein folding and secretion: mechanistic insights advancing recombinant protein production in S. cerevisiae. *Current Opinion in Biotechnology, 30*, 168-177. doi:10.1016/j.copbio.2014.06.018

Young, R. (2014). Phage lysis: Three steps, three choices, one outcome. *Journal of Microbiology, 52*(3), 243-258. doi:10.1007/s12275-014-4087-z

Zhang, K., Bhuripanyo, K., Wang, Y., & Yin, J. (2015). Coupling Binding to Catalysis: Using Yeast Cell Surface Display to Select Enzymatic Activities. *Methods Mol Biol, 1319*, 245-260. doi:10.1007/978-1-4939-2748-7_14

Zhang, Z., Schwartz, S., Wagner, L., & Miller, W. (2000). A Greedy Algorithm for Aligning DNA Sequences. *Journal of Computational Biology, 7*(1-2), 203-214. doi:10.1089/10665270050081478

Zorzet, A. (2014). Overcoming scientific and structural bottlenecks in

antibacterial discovery and development. *Ups J Med Sci*, *119*(2), 170-175. doi:10.3109/03009734.2014.897277

국문 초록

병원성 세균의 위협을 막아내기 위한 무수한 노력에도 불구하고, 세균들과 인간 사이의 군비 경쟁은 전혀 완화되지 못하고 있다. 그럼에도 불구하고, 다양한 병원균에 대한 폭넓은 연구 덕택에 우리는 이들의 특성에 대해 점점 더 많이 이해하게 되었다. 이러한 병원균 중, 황색 포도상 구균 (*Staphylococcus aureus*)은 가장 중요한 지역사회 및 병원 유래 질병 원인균으로 주목받고 있다. 황색 포도상 구균은, 그것이 유발하는 수많은 질병과 다양한 항생제에 대한 내성으로 인해 공공 보건에 심각한 위협이 되고 있다. 게다가, 인수공통 감염 능력은 이와 같은 문제점들을 더욱 악화시키고 있다.

최근, 생물정보학의 비약적인 발전으로 인해 다양한 병원성 세균에 대한 방대한 유전적, 유전체 정보를 활용할 수 있게 되었다. 그러나, 이러한 데이터는 여전히 몇몇 한정된 연구용 균주 또는 주요 분리 균주에서 얻어진 것이 대부분으로, 지구 각지에서 분리된 다양한 균주들의 특성을 대변하기는 어려울 것으로 보인다. 따라서, 본 연구자는 국내에서 분리된 병원성 황색 포도상 구균의 유전체 및 병원성, 항생제 저항성 형성에 기여하는 특질들에 대한

연구가 필요할 것으로 예상하였다. 본 연구에서는 한국에서 분리된 환자 유래 황색 포도상 구균 (*S. aureus* FORC_059)의 전체 염기서열을 밝히고, 해당 균주의 유전체에 대한 annotation 을 수행하였다. 또한, 유전체의 구조적 특성뿐 아니라 병원성 및 항생제 저항성의 형성에 관여하는 유전자들의 구체적인 정보를 유전형 및 표현형을 확인함으로써 밝혀내었다. 나아가, 한국에서 분리된 식품 유래 식중독 발병 원인 균주와의 유전체와의 유사성과 차이점을 비교 분석하였다. 이러한 유전체 연구를 통해, 환자 및 식품 유래 황색 포도상 구균 양쪽 모두 다수의 병원성 유전자와 항생제 저항성 유전자를 보유한 것을 알 수 있었고, 몇가지 핵심 유전자들에 대한 수평적 유전자 전이 가능성이 구조적으로 매우 높다는 것이 확인되었다. 이와 같은 현상에 의한 유전적 형질의 다변화가 빈번히 발생할 수 있다는 점 때문에, 항생제 저항성 유무와 무관하게 병원균을 억제할 수 있는 대안적 항균 요법에 대한 필요성을 통감하였다.

이러한 관점에서, 병원성 세균에 대한 대안적 생물 방제 요법의 개발을 위해 박테리오파지 (bacteriophage, 파지)에 대한 연구가 다각도로 진행되었다. 사실상 모든 세균에 대응되는 박테리오파지가 한가지 또는 그 이상 존재한다고 여겨지기 때문에, 파지 응용 연구는 유망한 해결책이 될 수 있다. 그러나, 숙주

의존적 증식, 숙주 특이성, 용원성 생활사, 숙주의 방어 체계 등과 같은 여러 이유로 인해 파지 응용은 항생제 저항성 사태를 해소할 수 없었다. 그러므로, 파지 라이신 (lysins), 특히 엔도라이신 (endolysin)이 더욱 주목받게 되었다. 지금껏, 파지 엔도라이신에 대한 연구는 주로 신규 엔도라이신의 발견과 개발, 그리고 특성 분석에 집중되어 있었다. 특히, 엔도라이신 연구가 세균 유래 단백질 발현 플랫폼을 기반으로 수행되었기 때문에, 엔도라이신의 응용은 제한적인 상황이었다. 따라서, 본 연구자는 산업적으로 적용 가능한 플랫폼을 개발하기 위하여, 효모 *Saccharomyces cerevisiae*의 표면 디스플레이 (yeast surface display) 및 분비 (secretion) 시스템을 엔지니어링 하고, 여기서 발현된 LysSA11 엔도라이신의 황색 포도상 구균에 대한 항균 효과를 확인하였다. 본 연구는 효모에서 표면 디스플레이와 분비 시스템 모두를 이용해 파지 엔도라이신을 발현 및 응용한 최초의 연구이다.

효모 *S. cerevisiae* EBY100 균주에서의 LysSA11 표면 디스플레이는 pYD5 플라스미드 상에서 LysSA11의 카르복실 말단부 (C-terminus)를 a-agglutinin subunit Aga2p와 융합하는 방법으로 수행되었다. 갈락토오스 (galactose)에 의해 발현이 유도된 *S. cerevisiae* EBY100/pYD5-LysSA11 배양액은 세포 증식 및 갈락토오스 섭취 양상을 기반으로, 초기 지수증식기 (OD_{600} = 6)와

후기 지수증식기 (OD_{600} = 13)에 확보되었다. 각각의 세포 증식 단계에서의 LysSA11-Aga2p 융합 단백질의 발현은 western blot 검사로 확인되었으며, 이 단백질이 당화 (glycosylation)되어있는 것 또한 확인되었다. Flow cytometry 분석법을 통해 각 세포 증식 단계에 확보된 배양액 내 효모 세포의 LysSA11 표면 디스플레이 특성을 분석하여, 지수증식기 동안 단일 개체 당 표면 디스플레이 된 LysSA11의 양이 증가하는 것을 확인할 수 있었다. 그리고, 배양액의 효모 세포를 단순히 반응 용액 (reaction buffer, 100 mM sodium phosphate, 200 mM sodium chloride, pH 7.4)으로 옮겨주었을 때, 효모 디스플레이된 LysSA11이 황색 포도상 구균의 type strain (*S. aureus* ATCC 13301)과 환자 분리 균주 (*S. aureus* FORC_059)에 대해 항균 활성을 나타내는 것을 확인하였다. 초기, 중기, 후기 지수증식기에 확보된 약 3×10^8 CFU/mL의 발현 유도된 효모 세포를 처리하였을 때, 각각 7시간, 6시간, 2시간 이내에 약 1×10^5 CFU/mL의 *S. aureus* ATCC 13301 균주를 사멸시키는 것으로 확인되었다. 또한, 반응 이후 황색 포도상 구균이 10시간 까지 사멸 상태를 유지하는 것을 확인하여, 저항성 형성이 불가능하다는 것을 유추할 수 있었다. 마찬가지로, 후기 지수증식기에 확보된 동량의 효모 세포를 처리하였을 때, 약 2×10^5 CFU/mL의 *S. aureus* FORC_059 균주가 4시간 이내에 완전히

사멸되는 것을 확인할 수 있었다. 게다가, 효모 디스플레이 된 LysSA11의 안정성이 획기적으로 향상되어, 어떠한 안정화 요소 없이도 4℃의 보관 환경에서 14일간 *S. aureus* ATCC 13301 균주에 대한 항균 능력이 거의 온전히 유지되는 것을 알 수 있었다. 반면, 대장균 (*Escherichia coli*) 시스템에서 발현 및 정제된 LysSA11은 글라이세롤이 없는 환경에서 매우 급격하게 변성되어, 7일과 14일 후에 각각 초기 항균 능력의 19.2%와 11.5%에 해당하는 효과가 유지되는 것이 확인되었다.

LysSA11의 분비는 YVH10/pYDS-K-LysSA11과 EBY100/p404TEF1-LysSA11의 두가지 서로 다른 재조합 효모 균주에서 진행되었다. 구체적으로, 전자의 경우 발현이 유도 가능한 (inducible) GAL1 promoter가, 후자는 발현 유도체 없이 지속적 (constitutive) 발현이 가능한 TEF1 promoter가 사용되었다. 우선, 각각의 재조합 효모 균주를 30℃에서 배양하여, LysSA11의 발현과 항균 활성을 측정하였다. YVH10/ pYDS-K-LysSA11의 경우, 세포 성장 및 갈락토오스 섭취 양상에 기반하여 초기 지수증식기 (OD_{600} = 5) 및 후기 지수증식기 (OD_{600} = 16)에 발현 유도된 배양액을 확보하였고, EBY100/p404TEF1-LysSA11의 경우 세포 성장 양상에 기반하여 후기 지수증식기 (OD_{600} = 10)에 배양액을 확보하였다. 각 재조합 효모 균주 모두 LysSA11를 세포 내부에

발현하거나 외부로 분비하는 것이 확인되었고, 특히, YVH10/pYDS-K-LysSA11에서는 LysSA11이 당화 (glycosylation)되는 것이 확인되었다. 각 세포 배양액을 원심분리한 상등액 내에 존재하는 분비된 LysSA11은 초기 부피의 125배로 농축된 후, 약 2×10^4 CFU/mL의 *S. aureus* ATCC 13301 균주에 대한 항균 활성이 측정되었다. 그 결과, YVH10/pYDS-K-LysSA11 유래 농축액은 4시간 이내에 대상균 전체를 사멸하였으나, EBY100/p404TEF1-LysSA11의 경우에서는 항균 활성을 전혀 나타내지 못하는 것을 확인하였다. 이후, YVH10/pYDS-K-LysSA11 균주를 각기 다른 조건 (낮은 세포 밀도/높은 세포 밀도, 20℃/30℃)에서 배양하여 LysSA11의 분비 및 항균 활성을 분석하였고, 그 결과 낮은 세포 밀도의 30℃ 배양액을 초기 지수증식기에 확보하는 것과 높은 세포 밀도의 20℃ 배양액을 후기 지수증식기에 확보하는 경우 주어진 수의 *S. aureus* ATCC 13301 균주를 사멸하기에 충분한 활성을 나타내는 것으로 확인되었다.

본 연구자는, 본 연구를 통해 생물정보학 기법들을 활용하여 황색 포도상 구균을 유전체적으로 연구하고, 효모 *S. cerevisiae*의 단백질 표면 디스플레이 및 분비 시스템을 엔지니어링하여 신규 엔도라이신 발현 플랫폼을 개발하고, 황색 포도상 구균의 생물 방제를 위한 적용 가능성을 입증하였다. 본 연구에서 획득한

결과들은 신규 항균 소재의 필요성을 역설하고, 더욱 발전된 엔도라이신 응용 방안을 위한 효모 개발의 초석이 될 것이다.

주제어: 황색 포도상 구균, 박테리오파지 엔도라이신, 사카로마이시스 세레비지애 (효모), 효모 표면 디스플레이, 효모 단백질 분비, 생물 방제재

학번: 2014-21911